

**MECHANISMS OF ASTROCYTIC CALCIUM WAVE PROPAGATION AND *IN*
VITRO HIPPOCAMPAL CELL DEATH ARE DETERMINED BY THE
MAGNITUDE OF MECHNICAL INJURY**

William J. Miller

A DISSERTATION
IN
BIOENGINEERING

Presented to the Faculties of the University of Pennsylvania
in Partial Fulfillment of the Requirements for the Degree of Doctor of Philosophy
2010

David F. Meaney, Ph.D.
Professor, Department Chair, Bioengineering
Supervisor of Dissertation

Susan Margulies, Ph.D.
Professor, Bioengineering and Neurosurgery
Graduate Group Chairperson, Bioengineering

Dissertation committee
Philip Haydon, Ph. D., Professor and Vice Chair, Neuroscience, U of Penn
Joseph Neary, Ph.D., Professor, Miami Veterans Affairs Medical Center
Beth Winkelstein, Ph.D., Associate Professor, Bioengineering, U of Penn
Akiva Cohen, Ph.D., Assistant Professor, Neurology, U of Penn

Abstract

MECHANISMS OF ASTROCYTIC CALCIUM WAVE PROPAGATION AND *IN VITRO* HIPPOCAMPAL CELL DEATH ARE DETERMINED BY THE MAGNITUDE OF MECHANICAL INJURY

William J. Miller

David F. Meaney

It has been estimated that traumatic brain injury (TBI) costs the U.S. economy over \$60 billion a year, with over 5.3 million people suffering some level of long term effects. Despite these figures, no effective pharmacological treatment has been successfully developed to help patients recover from TBI. A more complete understanding of both the immediate cellular reactions to injury and the longer-term responses may present new strategies for reducing damage and promoting repair. In this dissertation we first examine the ability for astrocytes to modulate the mechanisms of calcium wave propagation in response to increasing degrees of injury. As injury magnitude increases, the complexity of the calcium wave that is transmitted to surrounding uninjured regions also increases. At very mild levels of stretch calcium waves are primarily transmitted through extracellular ATP. As the level of stretch increases, gap junction communication and metabotropic glutamate receptor activation can be detected. The interaction between these three signaling pathways may transmit information about the severity of injury to surrounding astrocytes and may mediate

immediate cellular responses. We also observe that the mechanical properties of cultured astrocytes are altered 24 hours after injury. Rapid stretch induces a decrease in the apparent Young's modulus on non-nuclear regions of astrocytes, indicating that the cells are softer and more compliant. This change is associated with an upregulation of GFAP, which is a common marker for reactive gliosis. Finally, we investigate the interaction between glutamatergic and purinergic signaling in mediating cell death in hippocampal slices 24 hours following mechanical injury. Within the CA3 region of the hippocampus there is a significant increase in cell death after stretch-injury that can be attenuated by inhibiting the activity of the glutamatergic N-methyl D-aspartate (NMDA) receptors. Alternatively, blocking the activity of P2Y1 receptors is effective in limiting cell death. Our studies suggest that there is a high probability that P2Y1 receptor activity on astrocytes is responsible for inducing the over-excitation of extrasynaptic NMDA receptors, which is responsible for a major component of the observed cell death. Further studies into this pathway may lead to new approaches for pharmacological therapies after TBI.

Table of Contents

Abstract	ii
Table of Contents	iv
List of Tables	vii
List of Figures	viii
Chapter 1: Background and Significance	1
1.1 Introduction	1
1.2 Calcium Waves	3
1.3 ATP and P2 purinergic receptors	5
1.4 Activation of the NMDA Receptor as a Mediator of Cell Death	8
1.5 Summary of Following Chapters	10
Chapter 2: Astrocytes Modulate Mechanisms of Calcium Wave Propagation in Response to the Severity of Mechanical Injury	12
2.1 ABSTRACT	12
2.2 INTRODUCTION	14
2.3 MATERIALS AND METHODS	18
2.3.1 Cell Culture	18
2.3.2 Cell Stretch	19
2.3.3 Imaging	20
2.3.4 Western Blots	21
2.3.5 Luciferin-luciferase Assay	22
2.3.6 Statistics	22
2.4 RESULTS	23
2.4.1 Mild stretch evokes intracellular free calcium increases in a subset of astrocytes	23
2.4.2 Rapid stretch of astrocytes produces intercellular calcium waves in the penumbra	23
2.4.3 Extracellular ATP is released into the penumbra through an intracellular calcium-dependent mechanism	25
2.4.4 Stretch-induced calcium waves in the penumbra are inhibited by P2 receptor antagonists after 5%	

stretch	25
2.4.5 Gap junctions and P2 receptors participate in calcium wave propagation after 15% stretch	27
2.4.6 Calcium wave propagation after 25% stretch is not dependent on gap junction pathway	28
2.4.7 Metabotropic glutamate receptors participate in propagating calcium waves after a 25% stretch	29
2.4.8 Calcium waves do not trigger ERK activation in the penumbra of a stretch-induced injury	30
2.5 DISCUSSION	32
Chapter 3: Mechanical Properties of Cultured Rat Cortical Astrocytes after Stretch-induced Injury	52
3.1 ABSTRACT	52
3.2 INTRODUCTION	53
3.3 MATERIALS AND METHODS	55
3.3.1 Cell Culture	55
3.3.2 Cell Stretch	56
3.3.3 GFAP immunoreactivity	56
3.3.4 Atomic Force Microscopy	57
3.3.5 Statistics	58
3.4 RESULTS	60
3.4.1 Mechanical stretch induces an increase in GFAP immunoreactivity 24 hours following injury	60
3.4.2 Modeling of AFM indentation	60
3.4.3 Apparent Young's modulus is reduced in nuclear regions of naïve astrocytes compared to non-nuclear regions	61
3.4.4 Mechanically injured astrocytes are more compliant than naïve astrocytes	61
3.4.5 Non-nuclear regions of penumbra astrocytes are more compliant than naïve astrocytes	62
3.5 DISCUSSION	63
Chapter 4: The Role of Purinergic and Glutamatergic Signaling in Mediating Cell Death Following Mechanical Injury of Organotypic Hippocampal	

Slices	75
4.1 ABSTRACT	75
4.2 INTRODUCTION	76
4.3 MATERIALS AND METHODS	80
4.3.1 Organotypic hippocampal slice culture isolation	80
4.3.2 In vitro model of TBI	80
4.3.3 Cell death measurement	81
4.3.4 Calcium Crimson	83
4.3.5 Statistics	84
4.4 RESULTS	85
4.4.1 Rapid stretch of organotypic hippocampal slice cultures results in increased cell death in the CA3 24 hours after injury	85
4.4.2 Inhibiting NMDA receptor activation attenuates cell death in CA3 region of OHSCs	86
4.4.3 Extrasynaptic NMDAR inhibition produces a selective protection against cell death after stretch	86
4.4.4 Inhibition of intracellular calcium increase in astrocytes is protective after severe injury	87
4.4.5 mGluR5 is not involved in mediating stretch-induced NMDAR-mediated cell death in OHSCs	88
4.4.6 Extracellular ATP and activation of purinergic receptors are linked to cell death in OHSCs following mechanical injury	89
4.5 DISCUSSION	92
Chapter 5: Potential Limitations and Future Directions	107
5.1 Astrocytes Modulate Calcium Wave Communication in Response to Mechanical Injury	107
5.2 Mechanical Properties of Astrocytes Change after Injury	108
5.3 P2Y1 and NMDA Receptors Mediate Cell Death Patterns in the CA3 Region of Injured Organotypic Hippocampal Slice Cultures	110
Bibliography	112

List of Tables

Table 3.1: Conical and Parabolic estimations of the apparent Young's modulus in astrocytes following injury	75
---	----

List of Figures

Figure 2.1: Schematic of injury device and images of calcium wave propagation in astrocyte cultures following stretch	39
Figure 2.2: Astrocytes in the mechanical penumbra show more pronounced intracellular calcium increases than stretched astrocytes	41
Figure 2.3: Percentage of cells responding to calcium waves after stretch and the fura-2 ratio of responding cells	42
Figure 2.4: Luciferin-luciferase assay of ATP released and diffusing in the penumbra after stretch	44
Figure 2.5: Calcium waves following mild (5%) mechanical stretch are mediated primarily by P2 receptor activity	45
Figure 2.6: Calcium waves following a moderate (15%) stretch were inhibited by blocking gap junctions and P2 receptors simultaneously	47
Figure 2.7: Following the highest level of mechanical stretch (25%) P2 receptor antagonists attenuated but did not eliminate calcium waves in astrocytes.	49
Figure 2.8: Metabolic glutamate receptor antagonists attenuate calcium increases within the mechanical penumbra	50
Figure 2.9: Calcium waves did not initiate ERK activation	51
Figure 3.1: Overview of mechanical injury device	69
Figure 3.2: Height and deflection images of an astrocyte obtained by AFM scanning in contact mode	70
Figure 3.3: Immunocytochemistry for GFAP showing increased reactivity in stretched and penumbra regions	71
Figure 3.4: Force-indentation curve recorded from a group of penumbra astrocytes from separate cultures	72
Figure 3.5: Changes in apparent stiffness 24 hours following stretch injury differ with indentation region and are distinct between the penumbra and stretched regions	74
Figure 4.1: Overview of injury device and organotypic hippocampal slice cultures	100

Figure 4.2: PI labeling of OHSCs	101
Figure 4.3: Mechanical injury produced an increase in cell death in the CA3 of hippocampal slices cultures 24 hours after a mechanical injury	102
Figure 4.4: Treatment with NMDA receptor antagonists attenuated cell death after injury	103
Figure 4.5: BAPTA-AM loading in astrocytes reduced cell death after severe injury	104
Figure 4.6: Injury-induced CA3 cell death in OHSCs was not dependent on activation of mGluR5	105
Figure 4.7: P2 purinergic receptors mediated cell death in the CA3 region 24 hours after injury	106

Chapter 1: Background and Significance

1.1 Introduction

Approximately 1.4 million people sustain a traumatic brain injury (TBI) in the United States every year. Of this number, about 50,000 people suffer fatal injuries and 235,000 are hospitalized, including over 2,600 deaths and 37,000 hospitalizations of children under the age of 14 (Langlois et al. 2004). According to the CDC, 5.3 million Americans suffer some level of long-term disability as a result of a TBI, with an estimated net economic cost to the US of \$60 billion per year, including medical costs and lost productivity (Finkelstein et al. 2006). Since the highest risk age groups are 0-4 and 15-19 years old, a serious injury to the central nervous system can result in decades of disability and suffering for those afflicted (Langlois et al. 2004). Despite years of research and effort, no effective pharmacological intervention has emerged to help mitigate the short or long-term effects of TBI (Royo et al. 2003).

The most common causes of TBI are impacts and inertial loading, often experienced during falls or motor vehicle accidents (Langlois et al. 2004). The primary types of injury can be generally separated into focal injuries, such as contusions and hemorrhaging, and diffuse injuries, which are seen in concussion and in diffuse axonal injury. As a rule, diffuse injuries are caused by inertial loading, such as sudden acceleration/deceleration in a car accident, while focal injuries are caused by impact (Gennarelli 1993; McIntosh et al. 1996). Serious TBI is followed by necrotic and apoptotic cell death throughout the brain tissue, along with axonal degeneration in the white matter (Dietrich et al. 1994; Hicks et al. 1996; Sutton et al. 1993). Often this is

followed by a chronic neuronal death in which secondary processes increase the overall magnitude of the injury (Dietrich et al. 1994; Hicks et al. 1996; Raghupathi et al. 2000; Sato et al. 2001; Zhao et al. 2003). Astrocytes can respond to CNS injury by undergoing reactive gliosis, which is characterized by cellular swelling, increased process number and length, increase in glial fibrillary acidic protein (GFAP) content, and, in some cases, migration to the site of injury (Fawcett and Asher 1999; Fitch et al. 1999; Norton 1999; Yong 1998). Several days after injury nearby reactive astrocytes can begin to form a glial scar around the site of injury. This glial scar is a dense collection of cells, primarily composed of astrocytes, oligodendrocytes, and microglia, as well as cellular debris and extracellular matrix molecules that wall off the site of injury from the rest of the brain and might serve to minimize further spread of cell death (Faulkner et al. 2004; McKeon et al. 1999). However, the scar also has the effect of inhibiting neuronal and axonal regeneration (Fawcett and Asher 1999; Fitch et al. 1999; Yong 1998).

The exact processes involved in stimulated astrocyte reactivity and subsequent scarring is still not completely understood. Likewise, the mechanisms behind prolonged cell death after TBI have not been fully explained. The major themes of this thesis are to investigate how mechanically injured cultured astrocytes can transmit information about the severity of strain to the surrounding, uninjured astrocyte network by modulating calcium wave signaling and to examine how mechanical injury to organotypic hippocampal slices triggers astrocyte-mediated NMDA receptor-dependent cell death. In the remainder of this chapter we will review the major themes of this thesis.

1.2 Calcium Waves

A calcium wave is the standard communication mechanism used by astrocytes after acute stimulation. Calcium waves are defined as increases in cytosolic free calcium concentrations that propagate from the site of stimulation to surrounding cells. Calcium waves have been observed in cultured astrocytes after stimulation by various methods, including application of glutamate (Blomstrand et al. 1999b; Charles et al. 1991; Innocenti et al. 2000), ATP (Bennett et al. 2006; Coco et al. 2003; Cotrina et al. 2000; Guthrie et al. 1999; Newman 2001; Venance et al. 1997), endothelin-1 (Venance et al. 1997), noradrenaline (Tordjmann et al. 1997), 5-hydroxytryptamine (Blomstrand et al. 1999b), and mechanical stimulation by poking with a pipette tip (Charles et al. 1991; Muyderman et al. 1998; Newman 2001; Venance et al. 1997). However, the mechanism of calcium wave propagation from the stimulated cell to adjacent regions has generally been identified to be from two potential pathways: 1) through the release of ATP and the autocrine/paracrine activation of P2 purinergic receptors (Coco et al. 2003; Cotrina et al. 2000; Guthrie et al. 1999; Venance et al. 1997), and/or 2) through the diffusion of inositol 1,4,5-trisphosphate (IP₃) through open gap junctions that connect adjacent astrocytes (Blomstrand et al. 1999a; Charles 1998; Giaume and Venance 1998; Scemes 2000; Yamane et al. 2002). The exact interplay between the two mechanisms seems to depend on culture conditions and the stimulating event (Scemes 2000; Scemes et al. 2000).

During ATP-mediated calcium wave propagation, ATP released from the stimulated cell binds to G-protein-coupled P2Y purinergic receptors and activates phospholipase C (PLC), leading to the hydrolysis of phosphatidylinositol (4,5)-

bisphosphate (PIP₂) into IP₃ and diacyl glycerol (DAG). IP₃ can then activate IP₃ receptors on the endoplasmic reticulum (ER), which releases calcium into the cytosol (Clapham 1995). At the same time, ionotropic P2X receptors can open upon stimulation by ATP and allow calcium to enter the cytosol directly from the extracellular space, although this has not been shown to be a major pathway of calcium entry during calcium wave activity (Verkhratsky and Steinhauser 2000). Astrocytes undergo ATP-induced ATP release, which can occur in both a calcium-dependent or calcium-independent manner (Anderson et al. 2004; Bodin and Burnstock 1996; Haas et al. 2006; Stout et al. 2002; Suadicani et al. 2006). This release allows for a regenerating source of extracellular ATP to propagate a wave of calcium increases significant distances from the site of stimulation.

In gap junction-mediated calcium wave propagation, the increase in IP₃ concentration caused by the initial stimulation is transmitted to surrounding cells via diffusion through open gap junctions (Scemes and Giaume 2006). Astrocytes are extensively coupled by gap junctions, which are generally considered to be non-selective channels permeable to molecules under 1kDa in size (Kumar and Gilula 1996; Nagy and Rash 2000). An appropriate stimulus in the initiating cell evokes an acute rise in IP₃ production which diffuses into neighboring cells through open gap junction channels and activates IP₃ receptors on the ER of the neighboring cell. This results in calcium release from intracellular stores and the production of more IP₃, leading to increased diffusion into neighboring cells (Giaume and Venance 1998; Sanderson et al. 1994). Experiments on glioma cells show that the expression of connexin-43, the major gap junction protein

in astrocytes, is directly related to the extent of calcium wave propagation (Blomstrand et al. 1999a). In addition, gap junction blockers have effectively prevented calcium wave propagation in several experimental models (Venance et al. 1997; Yamane et al. 2002). In this thesis we investigate how stretch-induced injury can initiate calcium waves that propagate into the nearby, unstretched region – the ‘mechanical penumbra’ – and how astrocytic calcium wave signaling is modulated depending on the severity of strain used to initiate the injury.

1.3 ATP and P2 purinergic receptors

A greater appreciation has been developing for the importance of ATP signaling in physiological and pathological brain function. As mentioned above, extracellular ATP activates the P2 purinergic family of receptors (Fields and Burnstock 2006). There are two major groups of P2 receptors: P2X, which are ion channels, and P2Y, which are metabotropic G-protein coupled receptors (Araque et al. 2001). ATP is released in large quantities after a TBI (Hansson and Ronnback 2003), which makes this molecule a major potential target for explaining the pathological responses in the brain. The mechanism of release is still not completely understood and may be different in each cell type. ATP can be released from astrocytes and from neurons presynaptically or postsynaptically (Fields and Burnstock 2006). ATP has been found in vesicles that are released in a calcium-dependent manner (Fields and Burnstock 2006), and has been shown to be released through connexin hemichannels (Leybaert et al. 2003) or through the large pores formed during activation of the P2X7 receptor (Suadicani et al. 2006). ATP is also released in large quantities when cells are ruptured mechanically or during necrotic cell death

(Hansson and Ronnback 2003). In physiological conditions extracellular ATP is quickly degraded to adenosine by ectonucleotidases, but the activity of these enzymes may be inhibited in pathological conditions (Franke et al. 2006).

Extracellular ATP can have a large number of sometimes conflicting effects on neurons during normal function. For example, P2X receptors acting postsynaptically can contribute to excitatory synaptic transmission (Duan and Neary 2006). Likewise, P2X receptors acting presynaptically can increase the probability of vesicular release of glutamate (Franke et al. 2006; North and Verkhatsky 2006). Conversely, P2Y receptors generally act in an inhibitory manner on neurons. For instance, ATP acting on P2Y receptors in the CA1 region reduces the probability of vesicle release (Fields and Burnstock 2006; Hussl and Boehm 2006; North and Verkhatsky 2006). Indirectly, P2Y receptors are inhibitory in the hippocampus by being excitatory on inhibitory interneurons (Kawamura et al. 2004). Likewise, the breakdown product of ATP, adenosine, is an inhibitory signal for most neurons (Pascual et al. 2005). In fact, astrocytes in some brain regions act to inhibit nearby neurons by releasing ATP, which is converted to adenosine and reduces activity (Fellin et al. 2006a; Newman 2003; Pascual et al. 2005).

As mentioned in the previous section, extracellular ATP can activate calcium responses from astrocytes and is the primary signaling molecule in astrocyte communication (North and Verkhatsky 2006). In addition, ATP is involved in mediating the release of neurotransmitters through several different signaling mechanisms (Montana et al. 2004). ATP activation of P2X7 receptors, which are found

in large numbers on astrocytes, can lead to the release of glutamate (Duan et al. 2003; Fellin et al. 2006b; Franke et al. 2006). In addition, the activation of several P2Y receptors, and, specifically, the P2Y₁ receptor, can cause the release of glutamate from astrocytic vesicles in a PLC-mediated calcium-dependent manner (Domercq et al. 2006; Wirkner et al. 2006; Wirkner et al. 2002). ATP activation on astrocytes can also cause the release of additional ATP, as mentioned above (Anderson et al. 2004; Wang et al. 2000). In this way, astrocyte activation can have a direct effect on neuronal signaling pathways.

ATP may also be important in mediating the longer-term consequences of TBI and neurodegenerative diseases. Antagonists to P2 receptors are protective against cell death in hypoxia (Cavaliere et al. 2001; Fields and Burnstock 2006; Franke et al. 2006; Runden-Pran et al. 2005), ischemia (Chorna et al. 2004; Franke et al. 2006; Lammer et al. 2006), seizure (Franke et al. 2006), and TBI (Chorna et al. 2004; Franke et al. 2006; Neary and Kang 2005). ATP can be excitotoxic to neurons in culture, both directly (Fields and Burnstock 2006; Franke et al. 2006; Hussl and Boehm 2006) and by causing the release of excessive glutamate (Franke et al. 2006). Additionally, ATP stimulation of cultured astrocytes initiates ERK signaling, proliferation, stellation, GFAP upregulation, and other characteristics of reactive gliosis (Brambilla et al. 2002; Fields and Burnstock 2006; Franke et al. 2001; King et al. 1996; Neary et al. 2003). As a part of this thesis, we investigate the role ATP plays immediately after mechanical injury by looking at how ATP contributes to the propagation of calcium waves in astrocytes. We also examine how ATP participates in mediating cell death in organotypic hippocampal slice cultures

24 hours after mechanical injury. These studies will show that ATP is a critical component of the injury response in the brain and that P2 receptor antagonists may be a target for pharmacological therapies after TBI.

1.4 Activation of the NMDA Receptor as a Mediator of Cell Death

There is abundant evidence that activation of N-methyl-D-aspartate receptors (NMDARs) mediate cell death after brain injury and that antagonism of NMDARs is protective (Bullock and Fujisawa 1992; Dempsey et al. 2000; LaPlaca and Thibault 1998; Rao et al. 2001; Regan and Choi 1994; Shapira et al. 1990; Wang and Shuaib 2005). NMDARs are heterotetrameric ionotropic glutamate receptors that are particularly permeable to calcium ion flux (Loftis and Janowsky 2003). The receptor is composed of two NR1 subunits and two NR2 subunits. There are several subtypes of NR2 subunits, and it is generally found that the specific type of NR2 subunit is responsible for the cellular location and heterogeneous functions of the NMDARs (Loftis and Janowsky 2003). During physiological activity, the NMDAR is activated by the concurrent binding of glutamate and depolarization of the membrane, which releases Mg^{2+} from the ion pore and allows calcium flux (Scatton 1993). However, after mechanical injury the receptor has been shown to lose the Mg^{2+} block, allowing for activation by glutamate binding alone and potentially leading to excitotoxic cell death (Zhang et al. 1996).

Interestingly, there is some pharmacological evidence suggesting that activation of different subtypes of the NMDAR lead to opposing cellular fates. Activation of NR2A-containing NMDARs along with blockade of NR2B-containing NMDARs has been

associated with cell survival in some injury and disease models, while the reverse has been associated with cell death (Arundine and Tymianski 2004; Chazot 2004). However, the segregation of NR2A and NR2B receptor function in cell death is not undisputed, with some evidence that either NMDAR can result in cell death in conditions of overexcitation (Borsello et al. 2003; Sattler et al. 1998; Sattler et al. 2000), and the real difference in the cell death capacity of the NMDAR is determined by the location of the excitotoxic glutamate release (Sattler et al. 2000). While it is generally assumed that the majority of glutamate at the synapse is released from the presynaptic terminal, the source of glutamate that activates the extrasynaptic NR2B-containing NMDARs is not currently well characterized, although spill-over from the synapse (Rao et al. 1998; Selkirk et al. 2005), reversal of glutamate transporters (Kawahara et al. 2002; Rossi et al. 2000), and release from glial glutamate stores (Fellin and Haydon 2005) have been proposed as possibilities.

As mentioned above, astrocytes possess the cellular machinery for glutamate release (Anlauf and Derouiche 2005; Araque et al. 2000; Montana et al. 2004; Zhang et al. 2004a; Zhang et al. 2004b) and are uniquely positioned for activation of extrasynaptic NMDARs. Astrocytes enwrap a large number of synapses and can respond to neuronal signaling with intracellular calcium increases (Araque et al. 2001). These calcium increases can lead to regulated release of neurotransmitters like glutamate (Montana et al. 2004). Several recent studies have shown that astrocytes can release glutamate to specifically activate extrasynaptic NMDARs and cause a slow inward current (Angulo et al. 2004; Fellin et al. 2004; Fellin et al. 2006b). The role of this astrocyte release

mechanism is still not completely understood, although the effects of astrocyte-mediated extrasynaptic NMDAR activation has been shown to synchronize neuronal activity (Angulo et al. 2004; Fellin et al. 2004; Fellin et al. 2006a). In this dissertation we will investigate the possibility that a major source of extrasynaptic glutamate after traumatic injury is released from nearby astrocytes and that this glutamate is responsible for increased cell death in organotypic hippocampal slice cultures 24 hours after injury.

1.5 Summary of Following Chapters

The contents of the remainder of this thesis are as follows:

Chapter 2: We investigate how astrocytes regulate the propagation of calcium waves into the penumbra of a mechanical injury. We show that ATP released by mechanically stimulated astrocytes at three different strain magnitudes is the primary mediator of calcium waves that propagate into unstretched regions (penumbra) of the cultures. We also show that gap junctions are involved in propagating calcium waves after only the moderate strain magnitude, and that glutamate may be involved in calcium waves at the highest strain investigated. These results indicate that astrocytes are able to modulate calcium wave communication in response to varying levels of mechanical injury.

Chapter 3: We describe the changes in mechanical properties in astrocytes 24 hours following mechanical injury. Certain regions of astrocytes undergo a significant decrease in stiffness as measured by indentation with an atomic force microscope. This result is found both in injured cells and cells in the penumbra of the injury. Correlated with this

softening is an increase in GFAP immunoreactivity, indicating that these astrocytes are undergoing some level of reactive gliosis.

Chapter 4: We investigate the signaling pathways that lead to cell death 24 hours following mechanical injury to organotypic hippocampal slice cultures. At the threshold of mechanical injury we find that only extrasynaptic NMDARs are involved in cell death, while synaptic NMDARs are involved at higher levels of injury. We also find that astrocytic calcium is involved in mediating NMDAR-dependent cell death, and the antagonism of P2Y1 receptors is effective in limited cell death.

Chapter 5: We conclude with a discussion of problems, potential improvements, and some future directions to the current work presented in this thesis.

Chapter 2: Astrocytes Modulate Mechanisms of Calcium Wave Propagation in Response to the Severity of Mechanical Injury

2.1 ABSTRACT

We investigated the mechanisms by which cultured rat cortical astrocytes subjected to stretch-induced injury initiate calcium waves that propagated to surrounding regions (the mechanical penumbra) and whether the calcium transients in the stretched and penumbra cells resulted in increased ERK activation. Astrocytes were cultured on elastic membranes and a sub-region of the membrane was subjected to a transient strain of 5%, 15%, or 25%, mimicking the strains experienced during mild-to-moderate traumatic brain injury. With this method, a single culture contained a region of stretched cells surrounded by a penumbra of unstretched cells. Immediately after the stretch, robust calcium wave propagation was detected in the penumbra in 76% (25/33) of cultures subjected to a 5% strain, and 100% of cultures subjected to a 15% or 25% strain (28/28 and 24/24 cultures, respectively), as measured by fura-2 AM. Despite this intense activity in the penumbra, less than half of astrocytes in the stretched region of cultures experienced significant calcium increases. Calcium waves produced by a 5% stretch were completely inhibited by blockade of P2 purinergic receptor activation. After a 15% stretch a combination of gap junction blockers and P2 receptor blockers was effective in eliminating calcium wave propagation. Gap junction blockers were completely ineffective in altering wave dynamics after 25% stretch, while P2 receptor blockers were only partially effective. Group I metabotropic glutamate receptor antagonists were also effective in reducing the calcium transients seen in calcium waves initiated by a 25%

stretch. Astrocytes in the stretched region of the cultures exhibited a significant strain-dependent increase in phosphorylated ERK 15 minutes after 15% and 25% stretch magnitudes. However, in the penumbra, cells showed no significant increase in phosphorylated ERK. These findings show that while extracellular ATP is the primary mechanism of calcium wave propagation at all stretch levels, astrocytes can modulate the components of the calcium wave signal in response to different levels of mechanical strain, and that robust calcium waves in the penumbra of injury are largely independent of calcium increases in the stretched region.

2.2 INTRODUCTION

Approximately 1.4 million people sustain a traumatic brain injury (TBI) in the United States each year, leading to 50,000 deaths and 235,000 hospitalizations (Langlois et al. 2004). According to the CDC, 5.3 million Americans currently suffer with some degree of long-term disability as a result of a TBI, with an estimated net economic cost to the U.S. of \$60 billion per year (Finkelstein et al. 2006). There has been a growing appreciation of how even mild head trauma can lead to serious cognitive and functional deficits and dysfunction (Tashlykov et al. 2007). The mechanisms that regulate the cellular responses in the brain following mild injury, however, are poorly understood.

During a traumatic injury the brain experiences a complex pattern of deformations that results in localized regions of high strain and damage (Miller et al. 1998; Shreiber et al. 1997). In some cases, astrocytes in the surrounding tissue undergo reactive gliosis, a process which includes increased process stellation, proliferation, and production of extracellular matrix molecules that are inhibitory to neuronal regeneration (Nieto-Sampedro 1999; Pekny and Nilsson 2005; Sandvig et al. 2004; Wu and Schwartz 1998; Yiu and He 2006). Studies show that astrocyte-based changes after traumatic and neurodegenerative injury can profoundly affect neuronal function and recovery (Myer et al. 2006; Panickar and Norenberg 2005; Sofroniew 2005; Trendelenburg and Dirnagl 2005). Therefore, understanding how astrocytes signal to each other after mechanical injury and how these signals affect astrocytic and neuronal function may lead to strategies that can mitigate the long-term effects of TBI.

Both neurons and astrocytes show immediate pathophysiological changes in response to mechanical strains that mimic TBI (Ellis et al. 1995; Floyd et al. 2005; Rzigalinski et al. 1997; Weber et al. 2001; Wolf et al. 2001; Zhang et al. 1996). Much less, though, is known about how cells surrounding deformed regions in the brain – i.e., the ‘mechanical penumbra’ – respond to signals triggered by mechanically injured neurons and glia. In vitro, mechanical stimulation of a single astrocyte with a glass pipette tip can lead to the outward propagation of intercellular calcium waves, a process that can extend well beyond the initial focus of stimulation (Charles et al. 1991; Cornell-Bell and Finkbeiner 1991; Scemes and Giaume 2006). The consequences of these astrocytic-based calcium waves are only beginning to be understood, as some studies point to their role in neuromodulation (Charles 2005; Scemes and Giaume 2006), while others study point to their potential role in diseases such as epilepsy (Nadkarni and Jung 2003; Tashiro et al. 2002; Tian et al. 2005). Studies primarily implicate the participation of two mechanisms for astrocytic calcium waves: IP₃ diffusion through open gap junctions (Giaume and Venance 1998; Sanderson et al. 1994; Scemes 2000; Yamane et al. 2002), and the release of ATP resulting in the activation of P2 purinergic receptors in an autocrine/paracrine fashion (Cotrina et al. 2000; Cotrina et al. 1998; Guthrie et al. 1999; Venance et al. 1997). The interaction between these two mechanisms depends on developmental stage, brain region, and gap junction channel and/or purinergic receptor expression (Giaume and Venance 1998; Suadicani et al. 2004). Remarkably little, though, is known about how intercellular calcium waves are initiated and propagated under the mechanical conditions of TBI. Given the potential role that astrocytes can play in

neuronal signaling and the ability of calcium waves to spread long distances through the injured brain, the onset of calcium waves in astrocytes may play an important role in the pattern and severity of injury following TBI.

In addition to being a mediator of calcium wave communication in astrocytes, ATP can have other important effects on the injured brain. Several studies show that exogenous ATP is capable of initiating reactive gliosis in astrocytes (Abbracchio and Verderio 2006; Brambilla et al. 2002; Neary and Kang 2005). Moreover, application of ATP and P2 purinergic receptor agonists *in vitro* induce process stellation, proliferation, and up-regulation of GFAP, demonstrating that ATP can act as a pro-gliotic factor (Abbracchio et al. 1996; Bolego et al. 1997; Franke et al. 1999; Neary et al. 1996). ATP application also induces ERK phosphorylation, which has been associated with astrocyte gliosis in several models (Lenz et al. 2000; Munsch et al. 1998; Neary et al. 1999; Neary et al. 2003; Neary et al. 1998). In studies linking ATP and ERK activation in mechanically injured astrocytes, recent reports show that traumatic injury will activate ERK via both ionic (P2X) and metabotropic (P2Y) purine receptors (Neary et al. 2003), indicating the complex mechanisms that can be activated with a single physical stimulus.

In this study, we investigated how calcium waves propagate in astrocyte cultures after a rapid, transient strain that simulates mild TBI. We focused our investigation primarily on the mechanical penumbra – the region immediately adjacent to the area of stretch – since very little is known on how intercellular calcium signaling is regulated in this region after TBI *in vitro*. We found that calcium waves propagated from the injury into the penumbra after even the mildest strains, and that the mechanism of propagation

was dependent on the applied strain. Activation of P2 purinergic receptors by extracellular ATP was the primary contributor to calcium waves in the penumbra at all stretch levels, while gap junction communication significantly participated in propagating waves in the penumbra only after moderate strains. Evidence of activation of metabotropic glutamate receptors was detected after the highest strains. These data suggest that stretched astrocytes are capable of transmitting information about the severity of injury to the surrounding cells, allowing the surrounding, uninjured cells to modulate their responses depending on the level of strain experienced.

2.3 MATERIALS AND METHODS

2.3.1 Cell Culture

Pure cortical astrocyte cultures were generated from E18 Sprague-Dawley rat embryos (Charles River Laboratories). All procedures adhered strictly to the animal welfare guidelines established by the University of Pennsylvania's Institutional Animal Care and Use Committee. Embryos were removed from a pregnant rat anesthetized with CO₂ and euthanized by cervical dislocation. Brains were dissected from the embryos and the meninges were removed. The cortices were dissected and dissociated by incubating in Neurobasal media (Invitrogen) with trypsin (0.3mg/mL, Sigma) + DNase I (0.2mg/mL, Amersham Biosciences) at 37°C, 5% CO₂. Enzymatic activity was inhibited after 20 minutes by adding soybean trypsin inhibitor (.5mg/ml, Gibco). The tissue was mechanically disrupted by pipetting, then centrifuged for 5 minutes at 1000 rpm and resuspended in DMEM (Cambrex) + 5% FBS (Hyclone). Cells were filtered sequentially through a 60µm and 28µm Nitex Mesh (Cross Wire Cloth & Manufacturing Co.) and plated onto PLL-treated (Sigma) T75 tissue culture flasks (Fischer Scientific, Inc.) at a concentration of 1×10^5 cells/ml. Media was changed every 3-4 days.

At 13 days in vitro (DIV) cells were placed on an orbital shaker and shaken at 250 rpm overnight at 37°C, 5% CO₂ to remove loosely adherent cells. Flasks were rinsed with saline solution before adding 4 ml of trypsin/EDTA (0.25%, Invitrogen) for 2-3 minutes at 37°C, and then mechanically disrupted to dislodge the cell layer from the flask surface. DMEM + 5% FBS was added to inhibit enzymatic activity. The cells were centrifuged for 5 minutes at 1000 rpm and resuspended in DMEM + 5% FBS. The cell

suspension was diluted to 1×10^5 cells/ml and plated onto PLL-treated silicone-based elastic membranes (cured Sylgard 186:Sylgard 184 at a 7:4 mix, Dow Corning). Media was changed at 24 hours and then every 3-4 days until use at 13-14 DIV, at which point cultures had reached confluency. Cultures were determined to be >95% pure astrocytes by immunochemistry for GFAP (astrocytes), type-3 beta-tubulin (neurons), and CNPase (oligodendrocytes) counterstained with Hoechst 33342 (20 μ g/ml, Molecular Probes).

2.3.2 Cell Stretch

The mechanical injury model used in this study applied a rapid, transient strain to a 2 mm x 18 mm rectangular region of the astrocyte culture surface (Figure 2.1A). Past work showed the membrane strain causes a corresponding and proportional stretch of cells plated on the membrane (Lusardi et al. 2004). The culture region surrounding the region of stretch-injured cells – the “penumbra” – experiences no mechanical deformation (Lusardi et al. 2004). The duration (20ms) and magnitude of the strain (5-25%) were controlled to simulate mild traumatic brain injury (Shreiber et al. 1997). All confluent cultures were stretched once and either immediately used for calcium imaging or returned to the incubator. A fused-silica plate beneath the unstretched region of the culture allowed fluorescent imaging of the cytosolic calcium levels in the penumbra astrocytes. The silica plate did not interfere with the sensitivity of the calcium imaging as control experiments with ATP showed that fura-2 ratio increases were indistinguishable between the stretched and penumbra regions. Cell viability 24 hours after stretch was determined by adding propidium iodide (5 μ g/ml, Molecular Probes) and Hoechst 33342 for 15 minutes before fixing with 4% paraformaldehyde to measure dead/dying cells and

total cells, respectively. In a limited number of experiments, potential changes in cell membrane permeability to carboxyfluorescein immediately following stretch was measured as described in Geddes-Klein et al (2006) (Geddes-Klein et al. 2006).

2.3.3 Imaging

Intracellular free calcium was measured using the ratiometric calcium dye fura-2 AM (Molecular Probes). Cultures were rinsed twice with saline solution and incubated with 5 μ M fura-2 AM for 50 minutes in the dark at room temperature. Afterwards, the cultures were again rinsed with saline and incubated for 10 minutes in the dark at room temperature for ten minutes. Pharmacological agents were added during the second rinse. The cultures were then mounted onto the microscope and subjected to injury, as described above.

Fura-2 ratios were collected using a Hamamatsu C4742-98 camera and MetaFluor software (Universal Imaging, Inc.). Baseline fura-2 ratios were collected every three seconds for one minute prior to stretch. Cells were considered to be responding if the peak fura-2 ratio after stretch was greater than 50% higher than the average, pre-stretch baseline. For comparison, typical standard deviations in baseline prior to stretch were approximately 2-3% of the average. The distance calcium waves propagated into the penumbra was determined by measuring the distance from the edge of the stretched region to the farthest responding cell in the field of view within one minute after stretch. A typical calcium wave in the penumbra is shown in Figure 2.1C. For analysis, cells were grouped into regions 75 μ m wide, starting at the edge of the stretched region, as shown in Figure 2.1B.

2.3.4 Western Blots

To study ERK activation, astrocyte cultures were prepared and injured as described above and then returned to the incubator. At various time points (15 min, 30 min, 2 hr, and 6 hr) after stretch the astrocytes were lysed in the following manner. Cultures were rinsed twice with saline solution and the stretched and penumbra regions were separated. Ice cold lysis buffer (1mM EDTA, 150mM NaCl, 50mM Tris, 1 Complete Mini Protease Inhibitor Cocktail tablet (1 tablet/10mL, Roche Diagnostics), 1mM sodium orthovanadate) was added and the cells were scraped from the surface and mechanically disrupted. The cells were then centrifuged (10,000 rpm) for 15 minutes at 4°C and stored at -80°C. Protein concentration was determined using a DC Protein Assay Kit (Bio-Rad) according to the manufacturer's instructions.

For Western blotting, samples were thawed and heated to 75°C for 5 minutes after diluting 4:3 in NuPage LDS sample loading buffer (Invitrogen) and 3% β -mercaptoethanol. Equal quantities of protein (10 μ g) were added to 4-12% bis-tris gels (Invitrogen) and were resolved at 150V for 1.5 hours in 1x Running Buffer (Invitrogen). After gel electrophoresis, proteins were transferred onto polyvinylidene difluoride (PVDF) membranes (Invitrogen) for 12 hours at 10V in 1x Transfer Buffer (Invitrogen) containing 20% methanol. Membranes were blocked for 1 hr in a 5% dry milk solution containing 2mM Tris-HCl, 1.5mM NaCl, 0.1% Tween-20, and then incubated overnight at 4°C in primary antibody for phosphorylated ERK (1:500, clone 197G2, Cell Signaling Technology, Inc.). Membranes were then incubated for 2 hours at room temperature with horseradish peroxidase-conjugated anti-rabbit secondary (1:1000, Jackson Immuno-

Research). Enhanced chemiluminescence (Perkin Elmer) reagents were used to visualize the immunoreactivity on an X-ray film. Protein bands were quantified using Kodak 1D Image Analysis Software (Eastman Kodak Co.). The membranes were then stripped and re-probed using antibodies against ERK (Promega, 1:1000) and anti-rabbit secondary (1:3000), and then stripped and re-probed using antibodies against actin (Chemicon, 1:10,000)

2.3.5 Luciferin-luciferase Assay

Extracellular ATP was detected using the luciferin-luciferase reaction. Astrocytes were incubated in 0.5 mL of saline containing 140 μ g/ml firefly luciferase (L-1759, Sigma) and 100 μ g D-luciferin sodium salt (L-6882, Sigma). Luminescence detection was performed using a 40x objective attached to an upright microscope equipped with a photon counting intensified charge-coupled device camera (C2400-35). Photon counts were streamed to disk at a frequency of 30Hz and integrated after acquisition. Values reported are integrated counts per 3 seconds normalized to the average baseline values for the 15 seconds prior to injury.

2.3.6 Statistics

Data are reported as mean \pm standard error and analyzed by ANOVA followed by post-hoc analysis using Tukey's HSD test for unequal n. Fura data was transformed using a log transform to homogenize the variance. Data was considered significant at $p < 0.05$.

2.4 RESULTS

2.4.1 Mild stretch evokes intracellular free calcium increases in a subset of astrocytes

We first measured the intracellular free calcium response in the stretched region of cultures. An increase in intracellular calcium was detected after even the mildest stretch of 5%, leading to calcium increases of greater than 50% of pre-stretch baseline in $28 \pm 11\%$ of cells (mean \pm SE, Figure 2.2A), with an average fura-2 ratio after stretch of 1.4 ± 0.4 (Figure 2.2B). Increasing the strain to 15% led to $35 \pm 17\%$ of cells responding $> 50\%$ of baseline (Figure 2.2A), with an average fura-2 response of 2.9 ± 1.1 (Figure 2.2B). The highest strain of 25% evoked calcium responses in $46 \pm 22\%$ of cells (Figure 2.2A), with a fura-2 ratio of 1.6 ± 0.6 (Figure 2.2B). No significant change in viability was observed 24 hours after any stretch, as measured by propidium iodide uptake (data not shown). Likewise, no change in cell membrane permeability was detected immediately after stretch, based on measurement of carboxyfluorescein uptake immediately following stretch (data not shown) (Geddes-Klein et al. 2006). These data confirm that our mild stretch model can evoke a calcium response in stretched cells and that none of the stretch levels induce an immediate change in membrane permeability that could explain this increase in calcium. However, at all tested stretch levels there is a significant degree of heterogeneity in the response of these the stretched astrocytes, with a large number of cells exhibiting no calcium response to mild (5%) stretch.

2.4.2 Rapid stretch of astrocytes produces intercellular calcium waves in the penumbra

Given the variable levels of calcium response among cells in the stretched region it was surprising to observe that this stimulus resulted in robust calcium waves that quickly propagated outward into the penumbra. Waves were stimulated in the penumbra in 76% (25/33) of cultures that were subjected to a 5% stretch, while stretches of 15% and 25% stimulated calcium waves in 100% (28/28 and 24/24, respectively) of cultures. The percentage of cells responding in the wave depended on the magnitude of stretch and distance from the region of stretch. After a 5% stretch $59 \pm 8\%$ of cells within $75\mu\text{m}$ of the stretched region responded with an increase of fura-2 ratio $> 50\%$ of baseline, while $99.4 \pm 0.3\%$ and 100% of cells responded after a 15% or 25% stretch, respectively (Figure 2.3A). By comparison, less than 2% of astrocytes in control cultures had fura-2 ratio increases $> 50\%$ of baseline. The percentage of cells responding decreased with distance from the stretch region, with $44 \pm 8\%$ of cells responding in the farthest region ($375\mu\text{m}$) after 5%, $71 \pm 7\%$ after 15%, and $79 \pm 7\%$ after 25% (Figure 2.3A).

The peak calcium increase in the penumbra was proportional to the magnitude of the applied stretch. The peak fura-2 ratio in cells that responded to the calcium wave was lowest in cultures subjected to a 5% stretch, with an average of 2.7 ± 0.4 within $75\mu\text{m}$ of the penumbra. The fura-2 ratio dropped to 2.0 ± 0.3 at $150\mu\text{m}$, beyond which there was no further significant drop in fura-2 ratios (Figure 2.3B). In cultures subjected to a 15% stretch the peak fura ratio $75\mu\text{m}$ into the penumbra was 4.3 ± 0.5 , while 25% stretch resulted in a peak fura ratio of 4.9 ± 0.4 (Figure 2.3B). The fura ratio in 25%-stretched cultures remained significantly higher than in 5% or 15% cultures as the wave propagated farther into the penumbra. These data indicate that the calcium wave in the penumbra is

dependent on the magnitude of the applied strain but is not directly related to the calcium response in the stretched cells.

2.4.3 Extracellular ATP is released into the penumbra through an intracellular calcium-dependent mechanism

We next tested if mechanical injury led to an immediate increase in extracellular ATP in the penumbra region, given the role of ATP release in triggering intercellular waves from past studies (Scemes 2000). Imaging extracellular ATP in the penumbra with a luciferin-luciferase assay revealed an immediate increase ATP levels after 25% stretch. The concentration of extracellular ATP increased in untreated cultured for approximately one minute and then gradually decreased over the next 10 minutes (Figure 2.4). Similar to past reports, the rise in intracellular calcium was key for this stretch-induced ATP release, as pretreatment with BAPTA-AM (100 μ M) dramatically reduced the peak ATP concentration in the penumbra after stretch but did not alter the rise or recovery times (Figure 2.4). BAPTA-AM prevented calcium waves in the penumbra after stretch (data not shown), indicating that ATP release into the penumbra after stretch is transient and is largely dependent on intracellular calcium.

2.4.4 Stretch-induced calcium waves in the penumbra are inhibited by P2 receptor antagonists after 5% stretch

The addition of suramin (100 μ M, Sigma) and pyridoxalphosphate-6-azophenyl-2',4'-disulphonic acid (PPADS) (10 μ M, Sigma), antagonists of P2 purinergic receptors, as well as the extracellular ATP degrading enzyme apyrase (20U/mL, Sigma) were effective in nearly eliminating calcium waves in the penumbra of a 5% stretch experiment.

PPADS was most effective, significantly reducing the percentage of cells responding 75 μ m into the penumbra from $58 \pm 8\%$ in untreated cultures to $13 \pm 8\%$ (Figure 2.5A, $p < 0.01$). PPADS almost completely eliminated the propagation 375 μ m into the penumbra after one minute, reducing the percentage of cells responding to $0.35 \pm 0.35\%$ (Figure 2.5A, $p < 0.001$ compared to untreated stretched controls). Suramin and apyrase displayed a similar pattern of inhibition, but not to the same degree as PPADS, supporting the conclusion that this was a P2 receptor-related response.

Pretreatment with the gap junction blockers flufenamic acid (30 μ M, Sigma) and α -glycyrrhetinic acid (10 μ M, Sigma) caused a slight but statistically insignificant reduction in the percentage of cells responding to the calcium wave at every distance from the site of stretch. Flufenamic acid and α -glycyrrhetinic acid reduced the percentage at 75 μ m to $43 \pm 14\%$ and $46 \pm 14\%$, respectively, compared to $58 \pm 8\%$ in untreated cultures (Figure 2.5B). The treatments were similarly effective at 375 μ m, with flufenamic acid and α -glycyrrhetinic acid reducing the response to $19 \pm 11\%$ and $23 \pm 14\%$ compared to $44 \pm 8\%$ in controls. The reductions with gap junction blockers did not reach the level of significance at any distance from the region of stretch.

Applying flufenamic acid and PPADS together resulted in a significant reduction in the percentage of responding cells, with a nearly complete inhibition at distances greater than 150 μ m (Figure 2.5B). However, the results were not significantly different than using PPADS alone, indicating that gap junction communication contributes little to calcium waves after the lowest level of stretch and that calcium waves following 5% stretch are primarily mediated by extracellular ATP.

2.4.5 Gap junctions and P2 receptors participate in calcium wave propagation after 15% stretch

The mechanisms contributing to calcium waves in the penumbra were more complex after a 15% stretch-injury. Although suramin, apyrase, and PPADS each significantly reduced the percentage of responding cells at distance greater than 75 μ m from the region of stretch, a high percentage of responding cells was observed 150 μ m from the stretch. The most effective treatment, apyrase, reduced the percentage of responding cells from $99.4 \pm 0.3\%$ to $74 \pm 11\%$ at 75 μ m, and reduced the percentage from $71 \pm 7\%$ to $6 \pm 3\%$ at 375 μ m (Figure 2.6A). While apyrase produced a nearly complete block of the wave at distances greater than 300 μ m, there was significant calcium wave activity closer the region of stretch, suggesting that calcium waves were being propagated via a non-P2 receptor associated mechanism.

Flufenamic acid and α -glycyrrhetinic acid also reduced the calcium wave, reaching significance 375 μ m into the penumbra. Closer to the site of injury the effect was less pronounced, reducing the percentage of responding cells by 20-30% (Figure 2.6B). Combining flufenamic acid with PPADS was effective in almost completely inhibiting the calcium wave caused by a 15% stretch, and was more effective than PPADS or flufenamic acid alone, particularly closest to the stretched region (75 μ m and 150 μ m). PPADS alone resulted in a response of $71 \pm 11\%$ at 75 μ m, while flufenamic acid alone resulted in a response of $77 \pm 13\%$. When the two treatments were used together the response rate was reduced to $32 \pm 11\%$ (Figure 2.6B, $p < 0.001$ compared to untreated). We conclude that the double block produces a nearly complete inhibition of

the calcium wave, indicating that both extracellular ATP and gap junctions are responsible for transmitting the wave after 15% stretch.

2.4.6 Calcium wave propagation after 25% stretch is not dependent on gap junction pathway

Calcium waves were detected in the penumbra of every culture (24/24) subjected to a 25% stretch, as noted above. Based on the observations made after 5% and 15% stretches, we assumed that the mechanism of action at this stretch level would involve gap junctions and extracellular ATP. Accordingly, apyrase, suramin, and PPADS restricted the propagation of calcium waves after stretch to approximately 225 μ m into the penumbra, while untreated cultures had waves propagating beyond 375 μ m (Figure 2.7A). None of these three treatments had a significant effect at 75 μ m, with PPADS resulting in $99 \pm 1\%$ of cells responding, suramin resulting in $79 \pm 11\%$, and apyrase resulting in $88 \pm 11\%$. However, all were significant different from untreated cultures at 225 μ m from the site of stretch, reducing the percentage of responding cells from $90 \pm 4\%$ in untreated cultures to $42 \pm 9\%$, $40 \pm 15\%$, and $56 \pm 14\%$ in PPADS, suramin, and apyrase-treated cultures, respectively (Figure 2.7A). The wave was further reduced at 300 μ m and 375 μ m, bringing the percentage of responding cells below 20%, approximately a 75% reduction from untreated cultures.

The gap junction blockers flufenamic acid and α -glycyrrhetinic acid were completely ineffective in reducing wave propagation after a 25% stretch, unlike what was observed at lower stretch magnitudes. Figure 2.7B shows that the addition of these two agents resulted in essentially no change in propagation patterns compared to controls.

The average peak fura ratio in responding cells was also not significantly different than controls (data not shown), suggesting that this pathway does not significantly contribute to calcium waves that are initiated by a 25% stretch. The combined treatment of PPADS and flufenamic acid reduced the percentage of cells close to the region of stretch when compared to PPADS alone, but there was no significant difference between these two treatment groups beyond 150 μ m.

2.4.7 Metabotropic glutamate receptors participate in propagating calcium waves after a 25% stretch

Several investigations show a role for released glutamate in the transmission of astrocytic calcium waves (Charles et al. 1991; Cornell-Bell and Finkbeiner 1991; Innocenti et al. 2000; Yoshida et al. 2005), as well as ATP-induced glutamate release (Domercq et al. 2006; Fellin et al. 2006b; Jeremic et al. 2001). To determine if extracellular glutamate participated in transmitting stretch-induced calcium waves after a 25% stretch, we added antagonists of metabotropic glutamate receptors: LY367385 (100 μ M, Sigma), an mGluR1 antagonist, and 2-methyl-6-(phenylethynyl)-pyridine (MPEP, Sigma) (50 μ M), an mGluR5 antagonist. Treatment with MPEP and LY367385 or with MPEP, LY367385, and flufenamic acid had no effect in reducing the wave propagation, with >90% of cells responding at every distance from the region of injury (Figure 2.8A). However, using PPADS, MPEP, LY367385, and flufenamic acid together reduced the propagation of calcium waves to $2 \pm 2\%$ of cells at 375 μ m (Figure 2.8A). The four agents consistently resulted in lower responses than seen with the addition of

PPADS and flufenamic acid alone. This suggests that glutamate may be playing a partial role in calcium wave propagation.

More strikingly, the four agents together reduced the peak fura ratio significantly lower than any other treatment. Figure 2.8B shows the fura-2 ratio of cells responding to a calcium wave. MPEP and LY367385 alone had no significant effect on the peak fura-2 ratio, and flufenamic acid and PPADS had a moderate effect in reducing intracellular calcium increases. The four agents used together reduced the peak fura ratio in responding cells from 4.9 ± 0.4 75 μ m into the penumbra to 0.6 ± 0.1 . The results were nearly as pronounced at every other distance. Blocking the metabotropic glutamate receptors severely inhibited intracellular calcium increase, strongly suggesting that glutamate release is evoked from the calcium wave after a 25% stretch. However, these receptors apparently are much less involved in transmitting the wave from one cell to the next.

2.4.8 Calcium waves do not trigger ERK activation in the penumbra of a stretch-induced injury

An increase in the ratio of phosphorylated ERK to total ERK (pERK:ERK) has been reported after stretch injury of astrocytes (Mandell et al. 2001; Neary et al. 2003), as well as after stimulation with extracellular ATP (Brambilla et al. 2002). Given that ATP-mediated signaling contributes to calcium signaling in the penumbra at all stretch levels, we next considered if the ATP-induced calcium transients in the penumbra region also caused a corresponding increase in ERK activation, as suggested from past studies. We first measured ERK activation in the stretched astrocytes and, similar to other

investigators, we found significant increases in pERK in stretched astrocytes 15 minutes after a 15% or 25% stretch, but not after a 5% stretch (Figure 2.9B). However, there was no significant increase in pERK levels in the penumbra of the stretch region after any stretch level (Figure 2.9B). Westerns for pERK at later time points (30 min, 2 hr, 6 hr) showed no significant change from control in the stretched region or the penumbra at any stretch magnitude (data not shown).

2.5 DISCUSSION

In this study, we investigated how stretch-injured cultured astrocytes communicate to the surrounding, unstretched region – the mechanical penumbra – via calcium waves, and how the mechanism of wave propagation is dependent on strain magnitude. We determined that increases in intracellular calcium were more pronounced in the mechanical penumbra compared to astrocytes from the region of mechanical injury. In addition, we showed that ATP mediated signaling accounted for at least a portion of the intercellular wave in the penumbra region at all stretch levels. The complete set of mechanisms regulating the calcium wave in the penumbra differed with the magnitude of initial mechanical injury and included both gap junction communication and glutamate receptor activation at higher levels of stretch. Despite the common role of ATP on intercellular calcium signaling at all stretch levels tested, one common consequence of ATP stimulation – rapid ERK activation - was not consistently increased in the penumbra at the two highest stretch levels. In all, these data demonstrate differences in both intracellular and intercellular signaling that can occur between the zone of mechanical injury and the surrounding mechanical penumbra, even at mild levels of stretch that do not cause astrocytic death.

We used two outcome measures to determine the robustness of the calcium response across the two regions studied: percentage of cells displaying an increase in intracellular calcium >50% of baseline and the relative increase in intracellular calcium in responding cells as measured by the change in fura-2 ratio. Using strain magnitudes that do not cause cell death, we found that stretched astrocytes undergo a strain-dependent

increase in intracellular calcium concentration, as has been reported by others

(Rzagalinski et al. 1998). However, less than half of stretched cells showed an increase in intracellular calcium $> 50\%$ of the pre-stretch levels, and this fraction of cells did not significantly increase at the moderate or highest stretch levels. Given this finding, we were surprised to find calcium waves in the penumbra after every stretch at or above 15%. Even minor perturbation of the astrocytes, represented by our 5% strain, triggered robust calcium signaling in a large number of penumbra cells. These data imply astrocytes in the penumbra of a stretch injury can be much more responsive than the injured astrocytes at non-lethal stretch levels.

A potential explanation for the difference between the stretched astrocytes and the penumbra astrocytes is that cytoskeletal disruption during rapid stretch disturbs calcium signaling pathways by separating receptors on the plasma membrane from proximity to calcium release sites on the endoplasmic reticulum or by separating the receptors from downstream messengers. Past studies show that G-protein coupled receptors (GPCRs), such as opioid, dopamine, adenosine, and insulin receptors, are attached to the actin cytoskeleton through linkage proteins (Burgueno et al. 2003; He et al. 2003; Lin et al. 2001; Onoprishvili et al. 2003). As a result, it is possible that GPCRs undergo mechanically-induced alterations in function after stretch. Treatment with cytochalasin D to disassemble the actin cytoskeleton in cultured astrocytes nearly eliminates calcium wave propagation after mechanical stimulation (Cotrina et al. 1998), and prevents a calcium increase after ATP application, mainly by reducing the coupling between intracellular calcium stores and calcium entry (Sergeeva et al. 2000). Likewise, work in

pancreatic acinar cells has shown that the IP₃ receptor is linked to actin and disruption of this linkage prevents local calcium spikes (Turvey et al. 2005). The gap junction channel may also be mechanically altered, since gap junction communication can be inhibited through cytoskeletal disruption (Johnson et al. 2002). Interestingly, the threshold for the collapse of actin-based polymeric gels subjected to mechanical strain is approximately 10-15%, similar to stretch levels used in our study, although this threshold can change if the gel is polymerized with different actin crosslinking proteins (Janmey et al. 1994; Janmey et al. 1990; Janmey et al. 1988; MacKintosh et al. 1995). These results, along with our own, point to a mechanism that might explain the relative lack of calcium responsiveness in stretched astrocytes compared to the robust response in the penumbra.

With the ability to precisely control the level of mechanical injury, we found the mechanism of calcium wave propagation into the penumbra became more complex as the strain magnitude increased. To our knowledge, this is the first evidence of a strain-sensitive progression of intercellular waves in astrocytes. One common mechanism for the calcium waves at all strains was extracellular ATP, as evidenced by the ability of PPADS, suramin, and apyrase to significantly attenuate wave spreading at all stretch magnitudes. These data are consistent with a number of previous studies showing the role of ATP on intercellular waves originating from the stimulation of a single astrocyte (Cotrina et al. 2000; Cotrina et al. 1998; Guthrie et al. 1999; Venance et al. 1997). Gap junctions played an unusual role in our experiments, providing the most significant effect at moderate strain levels and very little contribution at the lowest and highest stretch level tested. The observed mechanical sensitivity of the gap junction mechanism may explain

why gap junction communication is observed in some intercellular calcium wave studies (Giaume and Venance 1998; Sanderson et al. 1994; Scemes 2000; Suadicani et al. 2004; Yamane et al. 2002) and not in others (Bennett et al. 2006; Cotrina et al. 2000; Guthrie et al. 1999; Hassinger et al. 1996; Venance et al. 1997). Past reports indicate gap junctions can be regulated by ATP or through the activity of other messengers (Meme et al. 2004), and our data showing the presence of ATP release at the highest level of stretch provides at least one mechanism for the reduction in the role of gap junctions at this stretch level. Moreover, the permeability of gap junctions can be inhibited by very high levels of intracellular calcium (Kumar and Gilula 1996), and our data show that the highest levels of intracellular calcium appeared in the penumbra at the highest level of stretch (Scemes et al. 2000). Less clear, though, is the significance of attenuating the role of gap junctions at the highest stretch levels. Certainly, the interaction of gap junctions and P2 receptors in astrocytes is noted in past work (Scemes et al. 2000; Suadicani et al. 2004; Yamane et al. 2002), however, the significance of this interaction has not been investigated. Some processes are thought to be regulated largely by gap junction communication in astrocytes, such as ion buffering and intercellular diffusion of small signaling molecules like cAMP and IP₃ (Loewenstein 1981). The role of astrocytic gap junction communication after traumatic or ischemic brain injury is only beginning to be understood, as some studies point to the potential protective role that the gap junctions can play in recovery while other studies observe less favorable outcomes (Farahani et al. 2005; Lin et al. 1998; Perez Velazquez et al. 2006). Our work points to the possible complexity in the astrocytic response after mechanical injury, where the factors that

control intercellular waves can be regulated by the initial severity of mechanical injury.

This variable signaling mechanism would help prevent a pathological response in the brain to normal, physiological strains and allows for the possibility of subtle pharmacological interventions to prevent only pathological wave progression after injury.

We considered one functional consequence of mechanical injury to astrocytes – ERK activation - that is a potential link to the onset of glial reactivity. Other investigators have detected ERK activation in astrocytes following stretch and/or ATP application (Abbracchio et al. 1996; Bolego et al. 1997; Franke et al. 1999; Lenz et al. 2000; Munsch et al. 1998; Neary and Norenberg 1992; Neary et al. 1996) , and our data from astrocytes in the stretched region are generally consistent with these past studies. With the role of ATP in producing ERK activation well established from previous work, it was surprising to observe no ERK activation in the penumbra at the higher stretch levels. The absence of ERK activation in the penumbra occurred despite large increases in intracellular calcium in this region following stretch, suggesting an uncoupling of these two events at these stretch levels. It has been shown that ERK activation in astrocytes can be produced through calcium-dependent and calcium-independent pathways, both of which can be activated by the application of ATP (Neary et al. 1999; Neary et al. 2003). The question from our data is why extracellular ATP fails to produce ERK activation in the penumbra in our model. One possibility is that other released factors are countering or inhibiting the ERK pathway, but this remains to be shown. Another possibility is that the local ATP concentration is too low to trigger ERK activation. However, this seems unlikely given the strong calcium propagation seen in these cultures. Nevertheless, our data show that

ATP-induced calcium waves are not sufficient stimuli to produce ERK activation in our cultured astrocyte model.

In all, the complex regulation of astrocytic calcium waves after injury suggest there may be several potential therapeutic targets that can modulate these waves, with the long term goal of improving outcome after TBI. Of note is recent work showing the ability of astrocytic calcium to trigger glutamate release from astrocytes, in turn activating extrasynaptic NMDA receptors on neurons (Fellin et al. 2004). The potential interplay between astrocyte signaling and neuronal fate after TBI is relatively unexplored, and our findings suggest at least one mechanism in which astrocytes may mediate significant changes to neuronal function in areas otherwise isolated from the mechanical injury. Further work is warranted to investigate how astrocytic calcium waves after TBI affect the ultimate fate of astrocytes, neurons, and other cell types in the affected regions, and whether interventions to prevent the spread of calcium waves would be beneficial for long-term recovery.

In conclusion, our results demonstrate that astrocytes can alter the mechanism of calcium wave production and spread in response to different levels of mechanical strain. The production of robust calcium waves in the penumbra of the injury is largely independent of the intracellular calcium increase in the stretched region. Extracellular ATP is the dominant mechanism of wave propagation at all strain magnitudes, while the involvement of gap junctions and glutamate was observed at the higher levels of stretch. Despite the widespread increase in calcium observed in the penumbra, there is no corresponding increase in ERK activation. The increasing complexity of the calcium

wave suggests that astrocytes are communicating information about the severity of injury to the penumbra, and this may have implications for pharmacological interventions.

Further work is needed to define the longer term effects of the calcium wave after injury and how calcium activation relates to astrocyte reactivity and neuronal dysfunction.

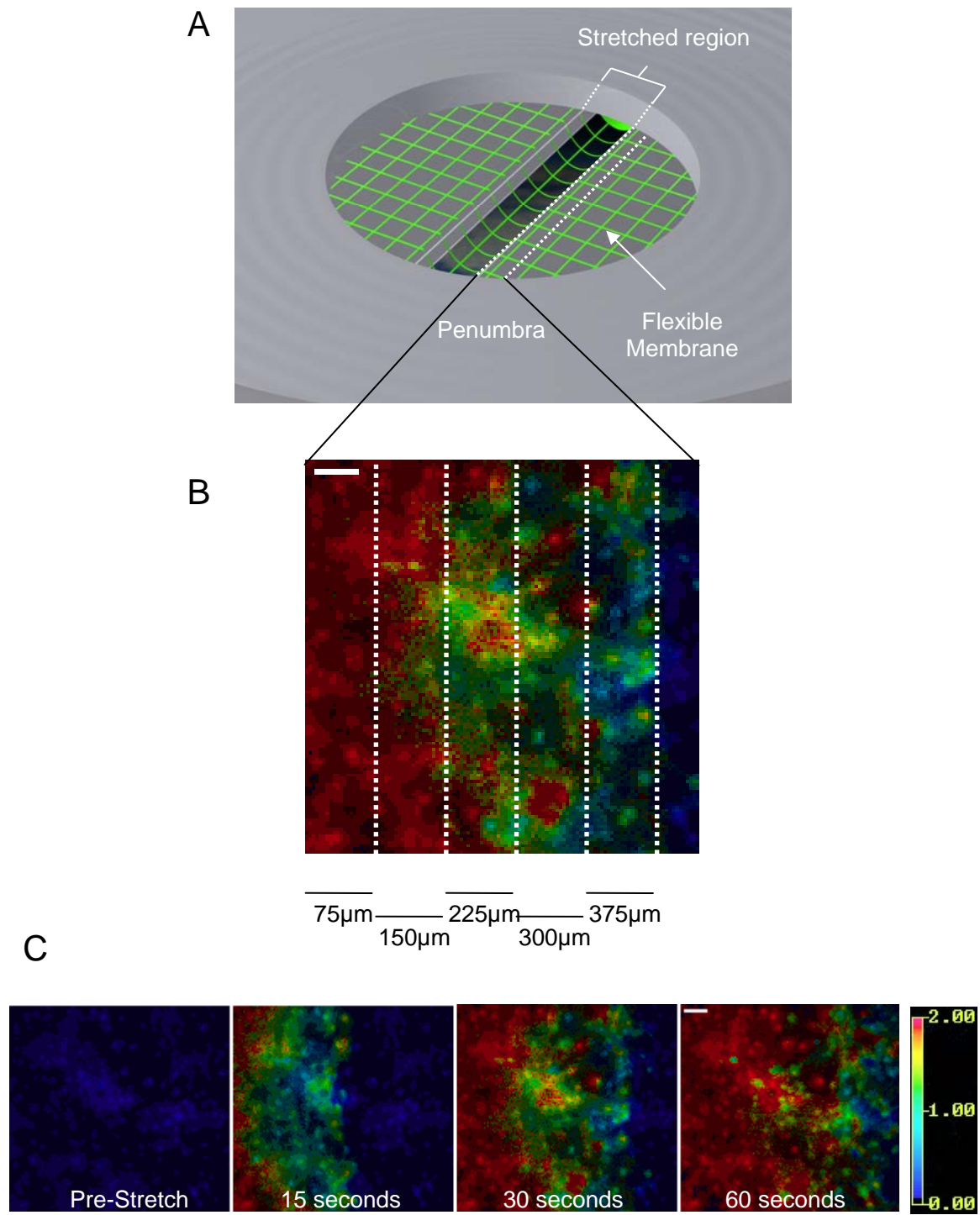


Figure 2.1 (previous page). A: Astrocytes were cultured on transparent elastic membranes. An air pressure pulse was delivered to the culture surface, deflecting the membrane downward. A fused silica plate beneath part of the culture restricted the region of stretch to a 2 mm x 18 mm region. The membrane strain produced by such geometry is uniaxial and nearly uniform throughout the stretched region; the adjacent membrane areas are unstretched. The penumbra was defined as the region immediately adjacent to the stretched region. B: Astrocytes were labeled with fura-2 AM to detect calcium waves propagating from the stretched region into the penumbra. For analysis, cells in the penumbra were grouped into regions 75 μ m wide, as shown. Scale bar = 50 μ m. C: The propagation of a calcium wave in the penumbra after a 15% stretch, measured by fura-2. Calcium waves typically advanced through the field of view in less than 1 minute. Scale bar = 50 μ m. Colorimetric scale bar represents fura-2 ratio (340/380).

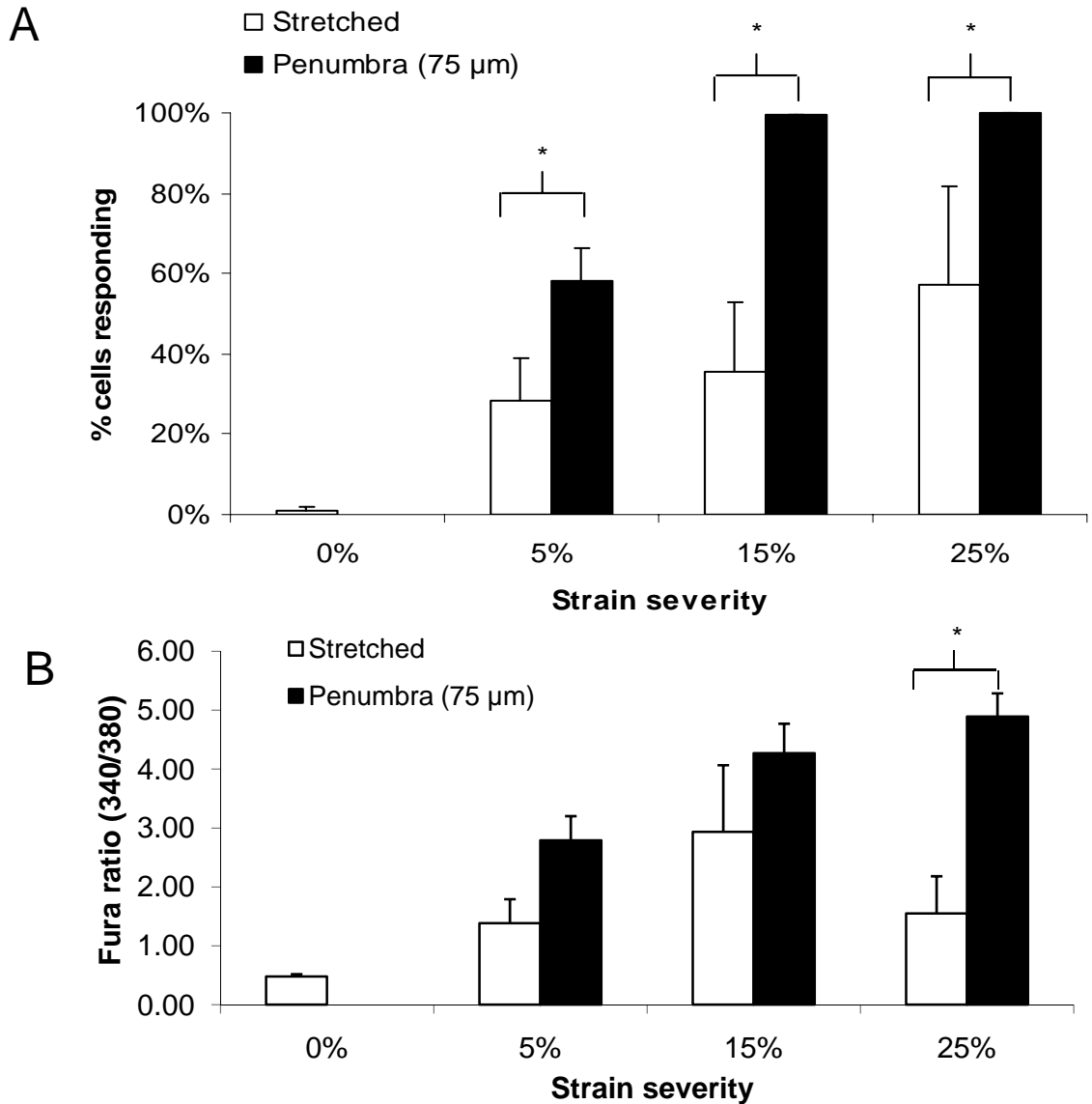


Figure 2.2. Astrocytes in the mechanical penumbra show more pronounced intracellular calcium increases than stretched astrocytes. **A:** After rapid stretch, intracellular free calcium in stretched astrocytes and penumbra astrocytes was measured for at least 1 minute using fura-2. The probability of a calcium increase $>50\%$ above baseline in an individual cell was significantly higher in the penumbra than in the region of stretch. In the stretched region, $28 \pm 11\%$, $36 \pm 17\%$, and $46 \pm 22\%$ of cells exhibited an intracellular calcium increase after a 5%, 15%, or 25% stretch, respectively, compared to $58 \pm 8\%$, $99.4 \pm 0.3\%$, and 100% of cells within $75\mu\text{m}$ of injury. (Mean \pm SE) * = $p < 0.001$. **B:** Peak intracellular calcium increases in stretched astrocytes and astrocytes in the penumbra, shown as changes in the fura-2 ratio. The average intracellular calcium level was lower in stretched cells than in cells in the penumbra that were involved in a calcium wave. $p < 0.05$.

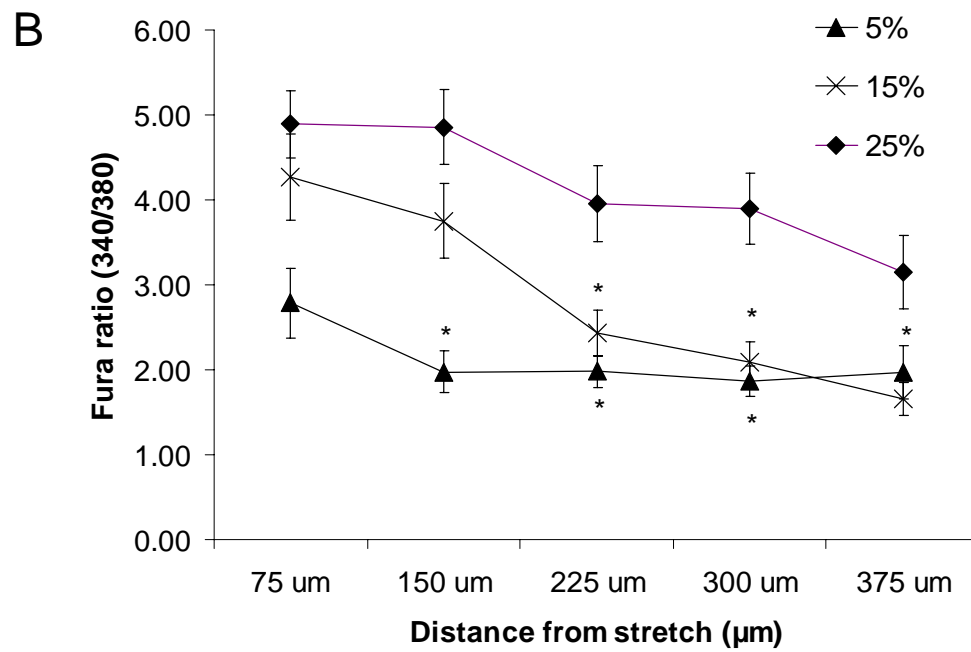
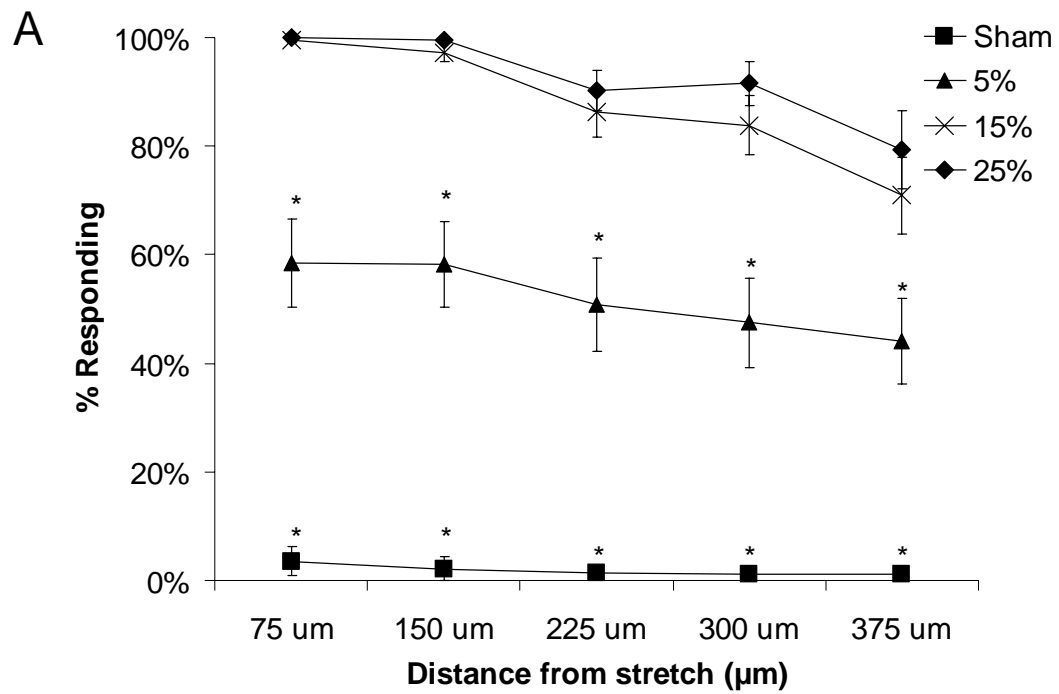


Figure 2.3 (previous page). A: Within one minute after a 15% or 25% stretch, 100% of astrocytes in the first 75 μ m of the penumbra showed calcium increases >50% of baseline. The percentage of responding cells 375 μ m into the penumbra was $71 \pm 7\%$ after a 15% stretch, and $79 \pm 7\%$ after a 25% stretch. In comparison, a stretch of 5% caused a response in $58 \pm 8\%$ of cells in the 75 μ m region, which decreased to $44 \pm 8\%$ in the 375 μ m region. (n = 13-33 cultures for each group). * = $p < 0.01$ compared to 25% stretched cultures. B: The fura-2 ratio in responding cells decreased with distance from the site of stretch. The cells in a calcium wave after a 25% stretch maintained a higher calcium level as a function of distance than cells after a 5% or 15% stretch. The fura-2 ratio in responding cells after a 5% stretch stabilized at approximately 2.0. * = $p < 0.01$ compared to 25%.

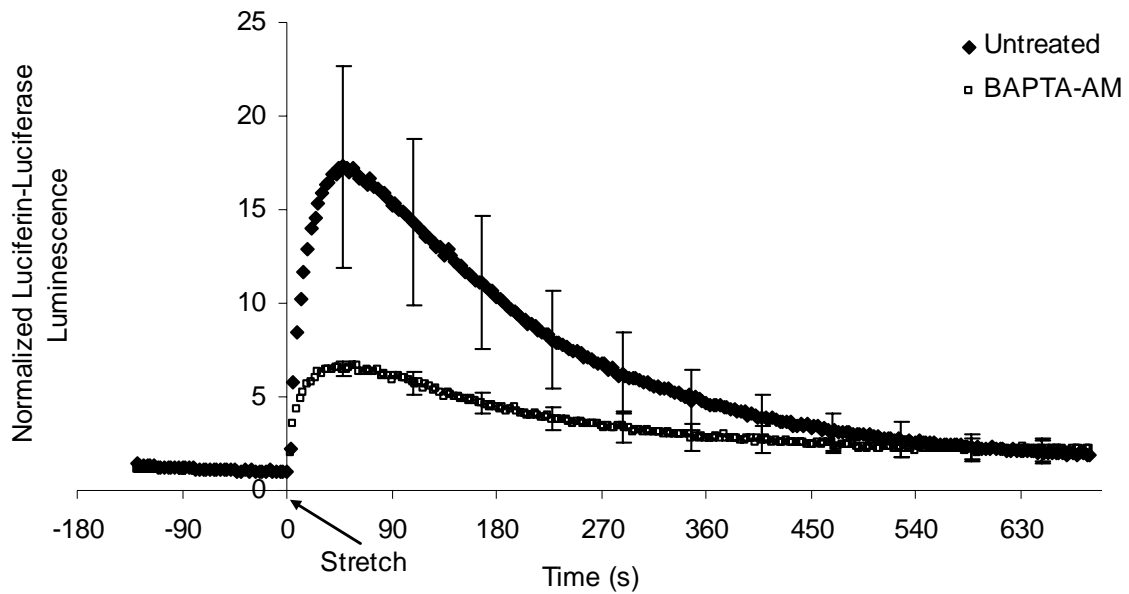


Figure 2.4. Extracellular ATP in the penumbra after 25% stretch was measured using a luciferin-luciferase assay. Immediately after stretch there was a sharp increase in extracellular ATP for the first minute followed by a gradual decrease towards baseline levels over the course of the next 10 minutes. Treatment with the calcium chelator BAPTA-AM greatly reduced the peak level of extracellular ATP in the penumbra, although the peak was still higher than pre-stretch levels. These data confirm the release and diffusion of ATP after stretch, primarily through a calcium-dependent release mechanism.

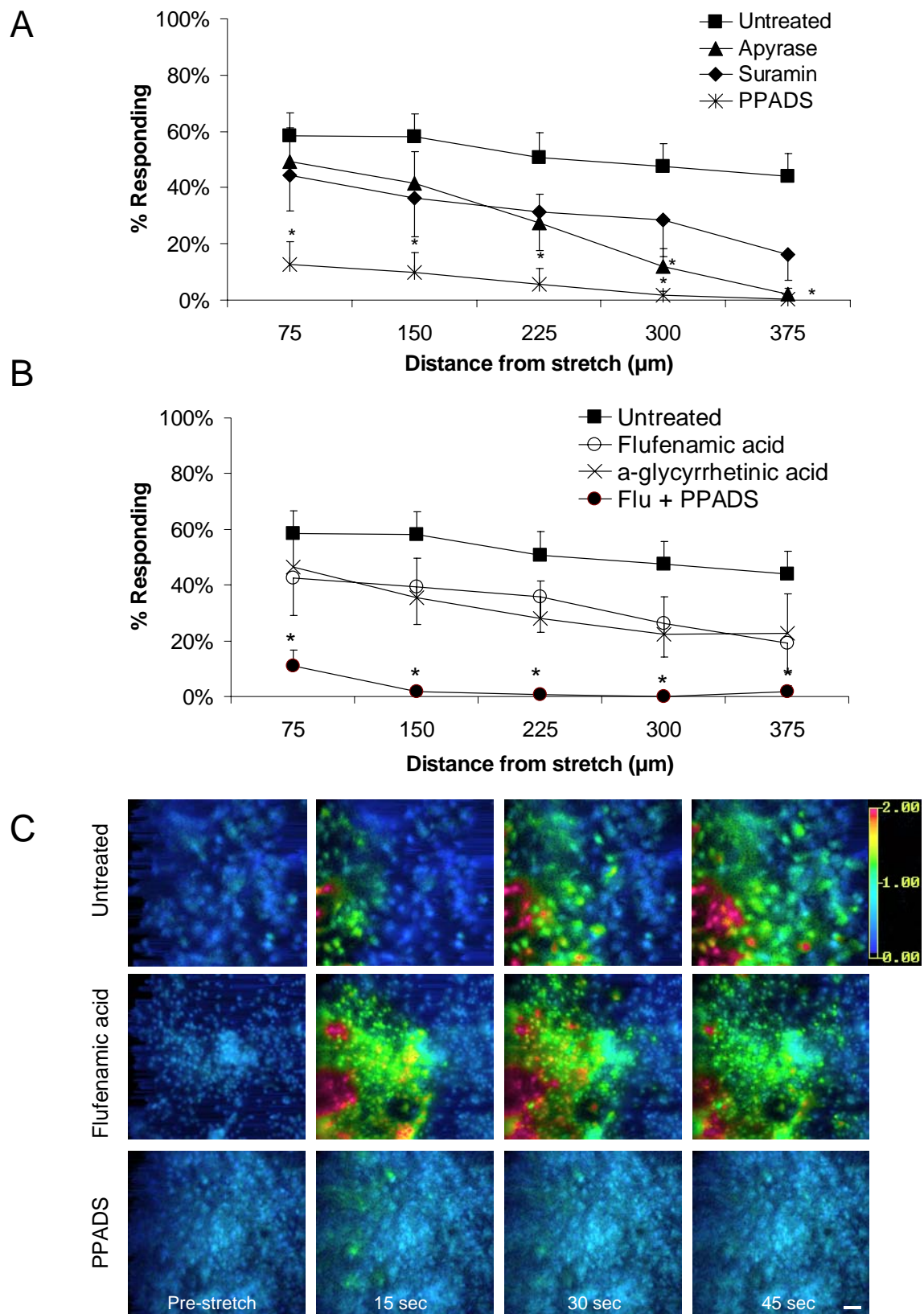


Figure 2.5 (previous page). Calcium waves following mild (5%) mechanical stretch are mediated primarily by P2 receptor activity. A: Apyrase (20U/ml), an extracellular ATPase, and suramin (100 μ M), a P2 receptor antagonist, partially inhibited the propagation of calcium waves, reducing the percentage of responding cells (>50% increase from baseline calcium) from $58\pm 8\%$ in the 75 μ m region in untreated cultures to $49\pm 12\%$ and $44\pm 13\%$, respectively. PPADS (10 μ M), a P2 receptor antagonist, was much more effective, reducing the percentage of responding cells to $13\pm 8\%$ at 75 μ m and completely blocking the propagation of calcium waves beyond 300 μ m. B: Gap junction blockers flufenamic acid (30 μ M) and α -glycyrrhetinic acid (10 μ M) had no statistically significant effect on calcium wave propagation, although a slight reduction in cell response rate was observed. PPADS and flufenamic acid used together severely inhibited calcium wave propagation, reducing the response in the 75 μ m region to $8\pm 5\%$. However, the double block was not significantly different than PPADS alone. C. Representative images of calcium waves in the penumbra of a stretched region. The region of stretch was immediately to the left of the image. Calcium waves were clearly evident in untreated and flufenamic acid-treated cultures at 15 seconds post-stretch, while PPADS-treated cultures showed less evidence of wave initiation and propagation. The wave propagated through the field of view by one minute post-stretch in untreated and flufenamic acid treated cultures but not typically in PPADS-treated cultures. * = $p < 0.05$ compared to untreated cultures. Scale bar = 50 μ m. Colorimetric scale bar represents fura-2 ratio.

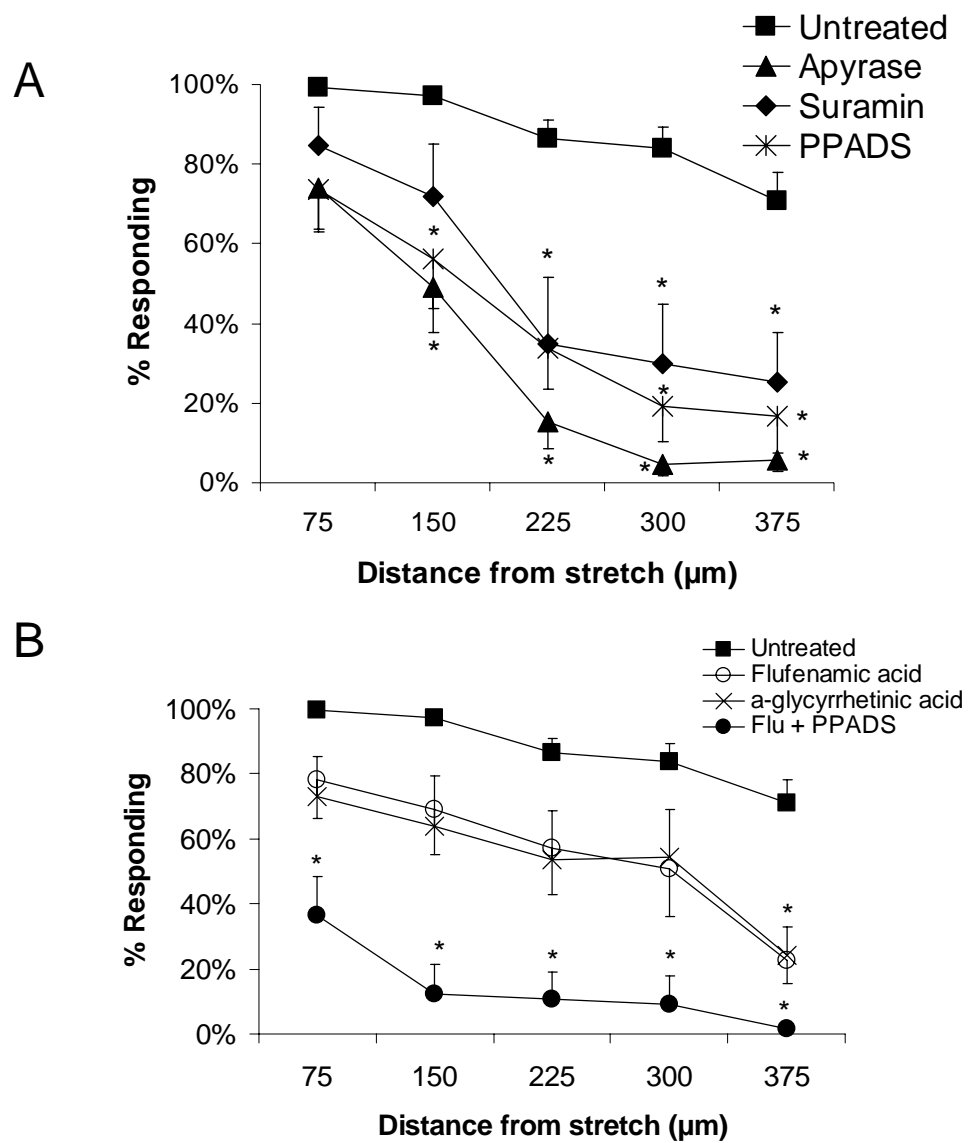


Figure 2.6 (previous page). Calcium waves following a moderate (15%) stretch were inhibited by blocking gap junctions and P2 receptors simultaneously. A: Calcium waves produced by a 15% stretch could not be completely inhibited by P2 receptor antagonists or apyrase alone, although the treatments did significantly reduced the percentage of cells responding to the wave as it propagated away from the region of stretch. In untreated cultures, 100% of penumbra cells responded 75 μ m from the stretch after one minute, while apyrase, suramin, and PPADS reduced the response rate to 74 \pm 10%, 80 \pm 11%, and 71 \pm 11%, respectively. The response at 375 μ m into the penumbra was reduced from 71 \pm 7% in untreated cultures to 6 \pm 3%, 25 \pm 13%, and 17 \pm 9% by apyrase, suramin, and PPADS, respectively. B: The gap junction blockers flufenamic acid and α -glycyrrhetinic acid also reduced the response rate, reaching a level of significance at 375 μ m. At 75 μ m, flufenamic acid reduced the response rate to 78 \pm 12% and α -glycyrrhetinic acid reduced the rate to 73 \pm 12%. At 375 μ m, flufenamic acid reduced the rate to 23 \pm 7% and α -glycyrrhetinic acid reduced the rate to 24 \pm 9%, both of which were significantly lower than controls. Application of PPADS and flufenamic acid together produced an additive block of the calcium wave, reducing the response rate at 75 μ m to 36 \pm 12% and nearly eliminating propagation into the 300 μ m and 375 μ m regions (9 \pm 9% and 1 \pm 1% of cells responding). * = p<0.05 compared to untreated cultures.

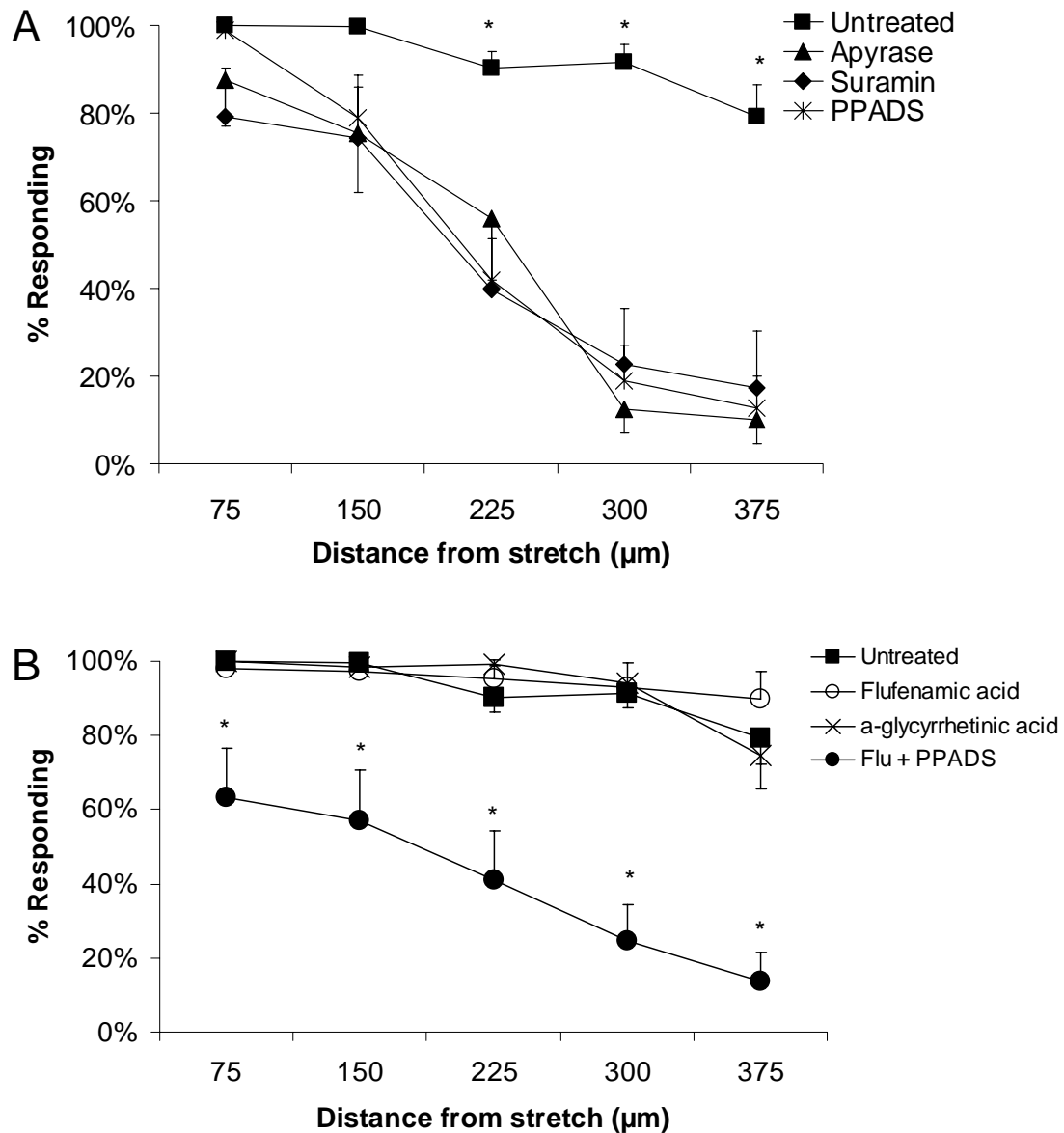


Figure 2.7. Following the highest level of mechanical stretch (25%) P2 receptor antagonists attenuated but did not eliminate calcium waves in astrocytes. A: P2 receptor antagonists significantly reduced the percentage of cells responding to a 25% stretch-induced calcium wave at distances greater than 225μm from the area of stretch. Apyrase, suramin, and PPADS were equally effective in reducing the cellular response to 10-20% of cells at 375μm, compared to 79±7% in untreated cultures. * = $p < 0.001$ compared to all three treated groups. B: Flufenamic acid and α-glycyrrhetinic acid were completely ineffective in reducing the propagation of calcium waves after a 25% stretch. The combination of flufenamic acid and PPADS significantly reduced the percentage of cells responding at every distance, but was only significantly different from using PPADS alone at 75μm. * = $p < 0.001$ compared to untreated cultures.

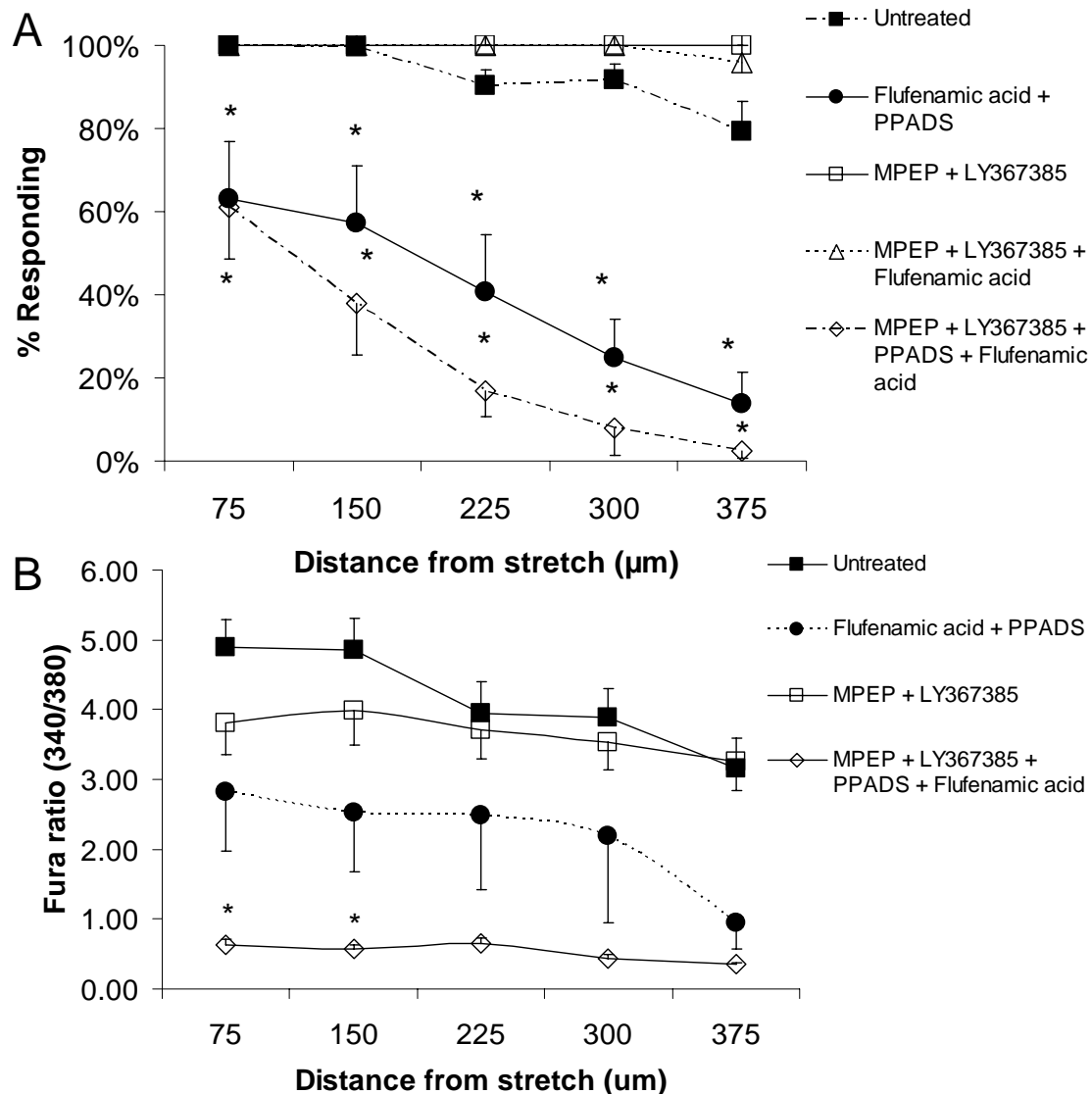


Figure 2.8. Following 25% stretch, metabotropic glutamate receptor antagonists significantly attenuated intracellular calcium increase within the mechanical penumbra, but had less effect on the wave propagation dynamics. A: LY367385, an mGluR1 antagonist, and MPEP, an mGluR5 antagonist, had no effect on the percentage of cells responding to the calcium wave after a 25% stretch, compared to untreated cultures. When LY367385 and MPEP were added to media containing PPADS and flufenamic acid, there was a slight but insignificant reduction in the percentage of cells responding to the wave compared to PPADS and flufenamic acid alone. B. The addition of LY367385 and MPEP to media containing PPADS and flufenamic acid had a profound effect on the peak fura-2 ratio of cells responding in the calcium wave at every distance from the injury region. LY367385 and MPEP alone had no significant effect, while PPADS and flufenamic acid had a moderate effect. * = $p < 0.05$ compared to untreated controls.

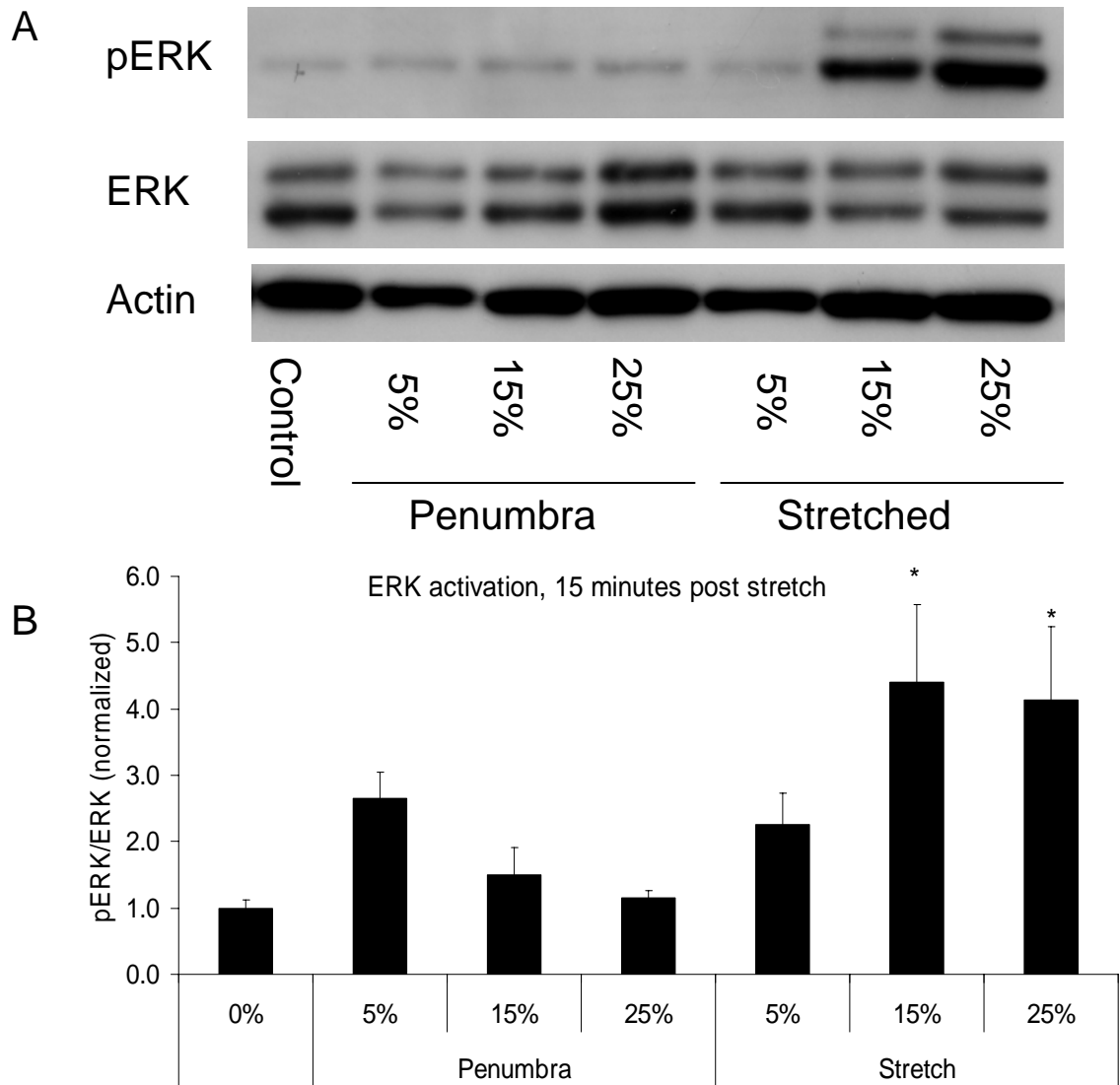


Figure 2.9. Calcium waves did not initiate ERK activation. A: Representative Western blots of ERK and phosphorylated ERK (pERK) 15 minutes following a stretch-induced injury. No elevation in pERK was observed in the penumbra after 15 minutes. B: Quantification of pERK/ERK ratios 15 minutes after stretch. Astrocytes showed a significant increase in pERK/ERK ratios at 15 minutes following a 15% or 25% stretch. Despite robust calcium wave propagation into the penumbra, there was no corresponding significant pERK activation. * = $p < 0.05$.

Chapter 3: Mechanical Properties of Cultured Rat Cortical Astrocytes after Stretch-induced Injury

3.1 ABSTRACT

This study evaluated the change in the mechanical properties of cultured cortical astrocytes after an in vitro model of traumatic brain injury (TBI) that induced characteristics of reactive gliosis. In injured cultures there was a significant increase in GFAP immunoreactivity 24 hours following a rapid, transient 15% strain. In these same cultures, the astrocytes in the surrounding region – the “mechanical penumbra” – also exhibited increased GFAP immunoreactivity compared to naïve cultures. Correlated with these changes in GFAP was a general softening of the non-nuclear regions of the astrocytes, both in the injured and penumbra cells, as measured by atomic force microscopy (AFM). The apparent Young’s modulus in naïve cultures was observed to be $57.7 \pm 5.8\text{kPa}$ in non-nuclear regions of naïve cultures, while 24 hours after injury the modulus was observed to be $26.4 \pm 4.9\text{kPa}$ in the same region of injured cells. In the penumbra, the modulus was $23.7 \pm 3.6\text{kPa}$ in non-nuclear regions of the cells. Indentations in regions above the cell nucleus resulted in a lower modulus ($22.7 \pm 5.8\text{kPa}$) than seen in non-nuclear regions in naïve cultures. There was no clear pattern of softening or stiffening after injury compared to naïve astrocytes when the stiffness was measured above the nucleus. Since neuronal cells generally prefer softer substrates for growth and neurite extension, these findings may indicate that the mechanical characteristics of reactive astrocytes are favorable for neuronal recovery after TBI.

3.2 INTRODUCTION

In vivo, focal traumatic brain injury (TBI) often results in reactive gliosis in surrounding astrocytes, which is a process that involves proliferation, increased process length, and upregulation of GFAP, an intermediate filament protein (Pekny and Nilsson 2005). A common element of these changes is that they involve a significant degree of cytoskeletal rearrangement. Studies have shown that changes in the intermediate filament network can also trigger the reorganization of the microtubule and actin microfilament networks (Chang and Goldman 2004). Since it has been reported that viscoelastic properties of cells are primarily determined by the microfilament and, to a lesser extent, the intermediate filament elements of the cytoskeleton (Trickey et al. 2004), we suspect that reactive gliosis may have implications for the mechanical properties of astrocytes.

In vitro, astrocyte monolayers provide a favorable environment for neurite outgrowth and neuronal attachment (Powell et al. 1997). In the traumatically injured brain, however, reactive astrocytes can form a glial scar that prevents neurites from regrowing through the injured region (Pekny and Nilsson 2005). Recently, a greater appreciation has developed for the importance of substrate stiffness for cell attachment, motility, and process extension, especially in neuronal cells (Balgude et al. 2001; Lo et al. 2000; Pelham and Wang 1997; Wang et al. 2001). Unlike astrocytes, which grow best on harder substrates (Georges et al. 2006), neurons prefer soft substrates, with neurite branching decreasing significantly when substrate stiffness is greater than that measured in human gray matter (Balgude et al. 2001; Discher et al. 2005; Flanagan et al. 2002; Lu

et al. 2006). While it is clear that astrocytes undergo cytoskeletal reorganization after injury, an important question that remains unanswered is whether the mechanical properties of astrocytes change during reactivity, given the lack of neuronal growth in the glial scar. In this study we used atomic force microscopy (AFM) to investigate whether a mechanical injury that induces changes in GFAP immunoreactivity also increases astrocyte stiffness and whether changes in cellular stiffness extend beyond the initial area of mechanical injury in vitro.

3.3 MATERIALS AND METHODS

3.3.1 Cell Culture

Pure cortical astrocyte cultures were generated from E18 Sprague-Dawley rat embryos (Charles River Laboratories) according to the animal welfare guidelines established by the University of Pennsylvania's IACUC. Briefly, brains were dissected from the embryos and the meninges were removed. The cortices were dissected and dissociated by incubating in Neurobasal media (Invitrogen) with trypsin (0.3mg/ml, Sigma) + DNase I (0.2mg/ml, Amersham Biosciences) at 37°C, 5% CO₂. Enzymatic activity was inhibited after 20 minutes by adding soybean trypsin inhibitor (.5mg/ml, Gibco). The tissue was mechanically disrupted by pipetting, then centrifuged for 5 minutes at 1000 rpm and resuspended in DMEM (Cambrex) + 5% FBS (Hyclone). Cells were filtered sequentially through a 60µm and 28µm Nitex Mesh (Cross Wire Cloth & Manufacturing Co.) and plated onto poly-L-lysine (PLL, Sigma)-treated T75 tissue culture flasks (Fischer Scientific, Inc.) at a concentration of 1×10^5 cells/ml. Media was changed every 3-4 days.

At 13 days in vitro (DIV) cells were placed on an orbital shaker and shaken at 250 rpm overnight at 37°C, 5% CO₂ to remove loosely adherent cells. Flasks were rinsed with saline solution before adding 4 ml of trypsin/EDTA (0.25%, Invitrogen) for 2-3 minutes at 37°C, and then mechanically disrupted to dislodge the cell layer from the flask surface. DMEM + 5% FBS was added to inhibit enzymatic activity. The cells were centrifuged for 5 minutes at 1000 rpm and resuspended in DMEM + 5% FBS. The cell suspension was diluted to 1×10^5 cells/ml and plated onto PLL-treated silicone-based

elastic membranes (cured Sylgard 186:Sylgard 184 at a 7:4 mix, Dow Corning). Media was changed at 24 hours and then every 3-4 days until use after 13-14 DIV, at which point cultures had reached confluency. Cultures were determined to be >95% pure astrocytes by immunocytochemistry for GFAP (astrocytes), type-3 beta-tubulin (neurons), and CNPase (oligodendrocytes) counterstained with Hoechst. Cultures were discarded if not confluent.

3.3.2 Cell Stretch

To simulate the strains experienced during mild TBI, a rapid, transient air pressure pulse was applied to the culture surface, deflecting the membrane downward. A metal plate beneath the culture restricted the deflection of the elastic membrane to a 2 mm x 18 mm rectangular region (Figure 3.1). Past work shows that this membrane strain causes a corresponding and proportional stretch of cells plated on the membrane (Shreiber et al. 1997). The duration (20ms) and magnitude of the strain (15%) were controlled to simulate mild TBI (Shreiber et al. 1997). The geometry of the stretched area created a nearly uniform uniaxial strain field throughout the stretched region (Lusardi et al. 2004). The culture region surrounding the region of stretch-injured cells – the “penumbra” – experienced no mechanical deformation (Lusardi et al. 2004). All cultures were stretched once and returned to the incubator environment for 24 hours before conducting AFM measurements or GFAP immunoreactivity.

3.3.3 GFAP immunoreactivity

As noted above, cultures were injured in a sterile environment in DMEM + 5% FBS and incubated for 24 hours. The cultures were then rinsed with PBS and fixed in 4%

paraformaldehyde for 15 minutes. The cells were permeabilized in 0.2% triton (Sigma) in TBS for 5 minutes. Primary monoclonal GFAP antibody (1:1000, Chemicon) in 5% NGS was added and the cultures were incubated overnight at 4°C. The cells were rinsed 2X with TBS and incubated for 30 minutes in 5% NGS and then the secondary antibody (Alexafluor 488, 1:1000, Chemicon) was added for 1 hour. The cells were rinsed and stored at 4°C until imaging.

Immunoreactivity was quantified by using Metamorph software (Universal Imaging) to compute an average fluorescence for a full field (350 μm x 350 μm). A threshold was set for the images such that only cellular areas were included and the average immunofluorescence was recorded. In stretched cultures, 3-6 images were taken randomly from the mechanically injured region and 4-10 images were taken from the adjacent, uninjured (penumbra) regions. In unstretched cultures, 6-10 images were taken randomly throughout the culture. Immunoreactivity was compared from week to week by including at least three naïve controls each week and normalizing each week's immunoreactivity data to the naïve controls for that week.

3.3.4 Atomic Force Microscopy

Images were acquired using a Bioscope AFM with a Nanoscope IIIa controller (Veeco Instruments) and a DAFM-2X Dimension Head Scanner (Veeco). Images were obtained in contact mode using silicon nitride DNP cantilevers (Veeco), which are nominally 200 μm long with 20 μm wide legs. Contact mode images were taken in DMEM media at room temperature with scan rates between 30-100 $\mu\text{m}/\text{s}$ and scan sizes between 10-100 μm in each direction. These images were used to identify nuclear and

non-nuclear regions of each astrocyte. After imaging a region of the culture, force curves were collected by indenting the cantilever onto the cell surface while holding the xy-axis constant. The nominal spring constant of these cantilevers is reported to be 0.06 N/m, although actual spring constants were determined using resonance frequency measurements of the tip prior to each experiment. The sensitivity of each cantilever was calibrated before use by lowering the cantilever onto a glass slide. After the cantilever reached the surface of the cell, it was lowered at least 300nm towards the cell surface at a rate of 1 Hz.

The apparent Young's modulus, E , was determined by fitting deflection curves for each culture to two different indentation models. In the Sneddon's modification of the Hertzian model (Landau and Lifshitz 1970; Sneddon 1965), the force-deflection relationship for a conical tip is given by

$$F = \frac{\delta^2 (2 E \tan \alpha)}{\pi (1-\nu^2)} \quad (1)$$

where F is the loading force, E is the elastic Young's modulus, α is the nominal tip angle, ν is the Poisson ration (0.5 was used, based on (Sato et al. 1990)), and δ was the deflection of the cantilever. For a parabolic tip the fit is given by

$$F = \frac{4 E R^{1/2} \delta^{3/2}}{3 (1-\nu^2)} \quad (2)$$

where R is the radius curvature at the apex (Sneddon 1965).

3.3.5 Statistics

Data are reported as mean \pm standard error except where specified otherwise. Significance for GFAP immunoreactivity and for differences in Young's modulus was

determined by ANOVA with strain (injured vs. naïve) and culture location (stretched vs. penumbra) as groups. Curve fitting was determined by linear regression and by a chi-squared test for goodness of fit.

3.4 RESULTS

3.4.1 Mechanical stretch induces an increase in GFAP immunoreactivity 24 hours following injury

In this study we measured the change in cellular stiffness in reactive astrocyte cultures 24 hours after applying a rapid, transient strain that mimics mild TBI. Astrocytes subjected to a 15% strain showed no morphological differences from astrocytes in naïve cultures in terms of process number or length, or in terms of increased cell density. However, increased GFAP immunoreactivity was noted at 24 hours following injury (Figure 3.3). Quantification of the fluorescence intensity (describe above) revealed that GFAP staining in stretched cells was significantly higher than in naïve cultures ($p < 0.05$, Figure 3.3D). Astrocytes in the penumbra regions of the injury, which we defined as the regions immediately adjacent to the stretch (Figure 3.1), also did not display any overt morphological changes but stained significantly more intensely for GFAP compared to naïve cultures ($p < 0.05$, Figure 3.3). There was no difference in GFAP immunoreactivity between stretched and penumbra astrocytes.

3.4.2 Modeling of AFM indentation

Using atomic force microscopy (AFM) we investigated whether these intermediate filament alterations were correlated with a change in mechanical properties. Using an indentation protocol, we made separate measurements for nuclear and non-nuclear regions of the cells. Each measurement consisted of indentation depths of at least 300nm. The average force-indentation curve for the non-nuclear region of penumbra astrocytes is shown in Figure 3.4. The apparent E was determined by fitting to either the

conical equation (1) or the parabolic equation (2), as described above (Sneddon 1965).

The goodness of fit for each model was determined by a chi-squared test, resulting in a chi-squared distribution value in non-nuclear regions of astrocytes of 0.43 for the conical model in penumbra cells, compared to a value of 0.99 for the parabolic model (Table 3.1). Likewise, the R^2 regression parameter for the parabolic model is higher than for the conical model (Table 3.1). Table 3.1 shows the R^2 regression parameter and the chi-squared distribution values for all conditions. These data indicate that the parabolic model is a superior approximation of the experimental data for determination of E. Therefore, we used the parabolic model for the remaining comparisons among injured and naïve culture regions.

3.4.3 Apparent Young's modulus is reduced in nuclear regions of naïve astrocytes compared to non-nuclear regions

We first measured E in naïve cultures, both in non-nuclear regions of the cell and areas above the nucleus. In these cultures there was a significant difference between E in the region above the nucleus compared to non-nuclear regions. The average E value was 22.7 ± 5.8 kPa above the nucleus, while in non-nuclear regions E was 57.7 ± 5.8 kPa ($p < 0.05$, Figure 3.5). Obviously, there is no “penumbra” region in naïve cultures, so there was no difference in the regions of the cultures, unlike in the injured cultures.

3.4.4 Mechanically injured astrocytes are more compliant than naïve astrocytes

We next investigated the stiffness of cells in the stretched region of injured cultures. As in naïve cultures, the value of E in the region above the nucleus was lower than in the non-nuclear areas (Figure 3.5). However, the difference between the two

locations was not significant. The stretched cells displayed no significant change in stiffness in the nuclear region compared to naïve (Figure 3.5). Despite this, in the non-nuclear region there was a significant decrease in E from $57.7 \pm 5.8\text{kPa}$ in naïve cultures to $26.4 \pm 4.9\text{kPa}$ in stretched cells ($p < 0.05$, Figure 3.5).

3.4.5 Non-nuclear regions of penumbra astrocytes are more compliant than naïve astrocytes

In the penumbra region of injured cultures, the area above the nucleus was stiffer than the non-nuclear regions, which was opposite of what was observed in naïve or stretched astrocytes (Figure 3.5). Due to the high variability in the nuclear region, the difference in E between the nuclear and non-nuclear region was not significant. Likewise, the difference between the nuclear region in the penumbra astrocyte and the nuclear region in naïve cultures was not significant. However, the nuclear region in the penumbra was significantly stiffer than the nuclear region in stretched astrocytes ($p < 0.05$, Figure 3.5). In the non-nuclear region of the penumbra astrocytes the value of E was significantly reduced compared to naïve cultures, with a apparent Young's modulus of $23.7 \pm 3.6\text{kPa}$ compared to $57.7 \pm 5.8\text{kPa}$ in naïve cultures ($p < 0.05$, Figure 3.5). The stiffness of penumbra astrocytes was nearly identical to what was observed in injured cells (Figure 3.5).

3.5 DISCUSSION

In this study we used AFM to investigate the cellular stiffness of cultured astrocytes after mechanical injury. AFM can be used to acquire exquisitely detailed topographical images of living cells, including information about height and the location of subcellular structures, without producing significant disturbance or damage to the cell (Alonso and Goldmann 2003; Haydon et al. 1996; Ohta et al. 2002). AFM has also been used to examine the mechanical properties of the cell by measuring the forces required to deflect the cell membrane (Alonso and Goldmann 2003; Collinsworth et al. 2002; Costa and Yin 1999; Hoh and Schoenenberger 1994; Lu et al. 2006; Rotsch et al. 1997; Sato et al. 2000). We used AFM to determine the apparent Young's modulus, E , in regions over the nucleus as well as in non-nuclear regions of the astrocytes both in naïve and injured cultures. In naïve cultures we found that the region above the nucleus was significantly less stiff than non-nuclear region. Cells in the stretched region of injured cultures also displayed stiffer non-nuclear regions compared to nuclear regions. However, the situation was reversed in the penumbra, which we defined as the area immediately adjacent to mechanical injury, with the nuclear region having a higher E than the non-nuclear region, although the difference did not reach the level of significance.

In addition, in injured astrocyte there was a dramatic softening of the non-nuclear regions 24 hours after injury compared to naïve cultures, although in the nuclear regions the results were not significantly different between injured and naïve cultures. Likewise, softening was detected in non-nuclear regions of astrocytes in the penumbra compared to naïve cultures. This suggests that the cell stiffness changes were not due directly to

mechanical injury, since non-stretched cells underwent the same level of stiffness change.

Correlated with this softening was a significant increase in GFAP immunoreactivity in both the stretched cells and the penumbra.

Increased GFAP expression is a standard marker for reactive gliosis, which is a process that astrocytes undergo following injury or during degenerative disease (Pekny and Nilsson 2005). In the case of a focal injury, reactive astrocytes can migrate to the area of injury and form a glial scar, which is composed of a dense wall of cells and extracellular matrix molecules that serve to divide the injured region from surrounding tissue. Generally, the glial scar is inhibitory to neuronal regrowth, and it has been suggested that the wall of glial cells physically block the regrowth of neurites through the scar (Pekny and Nilsson 2005). However, more recently the major inhibitory aspect of the glial scar has been reported to be increased production of chondroitin sulfate proteoglycans (McKeon et al. 1999; Yiu and He 2006) which are produced in large quantities from astrocytes, oligodendrocytes, and microglia in the glial scar (Sandvig et al. 2004). In support of this idea, some studies showed that enzymatic digestion of these large molecules allowed neurites to grow through the scar (Bradbury et al. 2002).

Likewise, our data suggests the actual mechanical aspects of reactive astrocytes may be favorable for repair, if these in vitro results are mimicked in vivo. As noted above, cultured neurons have been shown to prefer much softer substrates than typical cells (Balgude et al. 2001; Discher et al. 2005; Flanagan et al. 2002; Lu et al. 2006). For example, Flanagan et al (2002) reported that neurons showed more neurite branching on softer polyacrylamide gels. Similarly, the rate of dorsal root ganglion neurite extension

was found to be inversely related to the stiffness of the agarose gels used for culturing (Balgude et al. 2001). A recent study on the viscoelastic properties of glial cells revealed that they are much softer than other cell types (Lu et al. 2006), suggesting they may be a favorable substrate for neuronal growth. Interestingly, the optimal stiffness for neuronal growth seems to be much lower than the optimal level for astrocyte growth (Flanagan et al. 2002; Georges et al. 2006), which may be a mechanism for controlling cellular organization in the developing brain.

The relationship between cell stiffness and GFAP expression is potentially due to the influence of intermediate filaments on actin organization (Chang and Goldman 2004). As noted above, microfilaments are the major load-bearing components of the cytoskeleton, with intermediate filaments only playing a secondary role (Trickey et al. 2004). However, intermediate filament reorganization has been shown to induce the alteration actin organization (Chang and Goldman 2004), so we propose that the increase in GFAP expression is causing the actin network to rearrange, allowing for a more compliant structure. Studies using AFM after cytoskeletal treatments have shown that the actin network is particularly important in determine cell stiffness. In stiffness measurement of living astrocytes Yamane et al (2000) showed that areas above F-actin were much stiffer than the surroundings areas (Yamane et al. 2000). Another study showed that treatment of rat liver macrophages with latrunculin-A or cytochalasin B to depolymerize the actin network resulted in a drastic reduction in stiffness over time (7x less stiff in 40 minutes) (Rotsch et al. 1997), indicating that actin organization plays a major role in providing the mechanical stiffness of the cell. Based on these studies and

our own data, we suspect that there is a GFAP-induced actin change in injured astrocytes that contributes greatly to the softening seen after injury.

The mechanical properties of astrocytes and brain tissue have been measured by other investigators, and it has generally been found that brain tissue and cells are much softer than other tissue and cells (Discher et al. 2005; Lu et al. 2006). Earlier studies using AFM on cultured astrocytes measured the 3-D properties of cultured astrocytes and showed that AFM is capable of imaging sub-membrane structures of living glia without causing membrane leakage or other signs of overt cellular damage (Haydon et al. 1996; Parpura et al. 1993). More recent reports on the mechanical stiffness of astrocytes have found them to be more compliant than endothelial cells, cardiac cells, skeletal muscle cells, and fibroblasts, among others (Lu et al. 2006; Mathur et al. 2001). Lu et al (2006) found that the elastic component of the complex modulus in astrocytes was approximately 0.2-0.6 kPa, which is much lower than the values reported in this study. However, that study used a high frequency tapping protocol instead of a low speed indentation protocol, which may explain the difference from our values in apparent stiffness. Significantly, Lu et al found that the apparent complex shear modulus measured in astrocytes was close to that measured in hippocampal brain slices, as measured by bulk rheology (Lu et al. 2006), suggesting that astrocytes may play a large role in determining the macroscopic mechanical properties of the brain. In an AFM indentation study more similar to the one used in this study, astrocyte stiffness was measured to be 10-20kPa in non-nuclear regions while nuclear regions were much softer,

with a reported modulus of 2-3kPa (Yamane et al. 2000). This data correlates well with the values collected in the present study.

Studies that have directly measured the nucleus have generally shown that it is much stiffer than the rest of the cell (Caille et al. 2002; Dahl et al. 2005). Direct measurements of the mechanical properties of isolated nuclei have shown them to be approximately an order of magnitude stiffer than the cytoplasm (Caille et al. 2002; Dahl et al. 2005). However, indentation experiments above the nucleus have not consistently found that this region is stiffer than the surrounding areas of the cell. In fact, several reports using astrocytes and other cell types have shown that nuclear regions of the cell are significantly softer than the periphery regions (Radmacher et al. 1996; Ricci et al. 1997; Sato et al. 2000; Yamane et al. 2000). Others have found the opposite, with the nuclear region of the cell body showing a much greater modulus (Mathur et al. 2001). This discrepancy may be due to the fact that the indentation experiments are only measuring the stiffness immediately below the membrane and do not indent far enough to detect the nuclear stiffness component. Another possibility that has been proposed is that the measurements of the periphery are biased higher because of interactions with the underlying surface due to the decreased thickness of the cell in those regions compared to nuclear regions (Mathur et al. 2001). Of course, much of the discrepancy in values might be due to different protocols for measuring stiffness of living cells, or to the fact that different preparations may result in different mechanical properties for the cell. For example, in our model the cells are cultured on elastic membranes, which may give a very different mechanical profile than cells grown on glass.

The most important finding in this study was the dramatic softening of non-nuclear regions of cultured astrocytes after mechanical injury, a phenomenon that was found in both injured cells and nearby, uninjured cells. This effect was correlated with a significant upregulation of GFAP, indicating that these astrocytes were undergoing reactive gliosis. If this situation is reflected in vivo after injury, these data suggest that reactive astrocytes may be a mechanically favorable substrate for neuronal regrowth and repair in the absence of other inhibitory factors.

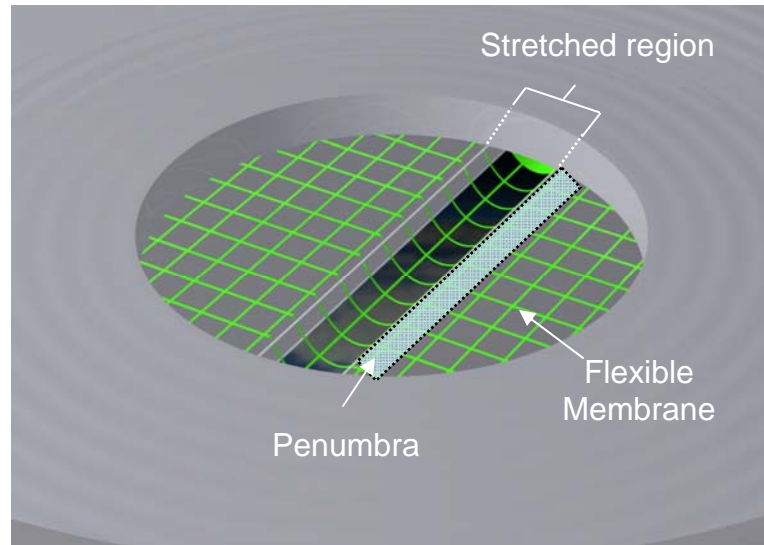


Figure 3.1. Overview of mechanical stretch injury device. Astrocytes were cultured on transparent, elastic membranes. An air pressure pulse was delivered to the culture surface, deflecting the membrane downward. A metal plate beneath part of the culture restricted the region of stretch to a 2mm x 18mm region. The membrane region adjacent to the deflected region, termed the penumbra (light blue area), experiences negligible strain. The membrane strain produced by such geometry is uniaxial and nearly uniform throughout the stretched region.

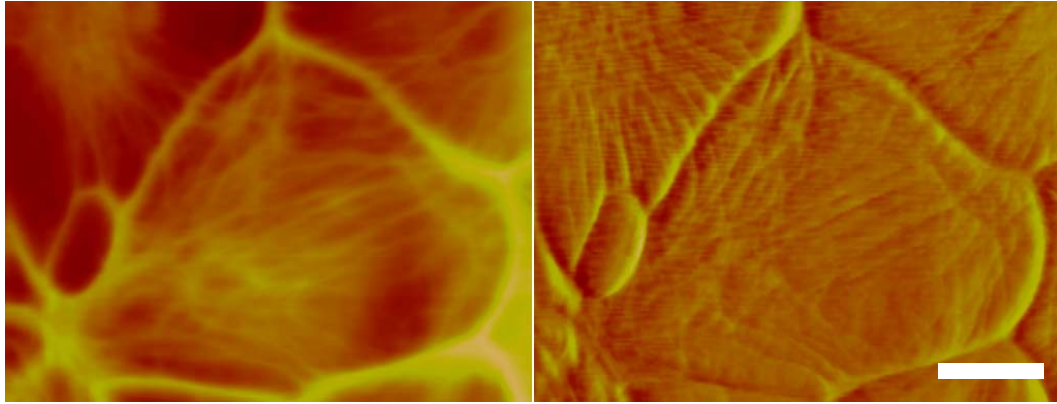


Figure 3.2. Height (left) and deflection (right) images of an astrocyte obtained by AFM scanning in contact mode. Images were used to determine nuclear and non-nuclear regions for measurement of cell stiffness. Scale bar = 10 μ m.

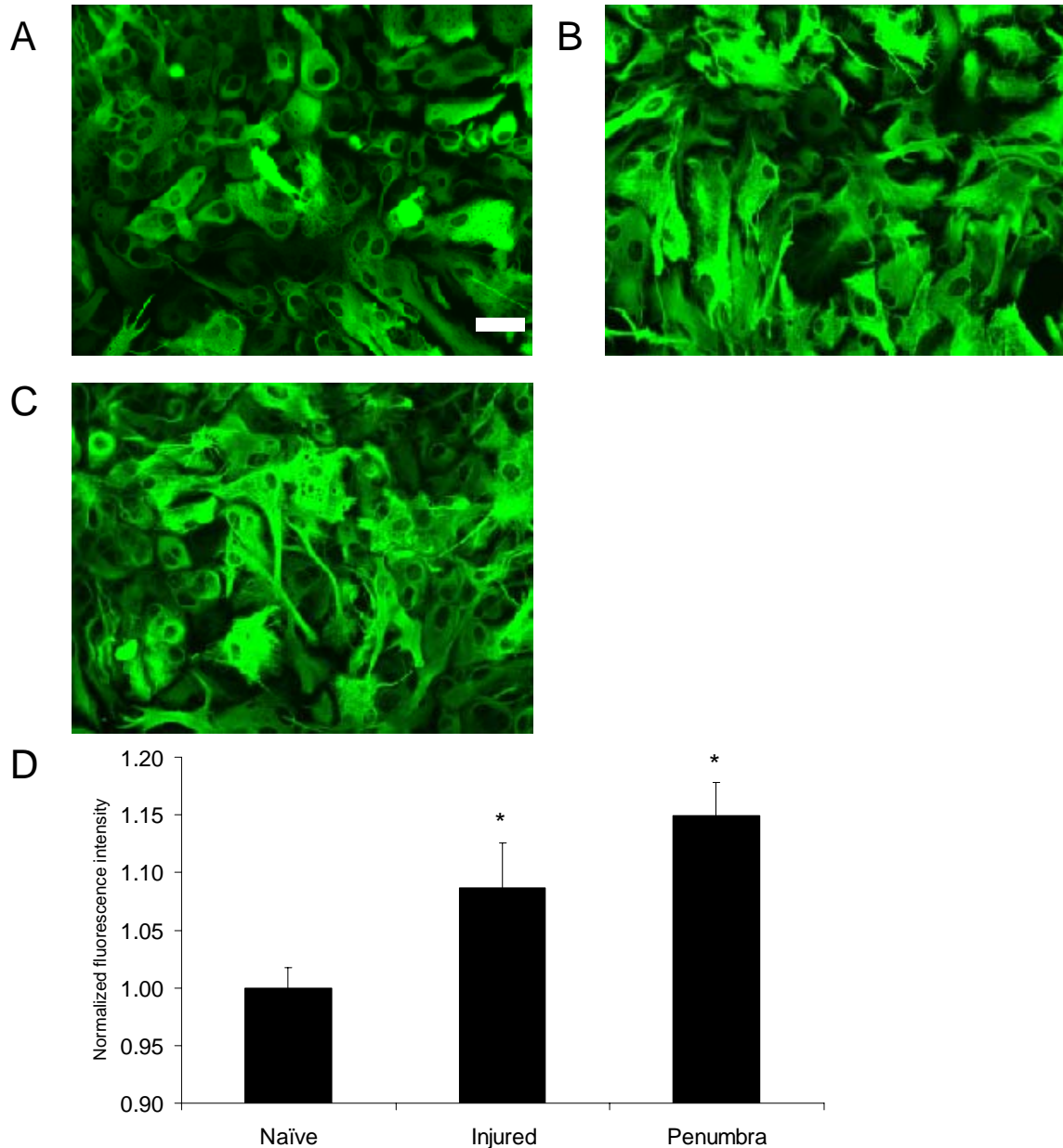


Figure 3.3. Immunocytochemistry for GFAP shows a single, dynamic stretch of 15% results in increased GFAP reactivity in the stretched and penumbra regions. (A) In naïve astrocytes, GFAP immunostaining appears consistently throughout all regions of the culture. Scale bar = 50 μ m. (B) In astrocytes receiving a direct mechanical injury, a noticeable increase in GFAP immunoreactivity occurs 24 hours after the stretch injury. (C) The extent of GFAP immunoreactivity is similar to injured cells in the penumbra of the astrocyte culture. (D) A quantitative measure of the immunofluorescence shows that the changes in the GFAP reactivity are significant in both the stretched (n = 24 independent cultures) and penumbra (n = 25) regions compared to naïve (n = 32). * = $p < 0.05$.

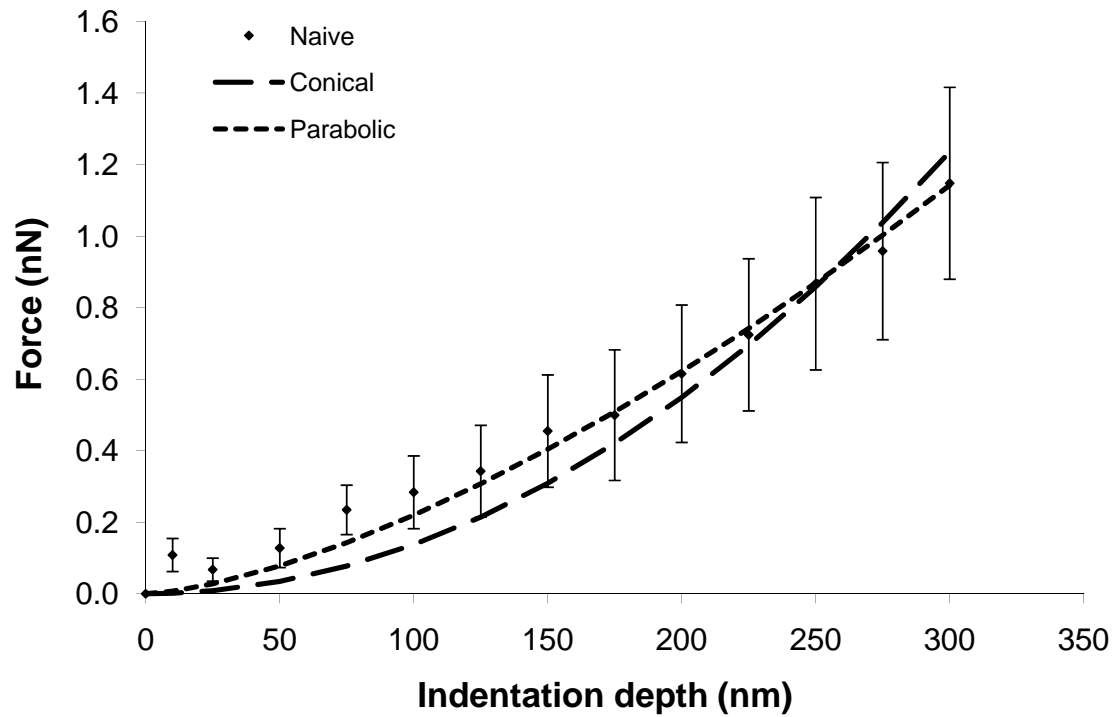


Figure 3.4. Force-indentation curve recorded from a group of penumbra astrocytes from separate cultures. Shown are the average \pm SD of the measured force from the experiments. The curves represent the fitting procedures used to develop estimates of the apparent stiffness from a group of tests.

Error! Objects cannot be created from editing field codes.

Table 3.1. Estimated apparent moduli (kPa) for different astrocyte regions across different zones of the culture. Numbers in parentheses and brackets indicate the R^2 regression parameter and the chi-squared distribution value for goodness of fit, respectively, from the fitting procedure using either a model that assumes a conical or parabolic approximation that accounts for the tip geometry.

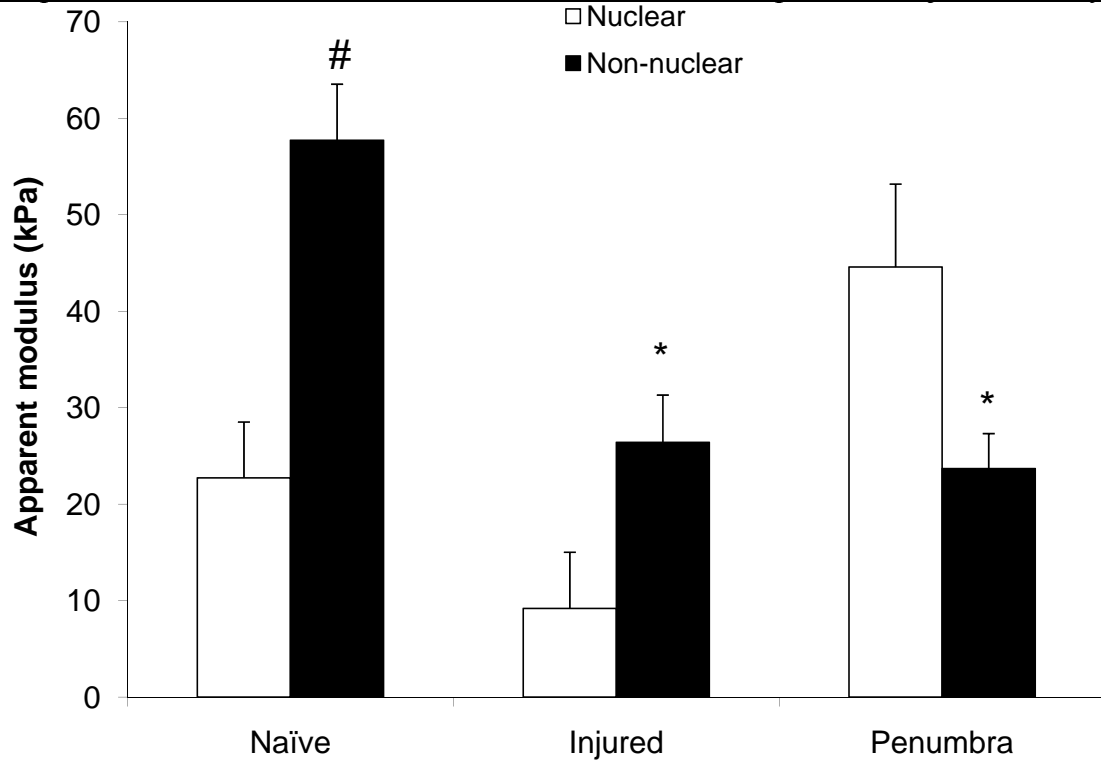


Figure 3.5. Changes in apparent stiffness 24 hours following stretch injury differ with indentation region, and are distinct between the penumbra and stretched regions. In naïve cultures, indentations above the nucleus yielded a significantly lower apparent modulus compared to non-nuclear areas. In injured cultures, the difference in apparent modulus between nuclear and non-nuclear regions followed the same pattern as naïve cultures, although apparent moduli in both regions were significantly lower than naïve cultures. The astrocytes measured in the penumbra region showed a reversal in the trend across indentation region, with nuclear areas now much stiffer than non-nuclear regions. Overall, injured cultures were considerably softer than naïve cultures in non-nuclear regions. * $p < 0.05$ compared to naïve, # = $p < 0.05$ compared to nuclear region.

Chapter 4: The Role of Purinergic and Glutamatergic Signaling in Mediating Cell Death Following Mechanical Injury of Organotypic Hippocampal Slices

4.1 ABSTRACT

The hippocampus has been reported to be selectively vulnerable to traumatic brain injury (TBI). In this study we investigated the role of glutamatergic and purinergic signaling in mediating cell death in organotypic hippocampal slice cultures (OHSCs) 24 hours following a stretch-induced injury. We found a significant increase in cell death in the CA3 subregion following a 75% or 100% stretch, as measured by propidium iodide uptake. In agreement with previous work, blockade of the NMDA receptor (NMDAR) eliminated increased PI uptake after either 75% or 100% stretch-injury. A specific blockade of extrasynaptic NMDARs with ifenprodil was equally effective in reducing cell death at 75% but not at 100%. Antagonism of the metabotropic glutamate receptor mGluR5 with MPEP was completely ineffective in preventing stretch-induced cell death in the CA3. Inhibiting the activation of P2 receptors, and, specifically the P2Y1 receptor, significantly reduced cell death at all injury levels. Interestingly, blocking an increase in astrocytic calcium by specifically loading these cells with the calcium chelator BAPTA-AM reduced cell death after 100% stretch. Overall, these data point to important linkages between purinergic and NMDA receptors in influencing cell death in the hippocampus after traumatic mechanical injury. The link between these receptors appears to indicate a coupling between astrocytes and neurons after injury, and supports the possibility of ATP-mediated release of glutamate from astrocytes in determining cell fate in the CA3 after TBI.

4.2 INTRODUCTION

The hippocampus has been reported to undergo an unusually high degree of immediate and progressive cell loss after traumatic brain injury (TBI), suggesting that this brain region may be selectively vulnerable to injury (Beer et al. 2000; Bramlett et al. 1997; Hicks et al. 1996; Lowenstein et al. 1992; Smith et al. 1995). In vitro experiments have confirmed that hippocampal neurons are more susceptible to cell death after mechanical injury than cortical neurons (Geddes et al. 2003), although the exact mechanisms that determine the selective vulnerability of the hippocampus have yet to be completely described.

Mechanical injury results in the release of large amounts of glutamate, which can be toxic to neurons and glia at high doses (Faden et al. 1989). Given this rapid increase in extracellular glutamate, a number of studies have examined the role of glutamatergic receptors and, particularly, the N-methyl-D-aspartate receptors (NMDARs), in cell death and dysfunction after experimental TBI (Arundine and Tymianski 2004; Bullock and Fujisawa 1992; Dempsey et al. 2000; Faden et al. 2003; Rao et al. 2001; Regan and Choi 1994; Shapira et al. 1990). The NMDAR is a heterotetramer consisting of two NR1 subunits and two NR2 subunits. The NR2 subunit generally determines the function and spatial distribution of the NMDAR (Loftis and Janowsky 2003). NR2A-containing receptors are found primarily in the synaptic region while NR2B-containing NMDARs, alternatively, are generally located extrasynaptically (Loftis and Janowsky 2003). Several reports have suggested that selective activation of NR2B-containing NMDARs leads to neuronal cell death (Hardingham et al. 2002; Wang and Shuaib 2005), and in

experimental models of TBI antagonists of extrasynaptic NMDARs generally result in increased cell survival and improved outcome (Dempsey et al. 2000; DeRidder et al. 2006; Toulmond et al. 1993). However, others have shown that either NR2A or NR2B-containing NMDARs are capable of inducing cell death under the proper excitatory conditions, and the distinction between the two may be due more to the source of glutamate than to the innate receptor activity (Sattler et al. 1998; Sattler et al. 2000). Significantly, recently published reports indicate that extrasynaptic NMDARs can be activated by astrocyte-released glutamate after stimuli that increase intracellular calcium, presenting potential a separate glutamate source for NMDAR activation (Angulo et al. 2004; Fellin et al. 2004).

In addition to activating NMDARs, glutamate released during injury is capable of affecting other receptors on neurons, such as the kainate, AMPA, and metabotropic glutamate receptors. Moreover, astrocytes are capable of responding to changes in extracellular glutamate; e.g., synaptic glutamate can activate the group I metabotropic glutamate receptor mGluR5 receptors on astrocytes, leading to the synaptically-driven increase in intracellular calcium (Biber et al. 1999; Nakahara et al. 1997; Schools and Kimelberg 1999). The stimulation of glutamatergic receptors on astrocytes may amplify the initial excitotoxic cascade by stimulating the release of additional glutamate (Zhang et al. 2004a) and indicate that non-NMDARs may also influence glutamate mediated neuronal death (Bao et al. 2001; Floyd et al. 2004; Movsesyan et al. 2001; Strasser et al. 1998).

A less well studied group of receptors that can influence glutamate excitotoxicity are the P2 purinergic receptors, which can affect the function of both astrocytes and neurons *in vivo* after injury. Large amounts of ATP are released into the extracellular space after TBI (Franke et al. 2006). In neurons, extracellular ATP can activate both ionotropic P2X receptors and metabotropic P2Y receptors, with varying effects. P2X receptors in the CNS are involved in direct synaptic transmission as well as in potentiating neurotransmitter release (Franke et al. 2006). P2Y receptors can modulate ion channels conductance, inhibit the release of neurotransmitters, and both inhibit and enhance synaptic transmission postsynaptically (Erb et al. 2006). Furthermore, adenosine produced from the breakdown of ATP can activate adenosine receptors on neurons, which is generally an inhibitory signal (Fields and Burnstock 2006). ATP acting at P2 receptors evokes intracellular calcium increases in astrocytes (King et al. 1996), and can result in the release of glutamate (Duan et al. 2003; Fellin et al. 2006b). In turn, the release of glutamate can lead to activation of extrasynaptic NMDARs on neurons (Fellin et al. 2004), potentially creating a neuronal-glia signaling network that can lead to neuronal death. Additionally, extracellular ATP can lead to astrocyte reactivity after injury (Franke et al. 1999), with some studies specifically implicating the P2Y1 receptor (Franke et al. 2001). Possibly from these mechanistic findings, blocking P2 receptor activation after focal cerebral ischemia and chemical hypoxia has been shown to be neuroprotective (Cavaliere et al. 2001; Kharlamov et al. 2002; Lammer et al. 2006), and P2 receptor antagonists can modulate glutamate-evoked death in cultured cerebellar granule neurons (Volonte and Merlo 1996).

In this study we compared the role of glutamatergic and purinergic receptors on the resulting cell death following mechanical injury to the hippocampus in vitro. Using an in vitro model of traumatic brain injury in organotypic hippocampal slice cultures (OHSCs), we found that mechanical injury causes a progressive increase in cell death within the CA3 region of the hippocampus 24 and 72 hours after injury. In agreement with previous work, blockade of all NMDARs eliminated the increase in cell death in the CA3. We found that inhibiting the activity of extrasynaptic NMDARs was consistent in limiting cell death only at moderate levels of injury. In comparison, blocking the activity of mGluR5 receptors was completely ineffective in reducing cell death after mechanical injury at any injury severity. Inhibiting the activity of P2 purinergic receptors resulted in significant decrease in cell death at all injury levels. These data indicate that extracellular ATP and NMDARs have a related role in activating cell death after mechanical injury of hippocampal slices, and that purinergic receptors may represent a more potent therapeutic target than other glutamatergic receptor blockade strategies.

4.3 MATERIALS AND METHODS

4.3.1 Organotypic hippocampal slice culture isolation

All procedures involving animal use were approved by the Institutional Animal Use and Care Committee at the University of Pennsylvania. The methods for isolating organotypic cultures are similar to those described previously (DeRidder et al. 2006), with some modifications. Briefly, elastic silicone membranes (Sylgard 184:186 mix, Dow Corning) were stretched across a 60mm stainless steel well containing an 18mm diameter hole in the center. The exposed region of the membrane was treated overnight with poly-L-lysine (20 µg/ml, Sigma-Aldrich) and laminin (50 µg/ml, BD Biosciences). The wells were rinsed with sterile water and culture media containing Neurobasal-A media (Invitrogen Corp.) supplemented with 6.5% glucose, B-27 (Invitrogen), and 1 µg/ml L-glutamine (Sigma) was added to the culture well. The wells were kept in a humidified incubator at 37°C, 5% CO₂ until needed.

Brains were aseptically removed from 6-8-day-old CD[®]IGS (Sprague-Dawley) rat pups (Charles River Laboratories, Inc), transferred to ice-cold Gey's salt solution (Sigma-Aldrich Corp.) supplemented with 6.5% glucose. The hippocampus was dissected out of each hemisphere and sectioned coronally (350µm sections) on a McIlwain Tissue Chopper (Brinkman Instruments). The hippocampal slices were carefully separated, and 1-3 slices were plated onto each elastic silicone membrane. Cultures were kept in a humidified incubator at 37°C, 5% CO₂ on a rocker (0.5 Hz, Elmeco Engineering) for 9-10 days in vitro (DIV) with media changes occurring every 2–3 days.

4.3.2 In vitro model of TBI

The mechanical injury model used in this study applies a rapid, transient strain to a 6 mm x 18 mm rectangular region of the culture surface (Figure 4.1A). Past work show the membrane strain causes a corresponding and proportional stretch of cultures plated on the membrane (Morrison et al. 1998). The duration (20ms) and magnitude of the strain (50-100%) were controlled to simulate traumatic brain injury (Shreiber et al. 1997). In a subset of cultures we applied the pressure pulse but the underlying membrane was not allowed to deflect. No increased cell death was observed in these “pressure” controls compared to naïve sham cultures (data not shown). The slices were aligned such that the strain field was primarily along the long axis of the hippocampal slice (Figure 4.1C). The geometry of the stretched area created a nearly uniform uniaxial strain field throughout the stretched region (Lusardi et al. 2004). Media was changed in all cultures 15-20 minutes prior to stretch, at which time all pharmacological pretreatments (including propidium iodide) were added.

In BAPTA-AM loaded cultures, BAPTA-AM (100 μ M, Molecular Probes) was loaded at room temperature for 40 minutes. Cultures were then rinsed 2x with warm media and incubated at 37°C, 5% CO₂ for 20 minutes prior to injury. All cultures were stretched once and returned to the incubator until imaging.

4.3.3 Cell death measurement

Cells were loaded with propidium iodide (PI, 5 μ g/mL, Molecular Probes) 15-20 minutes prior to injury. Hippocampal slices were removed from the incubator 24 or 72 hours after injury, and imaged with a confocal microscope. PI labeling was analyzed using MetaMorph software (Universal Imaging). For each slice a single image chosen

for analysis at a distance of 20 μ m above the membrane surface. In a subset of cultures the average PI labeling from five consecutive planes taken from a single slice separated by 5 μ m distance was compared to the PI labeling from a single image. There was no significant difference in the pattern of cell death, since the pattern of cell death was identical, although the absolute value of the PI labeling was slightly lower using 5 planes. As such, all of our analysis used a single image.

The hippocampal subregions were identified and the total area of each region was recorded (Figure 4.1C). In a subset of cultures each week an intensity threshold was determined by hand counting the number of PI positive cells and then determining a threshold level that included only those cells. The data are reported as a percentage of area staining positive for PI, which was determined in each subregion of the hippocampus by recording the total area that was above the threshold selected and dividing by the total area of the subregion. To check the accuracy of this measurement, Figure 4.2C shows the linear relationship between the # of PI-positive cells per μm^2 vs. the number of PI-positive pixels divided by total pixels. Uninjured OHSCs showed a low level of baseline PI labeling (Figure 4.2A), while treatment with 100 μ M NMDA for 24 hours resulted in a high level of cell death with corresponding high PI labeling (Figure 4.2B). NMDA treatment resulted in greater than 20% of the area of the CA1 and CA3 labeling positive for PI uptake, and greater than 15% of the dentate gyrus (DG) and the hilus labeled positive (Figure 4.2B). In untreated, uninjured cultures, by comparison, an average of less than 0.2% of each region labeled positive with PI (Figure 4.2A). The results reported are from a single confocal image taken at a set distance above the membrane surface.

However, the results of 5 sets of confocal images taken at 5 μ m intervals show no difference in the pattern of increased cell death (Figure 4.3B-C).

4.3.4 Calcium Crimson

Slices were loaded with Calcium Crimson-AM (25 μ M, Molecular Probes) in the dark for 40 minutes at room temperature in the dark. Cultures were rinsed 2x with media and then incubated for 90 minutes in 1-ethyl-3-(3-dimethylaminopropyl) carbodiimide-HCl (EDC, 20 mg/ml; Pierce, Rockford) in PBS. This compound fixes the BAPTA into the cell for tissue processing (Abdel-Hamid and Tymianski 1997). Slices were then fixed in 4% paraformaldehyde in PBS overnight.

After fixation, slices were rinsed four times with PBS, then immersed in PBS with 50% w/v sucrose and incubated for 24 hours at 4°C. Slices were sectioned to 20 μ m thickness on a freezing stage microtome, immersed in TBS with 0.1% Triton-X100, and mounted on microscope slides. Slides were rinsed three times in distilled de-ionized water, and then incubated for ten minutes in 50% v/v MeOH with 3% v/v H₂O₂ to quench endogenous peroxidase activity. Slides were washed another three times in DD water, then in TBS with 0.1% Tween-20; they were then blocked in TBS with 0.5% v/v normal goat serum for one hour. Sections were then covered with either rabbit anti-GFAP at 1:5000 in TBS with 0.5% v/v normal goat serum or rabbit anti-NeuN at 1:5000 in TBS with 0.5% v/v normal goat serum in a dark humidity chamber at 4°C for at least 8 hours. Slides were rinsed three times in TBS-Tween, then incubated in Alexa-488 goat anti-rabbit secondary antibody 1:1000 in TBS with 0.5% v/v normal goat serum for three

hours at room temperature in a dark humidity chamber. They were then cover-slipped using an aqueous mounting solution.

4.3.5 Statistics

Data are reported as mean \pm standard error and analyzed by ANOVA. The percentage of area staining PI positive was transformed using a log transform to homogenize the variance. Data was considered significant at $p < 0.05$.

4.4 RESULTS

4.4.1 Rapid stretch of organotypic hippocampal slice cultures results in increased cell death in the CA3 24 hours after injury

Previous work with this in vitro model shows that 50% strain is below the threshold required for cysteine protease activation organotypic hippocampal slice cultures (OHSCs), while 75% strain produced both calpain and caspase-3 activation throughout regions of the hippocampus (DeRidder et al. 2006). We first examined if a similar result could be found using propidium iodide (PI) labeling to measure cell death in the hippocampus. Applying a 50% strain to OHSCs resulted in a small but non-significant increase in cell death in the CA3, hilus, and DG regions of the hippocampus. The area of PI positive labeling increased in the CA3 from $0.07 \pm 0.02\%$ (mean \pm SE) ($n = 24$) in uninjured cultures to $0.17 \pm 0.06\%$ ($n = 21$) after 50% injury in the CA3 region, and $0.20 \pm 0.03\%$ in uninjured cultures to $0.33 \pm 0.07\%$ in 50% injured the dentate gyrus (Figure 4.3B). Increasing the strain to 75% resulted in a large and statistically significant increase in cell death in the CA3 compared to uninjured cultures, with PI labeling increasing to $0.33 \pm 0.08\%$ of total area ($p < 0.001$, $n = 28$) in the 75% injured cultures. The level of cell death in the CA3 increased further in the CA3 after a 100% strain, with the area of PI labeling increasing to $0.39 \pm 0.10\%$ of total area ($p < 0.001$ compared to uninjured, $n = 22$) (Figure 4.3B). The vast majority of PI labeling was detected in those areas which are highly enriched in neurons (Figure 4.3A). The results confirm that rapid mechanical strain produces increased cell death in OHSCs 24 hours after injury, with the amount of cell death related to the magnitude of the applied strain. The cell death is most

consistently increased in the CA3, with significant increases detected after 75% and 100% strains.

4.4.2 Inhibiting NMDA receptor activation attenuates cell death in CA3 region of OHSCs

With the CA3 region showing the highest relative amount of cell death indicated by PI labeling, we next considered if this cell death could be reduced using inhibitors targeting the NMDAR component of the glutamatergic receptors. Blocking both synaptic and extrasynaptic NMDARs by pretreatment with the broad spectrum NMDAR antagonist 2-amino-5-phosphovalerate (APV, 50 μ M) was effective in completely eliminating increased PI labeling in the CA3 after a 75% strain, with labeling decreasing from $0.33 \pm 0.08\%$ in untreated cultures to $0.03 \pm 0.01\%$ in APV-treated cultures ($n = 7$, $p < 0.01$) (Figure 4.4). APV also reduced cell death after a 100% strain to levels that were not significantly higher than uninjured controls, lowering PI labeling from $0.39 \pm 0.10\%$ in untreated cultures to $0.14 \pm 0.05\%$ in APV-treated cultures ($n = 9$, $p < 0.05$) (Figure 4.4).

4.4.3 Extrasynaptic NMDAR inhibition produces a selective protection against cell death after stretch

We next considered if the extrasynaptic NMDARs were primarily responsible for mediating cell death across the stretch levels studied by pretreating OHSCs with ifenprodil (3 μ M, Sigma-Aldrich) at concentrations reported to preferentially block extrasynaptic NMDARs (Williams 1993). At 24 hours after injury we found that ifenprodil was effective in significantly inhibiting cell death in the CA3 region of cultures

subjected to 75% strain, reducing PI labeling to $0.07 \pm 0.03\%$ ($p < 0.01$, $n = 10$) (Figure 4.4). However, unlike in our APV treatment, cell death was reduced after 100% strain, but not to the level of significance, with PI labeling an average of $0.23 \pm 0.08\%$ of the CA3 ($n = 13$) (Figure 4.4). Therefore, unlike the broad spectrum inhibition of the NMDAR population with APV pretreatment, these data show that targeting a subpopulation of NMDARs typically associated with cell death will lead to protection at some, but not all, levels of mechanical injury.

4.4.4 Inhibition of intracellular calcium increase in astrocytes is protective after severe injury

The participation of extrasynaptic NMDARs in mediating at least some cell death allows for the possibility that these receptors are being activated by neurotransmitters released from nearby astrocytes (Hardingham et al. 2002). To determine the role of calcium-induced release of neurotransmitter from astrocytes in the NMDAR-mediated toxicity, slices were pre-incubated with the calcium chelator BAPTA-AM (100 μ M). Several studies have indicated that in hippocampal slice cultures BAPTA-AM-like fluorescent probes are selectively loaded into astrocytes rather than neurons (Liu et al. 2004). To confirm this, the BAPTA-AM analog Calcium Crimson was loaded into OHSCs, fixed, and co-labeled for Neu-N for neurons and GFAP for astrocytes. Figure 4.5A-F show that Neu-N and Calcium Crimson labeling do not overlap to any significant degree, while GFAP and Calcium Crimson labeling overlap extensively. Based on this data and on previous studies, we concluded that BAPTA-AM was loading preferentially into astrocytes.

Pre-incubation with BAPTA-AM prior to injury significantly reduced cell death in the OHSCs after 100% stretch. A reduction, but not significant, was observed in cell death in the CA3 after 75%. However, cell death at 75% was also not significantly higher than uninjured, BAPTA-treated cultures, making interpretation of the results at this injury severity difficult. PI labeling after BAPTA-AM at 75% reduced the cell death to $0.20 \pm 0.08\%$ of the CA3 area ($n = 12$), while at 100% the cell death was $0.12 \pm 0.03\%$ ($n = 11$, $p < 0.05$, Figure 4.5G). These data suggest signaling in astrocytes contributes to CA3 cell death, at least at 100% stretch.

4.4.5 mGluR5 is not involved in mediating stretch-induced NMDAR-mediated cell death in OHSCs

Based on the BAPTA-AM results, we investigated whether inhibition of receptors that are known to be involved in generating calcium transients in astrocytes also could inhibit cell death. The group I metabotropic glutamate receptor mGluR5 is the dominant calcium-linked astrocytic metabotropic glutamate receptor (Schools and Kimelberg 1999) and activation of this receptor has been shown to enhance the release of glutamate from astrocytes (Araque et al. 1998a; Araque et al. 1998b). Moreover, mGluR5 receptors on neurons and can work cooperatively with the NMDAR to increase injury-induced activity (Lea et al. 2002). When we pretreated OHSCs with 2-methyl- 6-(phenylethynyl)-pyridine (MPEP, $50\mu\text{M}$, Sigma-Aldrich), a mGluR5 antagonist, before either a 75% or 100% strain there was no significant reduction in overall cell death in the CA3, with 75% strain resulting in PI labeling of $0.31 \pm 0.14\%$ of the CA3 area ($n = 15$) and 100% strain resulting in $0.29 \pm 0.09\%$ ($n = 13$) (Figure 4.6A). When OHSCs were incubated 72 hours

after injury before imaging, we again found MPEP failed to attenuate cell death in the CA3, with untreated cultures showing PI labeling in $0.34 \pm 0.13\%$ ($n = 16$) and $0.48 \pm 0.13\%$ ($n = 13$) of the CA3 area after 75% and 100% injuries, respectively, while MPEP-treated cultures showed PI labeling in $0.55 \pm 0.23\%$ ($n = 7$) and $0.48 \pm 0.16\%$ ($n = 8$) of the CA3 area (Figure 4.6B). Even with the shortcoming that MPEP administration inhibited mGluR5 receptors on both neurons and astrocytes, it is clear from these data that cell death after stretch is not dependent on the activation of metabotropic mGluR5 receptors.

4.4.6 Extracellular ATP and activation of purinergic receptors are linked to cell death in OHSCs following mechanical injury

An alternative mechanism for stimulating calcium increases in astrocyte is through the activation of P2 purinergic receptors. P2 purinergic receptors are found on both neurons and glia, but are the major signaling mechanism in glial communication. The purinergic receptor activation can lead to further astrocyte ATP release from astrocytes, potentially providing a persisting release of ATP. ATP is released in large quantities after TBI (Franke et al. 2006) and activation of P2 receptors has been connected with neurodegeneration and reactive gliosis (Franke et al. 2006). P2 receptors have also been closely linked with NMDAR function, both through direct modulation of receptor activity (Hussl and Boehm 2006) and through activation of intracellular calcium on nearby astrocytes, leading to neurotransmitter release, including the release of glutamate (Domercq et al. 2006; Wirkner et al. 2006; Wirkner et al. 2002). For this

reason, we examined if blocking the action of extracellular ATP was effective in reducing cell death.

Indeed, digesting extracellular ATP with the ATP hydrolyzing enzyme apyrase (20U/mL, Sigma-Aldrich) reduced PI labeling after 75% injury to $0.07 \pm 0.02\%$ ($n = 12$) of the CA3 area, and reduced labeling after 100% injury to $0.03 \pm 0.02\%$ ($n = 7$) of the CA3 area (Figure 4.7). Both reductions were significantly lower than untreated OHSCs ($p < 0.05$) and were indistinguishable from uninjured cultures. However, this treatment is relatively non-specific and part of the effect may be due to the acceleration of the production of adenosine, which may increase the protective effect by limiting synaptic glutamate via inhibitory adenosine receptors. A more specific treatment was PPADS (10 μ M, Sigma-Aldrich), a non-selective P2 receptor antagonist which reduced cell death after both moderate and severe injury at 24 hours, resulting in PI labeling of $0.09 \pm 0.03\%$ ($n = 19$) of the CA3 after 75% injury and $0.16 \pm 0.04\%$ ($n = 24$) after 100% injury (Figure 4.7). Since the results of the P2 receptor blockers mimic the effectiveness of APV and, at 75% stretch, ifenprodil, these results together suggest that NMDAR-dependent stretch-induced cell death in OHSCs is connected to activation of P2 receptors by extracellular ATP.

We next considered if the protection against stretch-induced cell death was associated with the metabolic P2Y₁ receptor, a receptor widely expressed on astrocytes and shown to be involved in releasing astrocytic glutamate as well as stimulating proliferation and gliotic responses (Domercq et al. 2006; Franke et al. 2004; Franke et al. 2001). Pretreatment with the specific P2Y₁ receptor antagonist MRS 2179 (10 μ M,

Sigma-Aldrich) reduced PI labeling to $0.04 \pm 0.02\%$ ($n = 10$) of CA3 area after 75%, to $0.14 \pm 0.05\%$ ($n = 12$) of CA3 area after 100%, which was significantly lower than untreated cultures ($p < 0.05$) (Figure 4.7). Interestingly, the reduction seen with MRS 2179 was similar to the broad-spectrum P2 receptor antagonist PPADS; no statistical difference was noted between PPADS and the more specific MRS 2179 treatment at all stretch levels studied.

4.5 DISCUSSION

Several past reports show that the hippocampus is specifically vulnerable to injury following TBI (Beer et al. 2000; Bramlett et al. 1997; Hicks et al. 1996; Lowenstein et al. 1992; Smith et al. 1995). In this study we confirmed that mechanical injury induces subregion-specific cell death in organotypic hippocampal slice cultures 24 hours after injury, with the CA3 region being most susceptible at every injury severity investigated. We found a strain-dependent increase in cell death in the CA3 after moderate (75%) and severe (100%) injury which could be inhibited by a broad-spectrum NMDA receptor antagonist; however, a more selective antagonist for extrasynaptic, NR2B-containing NMDARs significantly reduced cell death only after moderate injury. In addition, we examined the upstream mechanisms responsible for triggering glutamate release onto NMDARs. Increases in astrocytic calcium appeared to be a key requirement of cell death after severe stretch injury, as the selective loading of a calcium chelator (BAPTA-AM) in astrocytes provided protection against death. Although mGluR5 receptor activation on astrocytes can lead to persistent calcium waves, we found that inhibiting the metabotropic glutamate receptor mGluR5 was completely ineffective in reducing cell death after medium or severe injury. Conversely, blocking P2 purinergic signaling was significantly effective in inhibiting cell death after injury, with both non-specific P2 purinergic inhibitors (apyrase and PPADS) and a specific antagonist of the P2Y1 receptor subtype capable of reducing cell death significantly in comparison to untreated controls. These results suggest that NMDARs and P2 purinergic receptors, primarily through the P2Y1 receptor subtype linked to astrocytic calcium, are acting along the same pathway after

injury leading to cell death, since blocking P2Y1 activation, astrocytic calcium, or

NMDAR activation is sufficient to dramatically reduce cell death.

Antagonism of the NMDAR has been effective in limiting cell death and damage in the hippocampus after excitotoxicity (Sattler et al. 2000), ischemic insults (Arundine and Tymianski 2004), and TBI (Bullock and Fujisawa 1992; Dempsey et al. 2000; Faden et al. 1989; Faden et al. 2003; Rao et al. 2001; Regan and Choi 1994; Shapira et al. 1990). Several previous studies have implicated NR2B-containing NMDARs as being responsible for increased cell death after injury or disease (Hardingham et al. 2002; Wang and Shuaib 2005), while others have shown that over-activation of either extrasynaptic or synaptic NMDARs can lead to cell death under the proper conditions (Sattler et al. 1998; Sattler et al. 2000). We observed a transition from extrasynaptic NMDAR-mediated toxicity at moderate injury to a combination of extrasynaptic and synaptic NMDAR-mediated toxicity at the most severe injury. The lack of inhibition for the NR2B-containing NMDAR, when combined with the observation of complete blockade eliminating cell death, indicated that both extrasynaptic and synaptic NMDARs are responsible for cell death after the most severe injury in our model. Even though synaptic NMDAR activation has been linked to pro-survival stimuli (Hardingham et al. 2002), our data suggest a sufficiently high level of synaptic receptor activation can cause cell death, as has been reported by others (Sattler et al. 2000). These data suggest that, unlike in other diseases or injury conditions, both groups of NMDA receptors are involved in mediating cell death after high levels of mechanical injury, and that activation

of the death signal may be dependent on the upstream signaling from activating both NMDAR subpopulations.

The most obvious source of glutamate for activation of synaptic NMDARs is from synaptic vesicles, and the unregulated release of glutamate from synaptic regions has been suggested to be involved in excitotoxic cell death after injury in several models of TBI and ischemia (Rothman and Olney 1986). However, an alternative source of glutamate is from release by nearby astrocytes, which is capable of activating extrasynaptic NMDARs on adjacent neurons. Studies have shown that astrocytic release of glutamate can lead to synaptic alteration and, in some cases, neuronal death (Bezzi et al. 2004; Fellin et al. 2006a; Kang et al. 2005; Parpura and Haydon 2000). As noted above, astrocytes possess the protein machinery for vesicular release of glutamate (Anlauf and Derouiche 2005; Bezzi et al. 2004; Montana et al. 2004; Zhang et al. 2004b), and vesicle fusion and subsequent glutamate release has been shown to be dependent on increase in intracellular calcium (Montana et al. 2004; Zhang et al. 2004a). Based on our data and these previous studies we examined the potential role of glutamate release from astrocytes onto neuronal NMDARs.

The application of BAPTA-AM to specifically reduce calcium increases in astrocytes was sufficient to reduce cell death significantly after severe injury, and reduced death after moderate injury, but not to the level of statistical significance. BAPTA-AM treatment of OHSCs has been shown to last no more than 6 hours before the BAPTA is completely broken down or excluded from the cell (Abdel-Hamid and Tymianski 1997), so the inconsistency of the results may be due to the loss of

effectiveness of the treatment by 24 hours. Nonetheless, the persistence of some level of protection after moderate injury and a significant level of protection after severe injury suggested that astrocytes were involved in activating NMDARs after mechanical injury.

We examined both glutamatergic and purinergic pathways that were likely to induce calcium increases in astrocytes after injury to investigate how these pathways also affected cell death. The dominant calcium-associated metabotropic glutamate receptor on astrocytes is the mGluR5 (Biber et al. 1999; Schools and Kimelberg 1999), which found on processes near synapses and is involved in sensing glutamate levels in the synapse (Porter and McCarthy 1996). It is also involved in inducing reactive gliosis (Fields and Burnstock 2006), indicating that it is part of a major signaling pathway in astrocytes. Activation of the mGluR5 receptor triggers calcium increases (Nakahara et al. 1997) which can lead to release of vesicular glutamate release from astrocytes (Zhang et al. 2004a), thereby allowing astrocytes to activate extrasynaptic NMDARs (Fellin et al. 2006a; Kang et al. 2005; Parpura and Haydon 2000). Significantly, antagonists of this receptor were effective in reducing cell death after excitotoxic, ischemic, and TBI models (Bao et al. 2001; Movsesyan et al. 2001; Strasser et al. 1998), indicating that there a pathological role for the mGluR5 receptor. Based on these reports, we suspected that over-activation of the astrocytic mGluR5 receptor located near damaged synapses may induce a calcium-dependent release of glutamate, thereby inducing NMDAR activation across many neurons. However, in our model of mechanical injury, we found that an antagonist to the mGluR5 receptor was completely ineffective in preventing cell death.

A second and less commonly studied pathway typically leading to intracellular calcium increases in astrocytes is through the activation P2 purinergic receptors which are activated by extracellular ATP. ATP is released in large quantities after TBI, both through regulated release mechanisms and from the unregulated release from ruptured cells (Erb et al. 2006). P2 receptors are widespread in the brain, present on neurons, astrocytes, microglial, and other cells. In neurons, extracellular ATP can alter neuronal glutamate signaling through the action of pre- and post-synaptic ionotropic P2X receptors and metabotropic P2Y receptors (Duan and Neary 2006). In CA1 hippocampal neurons, P2X and P2Y receptors mediate the release of glutamate at presynaptic terminals, with P2X receptors increasing glutamate release and P2Y receptors inhibiting release (Rodrigues et al. 2005). Alternatively, ATP can excite hippocampal interneurons through the activation of the P2Y1 subtype of receptors, leading to enhanced inhibition in the hippocampus (Kawamura et al. 2004). Moreover, ATP can modulate neuronal signaling through its rapid conversion to adenosine and subsequent activation of adenosine receptors generally leading to suppression of synaptic activity (Newman 2003). However, these mechanisms do not have a direct relationship with astrocytic calcium increases, and therefore are unlikely to be involved in the BAPTA-AM sensitive cell death that we detected in our study.

A more direct link between extracellular ATP and astrocytic calcium-dependent NMDAR activation is through the activation of P2 receptors on nearby astrocytes. In astrocytes, ATP is the major signaling mechanism between adjacent cells, resulting in intracellular calcium waves that can propagate for long distances in vitro (Cotrina et al.

2000). ATP can also trigger the release of glutamate from astrocytes through calcium-dependent and calcium-independent mechanisms (Duan et al. 2003; Fellin et al. 2006b; Wirkner et al. 2006; Wirkner et al. 2002). Among the many P2 receptor subtypes, P2X7 activation on astrocytes can cause the formation of large pores through which ions and small molecules can flow (Duan and Neary 2006). P2X7 pores are permeable to both ATP and glutamate, and P2X7 activation has been shown to be directly linked to calcium-independent glutamate release from astrocytes with subsequent activation of NMDARs on adjacent neurons (Fellin et al. 2006b). Alternatively, P2Y1 receptors are widely expressed on astrocytes and are linked to intracellular calcium through a G-protein coupled mechanism (Domercq et al. 2006; Erb et al. 2006; Franke et al. 2006). Significantly, Domercq et al showed that this receptor subtype is involved in glutamate release specifically from astrocytes, finding that stimulation of P2Y1 does not release glutamate from hippocampal synaptosomes or microglia (Domercq et al. 2006). For these reasons, we investigated the role of P2Y1 receptors in mediating NMDAR-dependent cell death, given that P2Y1 receptor activation is linked to intracellular calcium and glutamate release in astrocyte.

In studying the purinergic pathways, we first applied non-specific purinergic receptor inhibitors to observe the overall contribution of extracellular ATP. P2 purinergic receptor blockers have been shown to be effective in preventing cell death several models of neuropathology (Abbracchio and Verderio 2006; Cavaliere et al. 2001; Lammer et al. 2006; Neary and Kang 2005). Because purine receptors are seen on almost all cell types in the brain, the application of apyrase, which hydrolyzes ATP, and PPADS,

which is a non-specific P2 receptor antagonist, could not be used to indicate cell specificity. However, they were both effective in dramatically reducing cell death after both moderate and severe injury, confirming the involvement of extracellular ATP in NMDAR-induced cell death after mechanical injury. We cannot discount the possibility that the effects of apyrase may also be mediated through the increased efficiency in adenosine production, which could lead to increased inhibition of glutamate release at the synapse through the activity of adenosine receptors. Likewise, PPADS is a broad-spectrum P2 receptor antagonist and may have resulted in decreased cell death through the antagonism of a wide range of neuronal and glial signal transduction pathways.

When we investigated whether the P2Y1 was involved in trauma-induced death, our data showed that inhibiting this receptor was sufficient to reduce NMDAR-mediated cell death at both moderate and severe injury. In the moderate injury condition, we were able to completely eliminate injury-induced cell death by blocking extrasynaptic NMDARs with ifenprodil or by blocking P2Y1 receptors with MRS 2179. Based on the prevalence of P2Y1 receptors on astrocytes the ability for astrocytic P2Y1 receptors to induce glutamate, as well as the ability for astrocytic glutamate to activate extrasynaptic NMDARs, we propose that cell death is primarily mediated through an astrocytic signaling pathway at this severity of injury in our model.

In the more severe injury condition we were able to reduce but not eliminate cell death by blocking P2Y1 receptors with MRS 2179 or by inhibiting calcium increases in astrocytes with BAPTA-AM, and were able to completely eliminate cell death with the broad-spectrum NMDAR antagonist APV or by enzymatically digesting extracellular

ATP with apyrase. In this condition we suspect that glutamate is becoming excitotoxic via both synaptic and extrasynaptic NMDARs, which would explain the loss of efficacy of ifenprodil but the continued efficacy of APV. Cell death is still mediated partially by P2Y1 receptor-mediated glutamate release from astrocytes, given the ability of MRS 2179 and BAPTA-AM to reduce but not eliminate cell death. We suspect that synaptic glutamate released from the pre-synaptic terminal is responsible for much of the remaining cell death, with the production of inhibitory adenosine most likely contributing to the protective effects of apyrase. Taken together, these results strongly suggest the involvement of calcium-induced glutamate release through a P2Y1 purinergic receptor pathway in NMDAR-mediate cell death after injury, with additional stimulation provided by synaptically released glutamate.

Overall, these data point to important linkages between purinergic and NMDA receptors in influencing cell death in the hippocampus after traumatic mechanical injury. The link between these receptors appears to indicate the tight coupling between astrocytes and neurons after traumatic injury, and how the ATP-mediated release of glutamate from astrocytes can, in turn, drive cell fate in the CA3 after TBI. With this potential coupling emerges new therapeutic opportunities for TBI which not only target neurons but also key activating mechanisms in astrocytes that can subsequently improve cell survival after TBI.

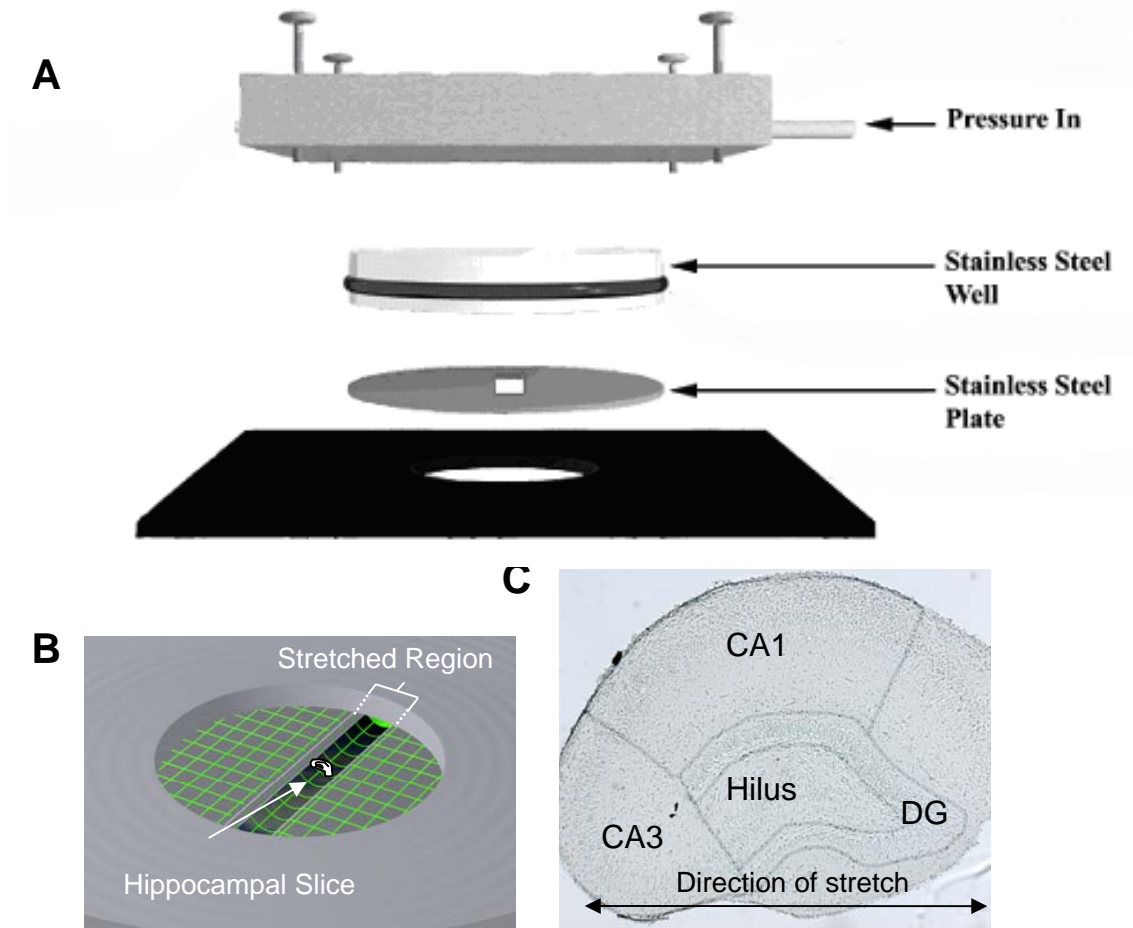


Figure 4.1. A: Overview of the injury device. B: Organotypic hippocampal slice cultures (OHSCs) were cultured for 9-10 DIV on transparent, elastic membranes. An air pressure pulse was delivered to the culture surface, deflecting the membrane downward, producing a 50%, 75%, or 100% strain. A metal plate beneath part of the culture restricted the region of stretch to a 6 mm x 18 mm region. The membrane strain produced by such geometry is nearly uniform throughout the stretched region. C: Representative OHSC stained with vector methyl green. For cell death measurements the CA1, CA3, hilus, and dentate gyrus (DG) subregions were separated as shown. The arrow indicates the orientation of the strain field during injury.

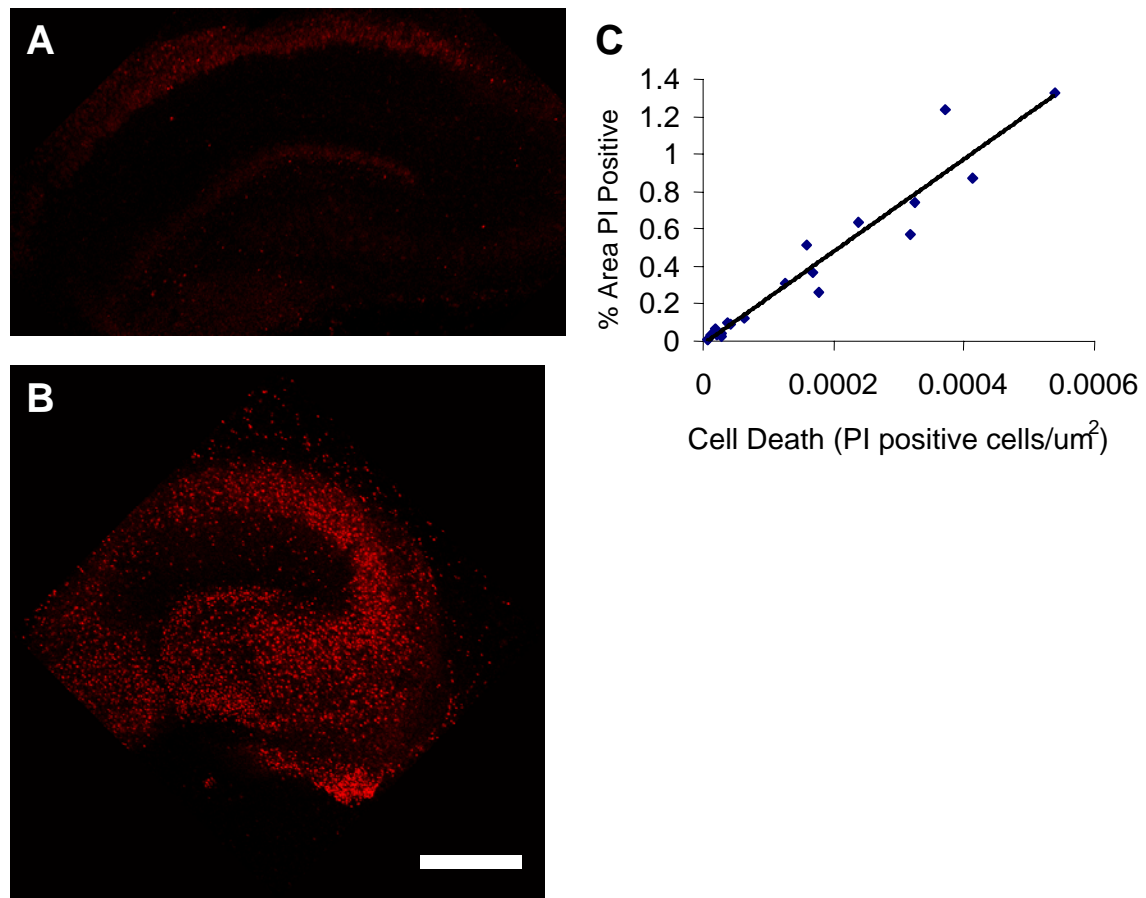


Figure 4.2. PI labeling of OHSCs. Propidium iodide was added to the cultures 15 minutes prior to injury and left on until imaging on a confocal microscope 24 hours later. NMDA-treated cultures (B) and naïve sham cultures (A) were used as controls. Scale bar = 500μm. C: The cell death data was reported as the percent of the area of each region that labeled positive for PI (# of PI positive pixels / total pixels). Figure 4.2C shows the relationship between % Area PI positive and the concentration of cell death per μm². This data was collected from a random subset of cultures. The relationship between the area of PI labeling and the concentration of cell death in the CA3 is linear.

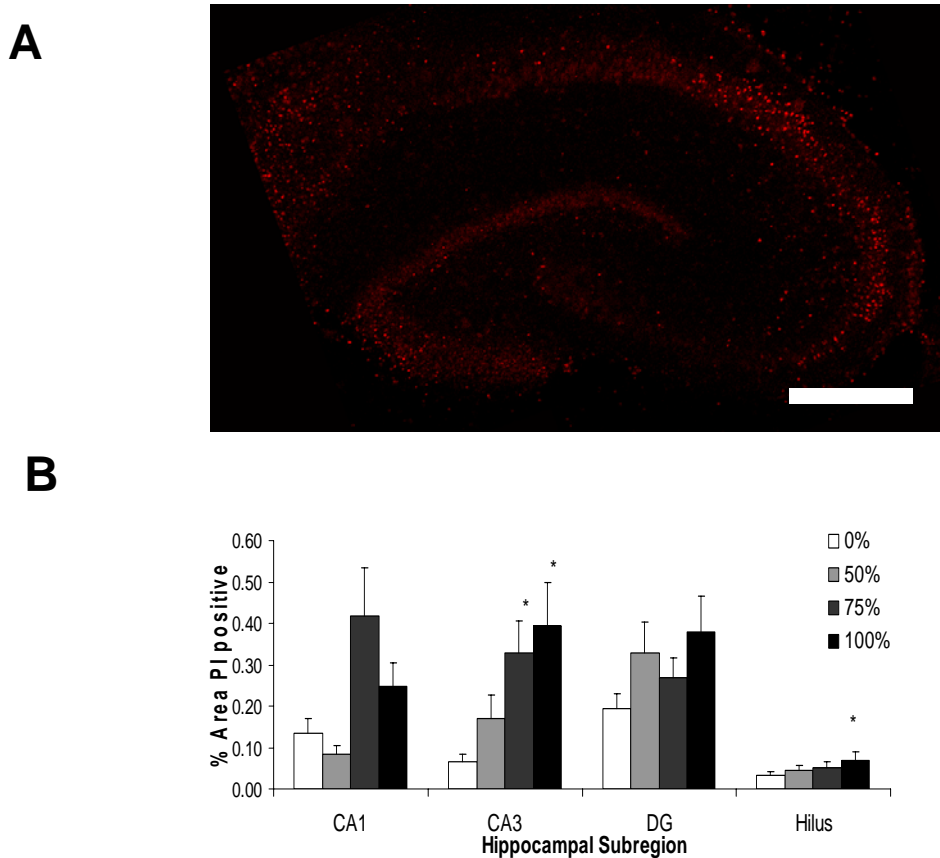


Figure 4.3. Mechanical injury produced an increase in cell death in the CA3 of hippocampal slice cultures 24 hours after a mechanical injury. A: Representative image of a hippocampal slice stained with PI 24 hours after a 100% strain-induced injury. Scale bar = 500 μ m. B: Quantification of a single image of PI staining in OHSCs 24 hours after injury. PI staining was significantly increased in the CA3 region after both 75% and 100% strains. * = $p < 0.05$ vs. 0%.

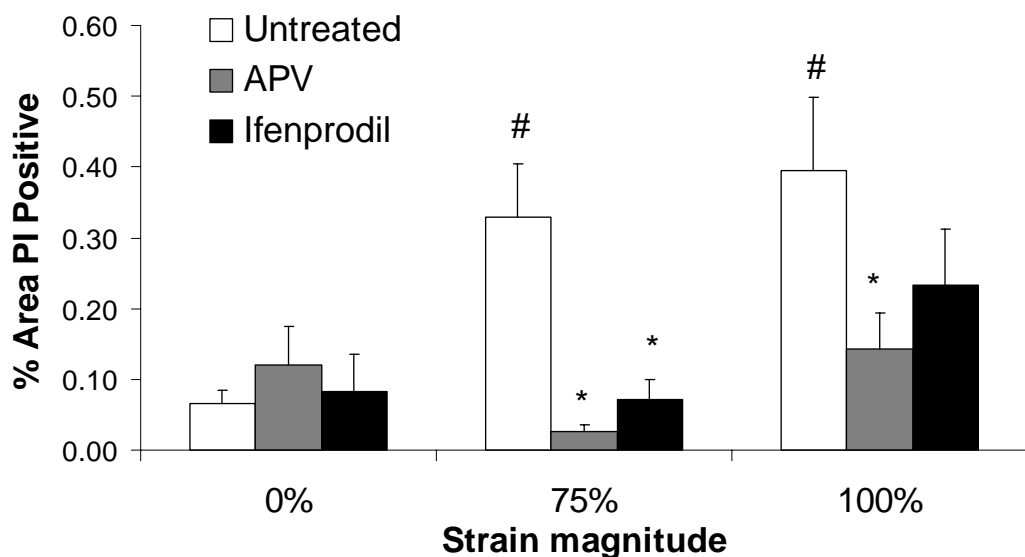


Figure 4.4. Treatment with NMDA receptor antagonists attenuated cell death after injury. APV, a non-specific NMDAR antagonist, significantly reduced cell death in the CA3 at 24 hours after injury after 75% and 100% strain. Ifenprodil, an antagonist of NR2b-containing NMDARs, was effective in reducing cell death after a 75% strain but lost effectiveness at the higher strain level. # = $p < 0.05$ vs 0%. * = $p < 0.05$ compared to untreated cultures.

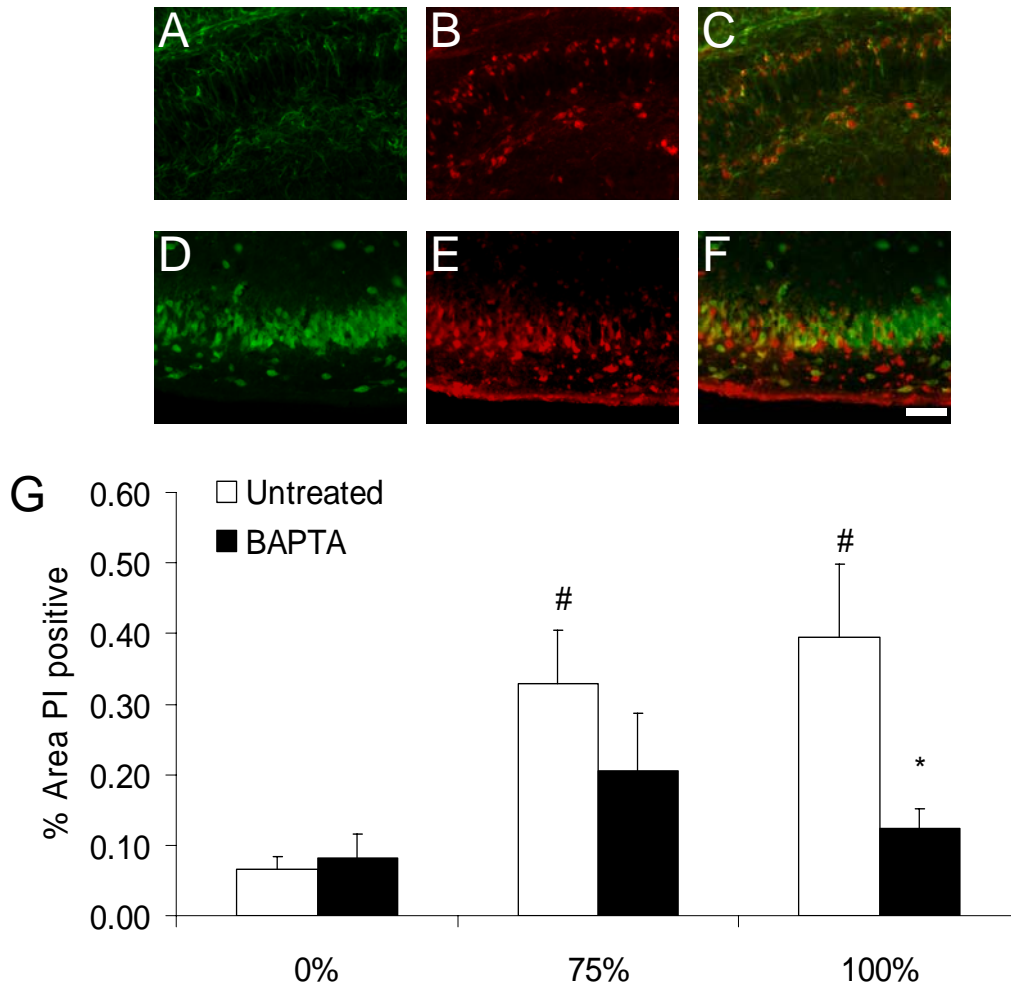


Figure 4.5. A-C: BAPTA-AM analog Calcium Crimson (B) loaded preferentially into astrocytes stained positive for GFAP (A) Figure 4.5C shows overlay of staining. D-F. Calcium Crimson (E) generally did not co-label cells staining positive for Neu-N (D) in hippocampal slices Figure 4.5F shows overlay of staining. Scale bar = 100 μ m G: Pre-incubating with BAPTA-AM (100 μ M) significantly reduced cell death at 24 hours after 100% injury. # = $p < 0.05$ vs 0%. * = $p < 0.05$ compared to untreated cultures.

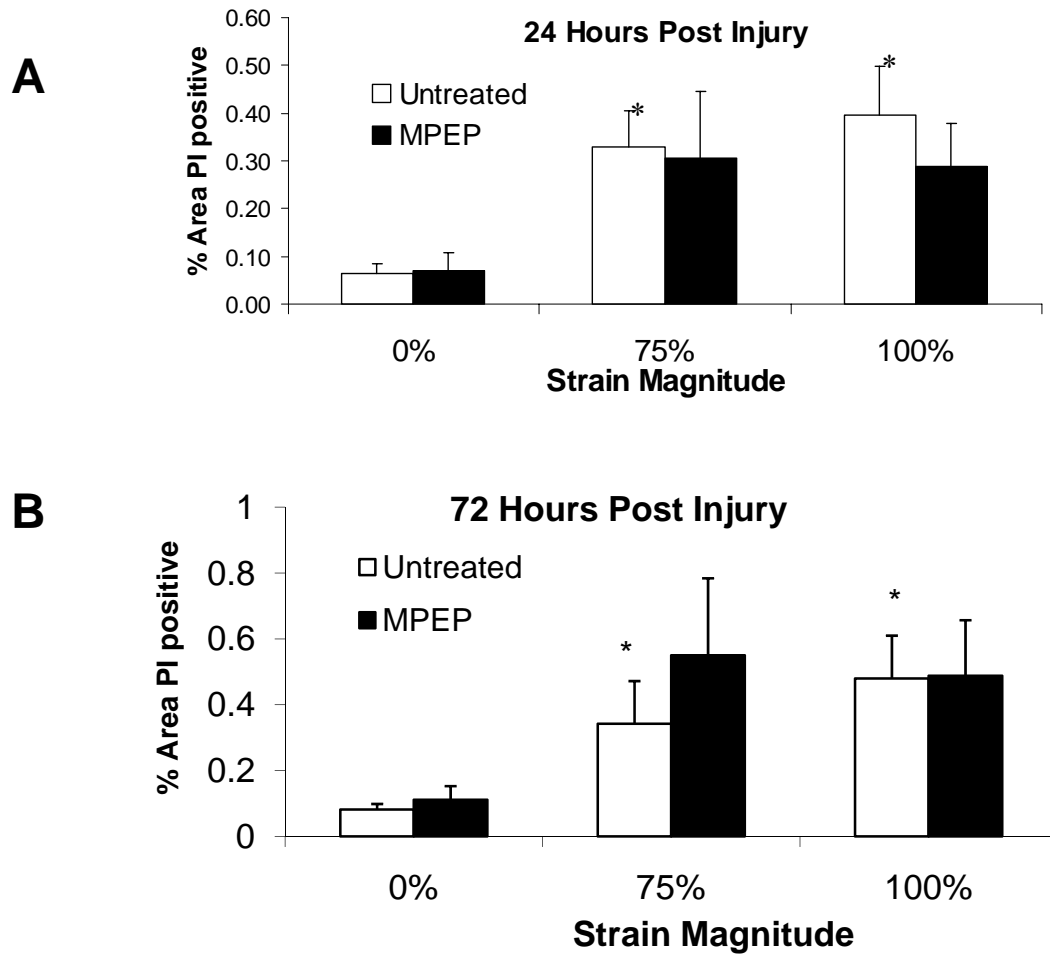


Figure 4.6. Injury-induced CA3 cell death in OHSCs was not dependent on activation of mGluR5. MPEP, an mGluR5 antagonist, was ineffective in reducing cell death in the CA3 region of OHSCs 24 hours (A) or 72 hours (B) after a 75% or 100% injury. * = $p < 0.01$ vs. 0%.

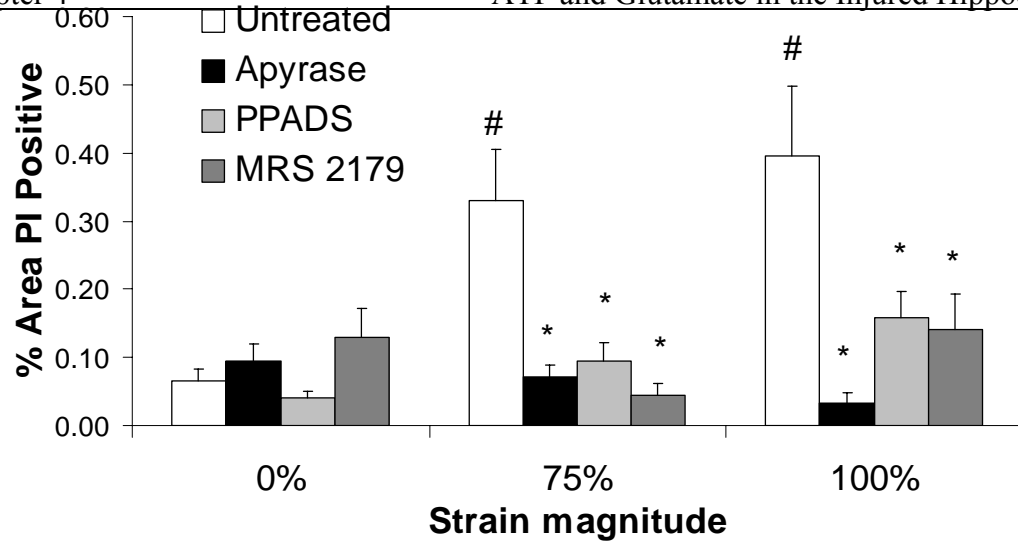


Figure 4.7. P2 purinergic receptors mediated cell death in the CA3 region 24 hours after injury. The application of PPADS, a non-specific P2 receptor antagonist, significantly reduced cell death after 75% and 100% strain. Likewise, enzymatically degrading extracellular ATP with apyrase completely eliminated stretch-induced cell death. The P2Y1 receptor antagonist MRS 2179 restricted cell death in a similar manner as PPADS. # = $p < 0.05$ vs 0%. * = $p < 0.05$ compared to untreated cultures.

Chapter 5: Potential Limitations and Future Directions

5.1 Astrocytes Modulate Calcium Wave Communication in Response to Mechanical Injury

Our calcium wave studies showed that injured astrocytes modulate communication to surrounding regions based on the level of applied injury. Currently there is little clear understanding of the role of calcium signaling in astrocyte networks during physiological signaling (Scemes and Giaume 2006). Even less is known about the long term effects of astrocytic calcium waves after TBI. We investigated one common signaling pathway seen in ATP stimulation of astrocytes, the ERK cascade, and found that calcium waves do not activate this cascade. However, there are many other possible signaling mechanisms that could be triggered by intense intercellular calcium waves. For example, other MAPK pathways, including JNK, might be activated selectively after specific levels of injury from either ATP signaling or excessive intracellular calcium. It is also possible that the ERK cascade or other cascades are activated at higher levels of injury. As noted previously, the injury severities used in this study were sub-lethal and at the low end of what has been measured in TBI models (Shreiber et al. 1997). It is very probably that as strains approach the threshold for lethal mechanical injury calcium wave communication will initiate more interesting cellular responses in surrounding astrocytes.

The role of injury-induced calcium waves in initiating reactive gliosis may be an avenue for future investigation. Application of exogenous ATP has been shown to induce reactive gliosis in several in vitro models (Neary and Kang 2005), so it is reasonable to assume that ATP-mediated calcium waves may trigger a similar result.

One problem with cultured astrocytes in general, however, is that they are morphologically more closely comparable to reactive astrocytes in vivo than normal astrocytes (Wu and Schwartz 1998). As a result, many of the features of reactive gliosis, such as increased GFAP expression, are harder to detect in vitro than in vivo.

For this reason, it may be valuable to look at injury-induced calcium waves in vivo. An in vivo model could verify whether astrocytes can actually modulate their communication in response to injury magnitude in a pathophysiological condition. In this paradigm the influence of non-astrocytic cells on astrocyte calcium signaling could also be observed, and the more realistic extracellular matrix would clarify the extent to which injury can induce calcium waves in surrounding tissue. This model also would show how far ATP signaling can transmit signals in the brain after injury, since the in vitro model lacks much of the cell distribution that inhibits diffusion and there is much lower activity of ectonucleotidases to degrade ATP. Another interesting phenomenon to look at would be how long calcium waves can elevate intracellular calcium in stimulated astrocytes in vivo, and whether this is dependent on the magnitude of the applied strain. This model would also be able to investigate the effects calcium signaling has on nearby neurons and microglia.

5.2 Mechanical Properties of Astrocytes Change after Injury

In our study of the change in stiffness in astrocytes after mechanical injury we found a correlation between increased GFAP and decreased apparent Young's modulus, especially in non-nuclear regions of the cell. We used a simple indentation protocol to measure cellular stiffness and determined the Young's modulus by fitting the data to a

well known model for interpreting AFM force-indentation curves. However, there are several other methods using AFM that could make these measurements. For instance, the protocol we used consisted of a relatively low frequency (1 Hz) indentation which resulted in measuring essentially only the elastic component of the cell's mechanical properties. Other investigators have measured both the viscous and elastic properties of various cells using high frequency indentation protocols (Lu et al. 2006). These protocols generally give a frequency-dependent value of the modulus and which is not easily comparable to our model.

We picked two regions to concentrate on in measuring the change in cellular stiffness: nuclear regions (membrane areas above the nucleus) and non-nuclear regions. While these were easily identifiable areas, there are many other substructures in the cytoplasm that may have a major role in determining the local stiffness. Beside the presence of actin filaments, organelles like mitochondria may have a significant impact on the results. Also, in especially thin areas of the cell the force-deflection profile may start to detect influences from the underlying substrate. We attempted to limit this effect in two ways. First, we used confluent cultures in which there were virtually no cell borders that were not touching other cells, and, as a result, we hoped that the edges of these cells would be generally thicker than in isolated cells. We also avoided indentation very close to the edge of the cell, on the assumption that the edges would be thinner than the more central areas.

We showed a correlation between increased GFAP immunoreactivity and cell softening after mechanical injury. In subsequent experiments this correlation should be

investigated to show a causal relationship. Of course, one major roadblock to this study would be determining the factor that is inducing GFAP immunoreactivity. There are several potential candidates, including ATP, glutamate, and inflammatory cytokines like IL-1 β . The complicating factors, however, are that treatments that block the injury-induced activity of these molecules might also block normal, baseline signaling and thus affect cytoskeletal organization. Likewise, induction of increased GFAP expression may also have a large number of effects that could affect actin organization, such as inducing proliferation or process growth, and these changes may cause a softening of the cell separate from the GFAP change. Because of these complicating factors, we believe the determining the causal relationship between GFAP expression and astrocyte softening may be very difficult.

5.3 P2Y1 and NMDA Receptors Mediate Cell Death Patterns in the CA3 Region of Injured Organotypic Hippocampal Slice Cultures

We found that P2Y1 receptors and NMDARs are involved in mediating cell death in OHSCs 24 hours following injury. In this study we attempted to show that astrocytes responding to excessive injury-induced release of ATP release glutamate onto neuronal NMDARs in a calcium-dependent manner. In general, the data support such a hypothesis. However, there are many questions that still need to be answered in this study. For example, our study gave us no information about the therapeutic window for NMDAR antagonists or P2Y1 antagonists. We pretreated all of our cultures, which is clearly not a clinically relevant model of treatment. In future studies these drugs could be applied at various time points to determine the effective treatment window. In addition,

we only report data for 24 hours after injury. It is possible that the treatments applied in this study simply delay cell death. Future studies can examine whether these treatments are protective over longer time periods.

This study also did not investigate if treatment with P2Y1 receptor antagonists reduced cell death in a specific cell type or if all cell types were protected equally. Previous work using our model of injury reported that cell death was relatively evenly mixed between astrocytes and neurons, with oligodendrocytes providing a much smaller number of dead cells at 24 hours (DeRidder et al. 2006). In this thesis we showed that at the severe injury level the P2Y1 receptor antagonist only offered partial protection in the CA3. A study that is planned for the near future will investigate whether the P2Y1 receptor antagonist is specifically protective to astrocytes or neurons. Likewise, the type of cell death, necrotic or apoptotic, was not investigated in our study, since propidium iodide staining does distinguish. However, studies using antibodies to caspase-3 and calpain-mediated spectrin-breakdown product can determine the mix between apoptotic and necrotic death, respectively (DeRidder et al. 2006). In addition, activation of cell death pathways or kinase pathways that are associated with cell death (ERK, JNK, etc.) could be studied to determine if there is a correlation between activation of these pathways and increased cell death. Inhibition of these pathways may help determine a causal link between activation and death.

Bibliography

- Abbracchio MP, Ceruti S, Bolego C, Puglisi L, Burnstock G, Cattabeni F. 1996. Trophic roles of P2 purinoceptors in central nervous system astroglial cells. *Ciba Found Symp* 198:142-7; discussion 147-8.
- Abbracchio MP, Verderio C. 2006. Pathophysiological roles of P2 receptors in glial cells. *Novartis Found Symp* 276:91-103; discussion 103-12, 275-81.
- Abdel-Hamid KM, Tymianski M. 1997. Mechanisms and effects of intracellular calcium buffering on neuronal survival in organotypic hippocampal cultures exposed to anoxia/aglycemia or to excitotoxins. *J Neurosci* 17(10):3538-53.
- Alonso JL, Goldmann WH. 2003. Feeling the forces: atomic force microscopy in cell biology. *Life Sci* 72(23):2553-60.
- Anderson CM, Bergher JP, Swanson RA. 2004. ATP-induced ATP release from astrocytes. *J Neurochem* 88(1):246-56.
- Angulo MC, Kozlov AS, Charpak S, Audinat E. 2004. Glutamate released from glial cells synchronizes neuronal activity in the hippocampus. *J Neurosci* 24(31):6920-7.
- Anlauf E, Derouiche A. 2005. Astrocytic exocytosis vesicles and glutamate: a high-resolution immunofluorescence study. *Glia* 49(1):96-106.
- Araque A, Carmignoto G, Haydon PG. 2001. Dynamic signaling between astrocytes and neurons. *Annu Rev Physiol* 63:795-813.
- Araque A, Li N, Doyle RT, Haydon PG. 2000. SNARE protein-dependent glutamate release from astrocytes. *J Neurosci* 20(2):666-73.
- Araque A, Parpura V, Sanzgiri RP, Haydon PG. 1998a. Glutamate-dependent astrocyte modulation of synaptic transmission between cultured hippocampal neurons. *Eur J Neurosci* 10(6):2129-42.
- Araque A, Sanzgiri RP, Parpura V, Haydon PG. 1998b. Calcium elevation in astrocytes causes an NMDA receptor-dependent increase in the frequency of miniature synaptic currents in cultured hippocampal neurons. *J Neurosci* 18(17):6822-9.
- Arundine M, Tymianski M. 2004. Molecular mechanisms of glutamate-dependent neurodegeneration in ischemia and traumatic brain injury. *Cell Mol Life Sci* 61(6):657-68.
- Balgude AP, Yu X, Szymanski A, Bellamkonda RV. 2001. Agarose gel stiffness determines rate of DRG neurite extension in 3D cultures. *Biomaterials* 22(10):1077-84.
- Bao WL, Williams AJ, Faden AI, Tortella FC. 2001. Selective mGluR5 receptor antagonist or agonist provides neuroprotection in a rat model of focal cerebral ischemia. *Brain Res* 922(2):173-9.
- Beer R, Franz G, Srinivasan A, Hayes RL, Pike BR, Newcomb JK, Zhao X, Schmutzhard E, Poewe W, Kampfl A. 2000. Temporal profile and cell subtype distribution of activated caspase-3 following experimental traumatic brain injury. *J Neurochem* 75(3):1264-73.
- Bennett MR, Buljan V, Farnell L, Gibson WG. 2006. Purinergic junctional transmission and propagation of calcium waves in spinal cord astrocyte networks. *Biophys J*.

Bibliography

- Bezzi P, Gundersen V, Galbete JL, Seifert G, Steinhauser C, Pilati E, Volterra A. 2004. Astrocytes contain a vesicular compartment that is competent for regulated exocytosis of glutamate. *Nat Neurosci* 7(6):613-20.
- Biber K, Laurie DJ, Berthele A, Sommer B, Tolle TR, Gebicke-Harter PJ, van Calker D, Boddeke HW. 1999. Expression and signaling of group I metabotropic glutamate receptors in astrocytes and microglia. *J Neurochem* 72(4):1671-80.
- Blomstrand F, Aberg ND, Eriksson PS, Hansson E, Ronnback L. 1999a. Extent of intercellular calcium wave propagation is related to gap junction permeability and level of connexin-43 expression in astrocytes in primary cultures from four brain regions. *Neuroscience* 92(1):255-65.
- Blomstrand F, Khatibi S, Muyderman H, Hansson E, Olsson T, Ronnback L. 1999b. 5-Hydroxytryptamine and glutamate modulate velocity and extent of intercellular calcium signalling in hippocampal astroglial cells in primary cultures. *Neuroscience* 88(4):1241-53.
- Bodin P, Burnstock G. 1996. ATP-stimulated release of ATP by human endothelial cells. *J Cardiovasc Pharmacol* 27(6):872-5.
- Bolego C, Ceruti S, Brambilla R, Puglisi L, Cattabeni F, Burnstock G, Abbracchio MP. 1997. Characterization of the signalling pathways involved in ATP and basic fibroblast growth factor-induced astrogliosis. *Br J Pharmacol* 121(8):1692-9.
- Borsello T, Croquelois K, Hornung JP, Clarke PG. 2003. N-methyl-D-aspartate-triggered neuronal death in organotypic hippocampal cultures is endocytic, autophagic and mediated by the c-Jun N-terminal kinase pathway. *Eur J Neurosci* 18(3):473-85.
- Bradbury EJ, Moon LD, Popat RJ, King VR, Bennett GS, Patel PN, Fawcett JW, McMahon SB. 2002. Chondroitinase ABC promotes functional recovery after spinal cord injury. *Nature* 416(6881):636-40.
- Brambilla R, Neary JT, Cattabeni F, Cottini L, D'Ippolito G, Schiller PC, Abbracchio MP. 2002. Induction of COX-2 and reactive gliosis by P2Y receptors in rat cortical astrocytes is dependent on ERK1/2 but independent of calcium signalling. *J Neurochem* 83(6):1285-96.
- Bramlett HM, Dietrich WD, Green EJ, Busto R. 1997. Chronic histopathological consequences of fluid-percussion brain injury in rats: effects of post-traumatic hypothermia. *Acta Neuropathol (Berl)* 93(2):190-9.
- Bullock R, Fujisawa H. 1992. The role of glutamate antagonists for the treatment of CNS injury. *J Neurotrauma* 9 Suppl 2:S443-62.
- Burgueno J, Blake DJ, Benson MA, Tinsley CL, Esapa CT, Canela EI, Penela P, Mallol J, Mayor F, Jr., Lluís C and others. 2003. The adenosine A2A receptor interacts with the actin-binding protein alpha-actinin. *J Biol Chem* 278(39):37545-52.
- Caille N, Thoumine O, Tardy Y, Meister JJ. 2002. Contribution of the nucleus to the mechanical properties of endothelial cells. *J Biomech* 35(2):177-87.
- Cavaliere F, D'Ambrosi N, Ciotti MT, Mancino G, Sancesario G, Bernardi G, Volonte C. 2001. Glucose deprivation and chemical hypoxia: neuroprotection by P2 receptor antagonists. *Neurochem Int* 38(3):189-97.
- Chang L, Goldman RD. 2004. Intermediate filaments mediate cytoskeletal crosstalk. *Nat Rev Mol Cell Biol* 5(8):601-13.

Bibliography

- Charles A. 1998. Intercellular calcium waves in glia. *Glia* 24(1):39-49.
- Charles A. 2005. Reaching out beyond the synapse: glial intercellular waves coordinate metabolism. *Sci STKE* 2005(270):pe6.
- Charles AC, Merrill JE, Dirksen ER, Sanderson MJ. 1991. Intercellular signaling in glial cells: calcium waves and oscillations in response to mechanical stimulation and glutamate. *Neuron* 6(6):983-92.
- Chazot PL. 2004. The NMDA receptor NR2B subunit: a valid therapeutic target for multiple CNS pathologies. *Curr Med Chem* 11(3):389-96.
- Chorna NE, Santiago-Perez LI, Erb L, Seye CI, Neary JT, Sun GY, Weisman GA, Gonzalez FA. 2004. P2Y receptors activate neuroprotective mechanisms in astrocytic cells. *J Neurochem* 91(1):119-32.
- Clapham DE. 1995. Calcium signaling. *Cell* 80(2):259-68.
- Coco S, Calegari F, Pravettoni E, Pozzi D, Taverna E, Rosa P, Matteoli M, Verderio C. 2003. Storage and release of ATP from astrocytes in culture. *J Biol Chem* 278(2):1354-62.
- Collinsworth AM, Zhang S, Kraus WE, Truskey GA. 2002. Apparent elastic modulus and hysteresis of skeletal muscle cells throughout differentiation. *Am J Physiol Cell Physiol* 283(4):C1219-27.
- Cornell-Bell AH, Finkbeiner SM. 1991. Ca²⁺ waves in astrocytes. *Cell Calcium* 12(2-3):185-204.
- Costa KD, Yin FC. 1999. Analysis of indentation: implications for measuring mechanical properties with atomic force microscopy. *J Biomech Eng* 121(5):462-71.
- Cotrina ML, Lin JH, Lopez-Garcia JC, Naus CC, Nedergaard M. 2000. ATP-mediated glia signaling. *J Neurosci* 20(8):2835-44.
- Cotrina ML, Lin JH, Nedergaard M. 1998. Cytoskeletal assembly and ATP release regulate astrocytic calcium signaling. *J Neurosci* 18(21):8794-804.
- Dahl KN, Engler AJ, Pajerowski JD, Discher DE. 2005. Power-law rheology of isolated nuclei with deformation mapping of nuclear substructures. *Biophys J* 89(4):2855-64.
- Dempsey RJ, Baskaya MK, Dogan A. 2000. Attenuation of brain edema, blood-brain barrier breakdown, and injury volume by ifenprodil, a polyamine-site N-methyl-D-aspartate receptor antagonist, after experimental traumatic brain injury in rats. *Neurosurgery* 47(2):399-404; discussion 404-6.
- DeRidder MN, Simon MJ, Siman R, Auberson YP, Raghupathi R, Meaney DF. 2006. Traumatic mechanical injury to the hippocampus in vitro causes regional caspase-3 and calpain activation that is influenced by NMDA receptor subunit composition. *Neurobiol Dis* 22(1):165-76.
- Dietrich WD, Alonso O, Halley M. 1994. Early microvascular and neuronal consequences of traumatic brain injury: a light and electron microscopic study in rats. *J Neurotrauma* 11(3):289-301.
- Discher DE, Janmey P, Wang YL. 2005. Tissue cells feel and respond to the stiffness of their substrate. *Science* 310(5751):1139-43.

Bibliography

- Domercq M, Brambilla L, Pilati E, Marchaland J, Volterra A, Bezzi P. 2006. P2Y₁ receptor-evoked glutamate exocytosis from astrocytes: control by tumor necrosis factor- α and prostaglandins. *J Biol Chem* 281(41):30684-96.
- Duan S, Anderson CM, Keung EC, Chen Y, Swanson RA. 2003. P2X₇ receptor-mediated release of excitatory amino acids from astrocytes. *J Neurosci* 23(4):1320-8.
- Duan S, Neary JT. 2006. P2X(7) receptors: properties and relevance to CNS function. *Glia* 54(7):738-46.
- Ellis EF, McKinney JS, Willoughby KA, Liang S, Povlishock JT. 1995. A new model for rapid stretch-induced injury of cells in culture: characterization of the model using astrocytes. *J Neurotrauma* 12(3):325-39.
- Erb L, Liao Z, Seye CI, Weisman GA. 2006. P2 receptors: intracellular signaling. *Pflugers Arch* 452(5):552-62.
- Faden AI, Demediuk P, Panter SS, Vink R. 1989. The role of excitatory amino acids and NMDA receptors in traumatic brain injury. *Science* 244(4906):798-800.
- Faden AI, Knoblach SM, Cernak I, Fan L, Vink R, Araldi GL, Fricke ST, Roth BL, Kozikowski AP. 2003. Novel diketopiperazine enhances motor and cognitive recovery after traumatic brain injury in rats and shows neuroprotection in vitro and in vivo. *J Cereb Blood Flow Metab* 23(3):342-54.
- Farahani R, Pina-Benabou MH, Kyrozis A, Siddiq A, Barradas PC, Chiu FC, Cavalcante LA, Lai JC, Stanton PK, Rozental R. 2005. Alterations in metabolism and gap junction expression may determine the role of astrocytes as "good samaritans" or executioners. *Glia* 50(4):351-361.
- Faulkner JR, Herrmann JE, Woo MJ, Tansey KE, Doan NB, Sofroniew MV. 2004. Reactive astrocytes protect tissue and preserve function after spinal cord injury. *J Neurosci* 24(9):2143-55.
- Fawcett JW, Asher RA. 1999. The glial scar and central nervous system repair. *Brain Res Bull* 49(6):377-91.
- Fellin T, Haydon PG. 2005. Do astrocytes contribute to excitation underlying seizures? *Trends Mol Med* 11(12):530-3.
- Fellin T, Pascual O, Gobbo S, Pozzan T, Haydon PG, Carmignoto G. 2004. Neuronal synchrony mediated by astrocytic glutamate through activation of extrasynaptic NMDA receptors. *Neuron* 43(5):729-43.
- Fellin T, Pascual O, Haydon PG. 2006a. Astrocytes coordinate synaptic networks: balanced excitation and inhibition. *Physiology (Bethesda)* 21:208-15.
- Fellin T, Pozzan T, Carmignoto G. 2006b. Purinergic receptors mediate two distinct glutamate release pathways in hippocampal astrocytes. *J Biol Chem* 281(7):4274-84.
- Fields RD, Burnstock G. 2006. Purinergic signalling in neuron-glia interactions. *Nat Rev Neurosci* 7(6):423-36.
- Finkelstein E, Corso P, Miller T. 2006. The Incidence and Economic Burden of Injuries in the United States. New York, NY: Oxford University Press.
- Fitch MT, Doller C, Combs CK, Landreth GE, Silver J. 1999. Cellular and molecular mechanisms of glial scarring and progressive cavitation: in vivo and in vitro

Bibliography

- analysis of inflammation-induced secondary injury after CNS trauma. *J Neurosci* 19(19):8182-98.
- Flanagan LA, Ju YE, Marg B, Osterfield M, Janmey PA. 2002. Neurite branching on deformable substrates. *Neuroreport* 13(18):2411-5.
- Floyd CL, Gorin FA, Lyeth BG. 2005. Mechanical strain injury increases intracellular sodium and reverses Na(+)/Ca(2+) exchange in cortical astrocytes. *Glia* 51(1):35-46.
- Floyd CL, Rzigalinski BA, Sitterding HA, Willoughby KA, Ellis EF. 2004. Antagonism of group I metabotropic glutamate receptors and PLC attenuates increases in inositol trisphosphate and reduces reactive gliosis in strain-injured astrocytes. *J Neurotrauma* 21(2):205-16.
- Franke H, Krugel U, Grosche J, Heine C, Hartig W, Allgaier C, Illes P. 2004. P2Y receptor expression on astrocytes in the nucleus accumbens of rats. *Neuroscience* 127(2):431-41.
- Franke H, Krugel U, Illes P. 1999. P2 receptor-mediated proliferative effects on astrocytes in vivo. *Glia* 28(3):190-200.
- Franke H, Krugel U, Illes P. 2006. P2 receptors and neuronal injury. *Pflugers Arch* 452(5):622-44.
- Franke H, Krugel U, Schmidt R, Grosche J, Reichenbach A, Illes P. 2001. P2 receptor-types involved in astrogliosis in vivo. *Br J Pharmacol* 134(6):1180-9.
- Geddes DM, LaPlaca MC, Cargill RS, 2nd. 2003. Susceptibility of hippocampal neurons to mechanically induced injury. *Exp Neurol* 184(1):420-7.
- Geddes-Klein DM, Schiffman KB, Meaney DF. 2006. Mechanisms and consequences of neuronal stretch injury in vitro differ with the model of trauma. *J Neurotrauma* 23(2):193-204.
- Gennarelli TA. 1993. Mechanisms of brain injury. *J Emerg Med* 11 Suppl 1:5-11.
- Georges PC, Miller WJ, Meaney DF, Sawyer ES, Janmey PA. 2006. Matrices with Compliance Comparable to that of Brain Tissue Select Neuronal over Glial Growth in Mixed Cortical Cultures. *Biophys J* 90(8):3012-8.
- Giaume C, Venance L. 1998. Intercellular calcium signaling and gap junctional communication in astrocytes. *Glia* 24(1):50-64.
- Guthrie PB, Knappenberger J, Segal M, Bennett MV, Charles AC, Kater SB. 1999. ATP released from astrocytes mediates glial calcium waves. *J Neurosci* 19(2):520-8.
- Haas B, Schipke CG, Peters O, Sohl G, Willecke K, Kettenmann H. 2006. Activity-dependent ATP-waves in the Mouse Neocortex are Independent from Astrocytic Calcium Waves. *Cereb Cortex* 16(2):237-46.
- Hansson E, Ronnback L. 2003. Glial neuronal signaling in the central nervous system. *Faseb J* 17(3):341-8.
- Hardingham GE, Fukunaga Y, Bading H. 2002. Extrasynaptic NMDARs oppose synaptic NMDARs by triggering CREB shut-off and cell death pathways. *Nat Neurosci* 5(5):405-14.
- Hassinger TD, Guthrie PB, Atkinson PB, Bennett MV, Kater SB. 1996. An extracellular signaling component in propagation of astrocytic calcium waves. *Proc Natl Acad Sci U S A* 93(23):13268-73.

Bibliography

- Haydon PG, Lartius R, Parpura V, Marchese-Ragona SP. 1996. Membrane deformation of living glial cells using atomic force microscopy. *J Microsc* 182(Pt 2):114-20.
- He HJ, Kole S, Kwon YK, Crow MT, Bernier M. 2003. Interaction of filamin A with the insulin receptor alters insulin-dependent activation of the mitogen-activated protein kinase pathway. *J Biol Chem* 278(29):27096-104.
- Hicks R, Soares H, Smith D, McIntosh T. 1996. Temporal and spatial characterization of neuronal injury following lateral fluid-percussion brain injury in the rat. *Acta Neuropathol (Berl)* 91(3):236-46.
- Hoh JH, Schoenenberger CA. 1994. Surface morphology and mechanical properties of MDCK monolayers by atomic force microscopy. *J Cell Sci* 107 (Pt 5):1105-14.
- Hussl S, Boehm S. 2006. Functions of neuronal P2Y receptors. *Pflugers Arch* 452(5):538-51.
- Innocenti B, Parpura V, Haydon PG. 2000. Imaging extracellular waves of glutamate during calcium signaling in cultured astrocytes. *J Neurosci* 20(5):1800-8.
- Janmey PA, Hvidt S, Kas J, Lerche D, Maggs A, Sackmann E, Schliwa M, Stossel TP. 1994. The mechanical properties of actin gels. Elastic modulus and filament motions. *J Biol Chem* 269(51):32503-13.
- Janmey PA, Hvidt S, Lamb J, Stossel TP. 1990. Resemblance of actin-binding protein/actin gels to covalently crosslinked networks. *Nature* 345(6270):89-92.
- Janmey PA, Hvidt S, Peetermans J, Lamb J, Ferry JD, Stossel TP. 1988. Viscoelasticity of F-actin and F-actin/gelsolin complexes. *Biochemistry* 27(21):8218-27.
- Jeremic A, Jeftinija K, Stevanovic J, Glavaski A, Jeftinija S. 2001. ATP stimulates calcium-dependent glutamate release from cultured astrocytes. *J Neurochem* 77(2):664-75.
- Johnson RG, Meyer RA, Li XR, Preus DM, Tan L, Grunenwald H, Paulson AF, Laird DW, Sheridan JD. 2002. Gap junctions assemble in the presence of cytoskeletal inhibitors, but enhanced assembly requires microtubules. *Exp Cell Res* 275(1):67-80.
- Kang N, Xu J, Xu Q, Nedergaard M, Kang J. 2005. Astrocytic glutamate release-induced transient depolarization and epileptiform discharges in hippocampal CA1 pyramidal neurons. *J Neurophysiol* 94(6):4121-30.
- Kawahara K, Hosoya R, Sato H, Tanaka M, Nakajima T, Iwabuchi S. 2002. Selective blockade of astrocytic glutamate transporter GLT-1 with dihydrokainate prevents neuronal death during ouabain treatment of astrocyte/neuron cocultures. *Glia* 40(3):337-49.
- Kawamura M, Gachet C, Inoue K, Kato F. 2004. Direct excitation of inhibitory interneurons by extracellular ATP mediated by P2Y1 receptors in the hippocampal slice. *J Neurosci* 24(48):10835-45.
- Kharlamov A, Jones SC, Kim DK. 2002. Suramin reduces infarct volume in a model of focal brain ischemia in rats. *Exp Brain Res* 147(3):353-9.
- King BF, Neary JT, Zhu Q, Wang S, Norenberg MD, Burnstock G. 1996. P2 purinoceptors in rat cortical astrocytes: expression, calcium-imaging and signalling studies. *Neuroscience* 74(4):1187-96.

Bibliography

- Kumar NM, Gilula NB. 1996. The gap junction communication channel. *Cell* 84(3):381-8.
- Lammer A, Gunther A, Beck A, Krugel U, Kittner H, Schneider D, Illes P, Franke H. 2006. Neuroprotective effects of the P2 receptor antagonist PPADS on focal cerebral ischaemia-induced injury in rats. *Eur J Neurosci* 23(10):2824-8.
- Landau LD, Lifshitz EM. 1970. *Theory of Elasticity*. Oxford: Pergamon Press.
- Langlois J, Rutland-Brown W, Thomas K. 2004. Traumatic brain injury in the United States: emergency department visits, hospitalizations, and deaths. Atlanta (GA): Centers for Disease Control and Prevention, Nation Center for Injury Prevention and Control.
- LaPlaca MC, Thibault LE. 1998. Dynamic mechanical deformation of neurons triggers an acute calcium response and cell injury involving the N-methyl-D-aspartate glutamate receptor. *J Neurosci Res* 52(2):220-9.
- Lea PM, Custer SJ, Vicini S, Faden AI. 2002. Neuronal and glial mGluR5 modulation prevents stretch-induced enhancement of NMDA receptor current. *Pharmacol Biochem Behav* 73(2):287-98.
- Lenz G, Gottfried C, Luo Z, Avruch J, Rodnight R, Nie WJ, Kang Y, Neary JT. 2000. P(2Y) purinoceptor subtypes recruit different mek activators in astrocytes. *Br J Pharmacol* 129(5):927-36.
- Leybaert L, Braet K, Vandamme W, Cabooter L, Martin PE, Evans WH. 2003. Connexin channels, connexin mimetic peptides and ATP release. *Cell Commun Adhes* 10(4-6):251-7.
- Lin JH, Weigel H, Cotrina ML, Liu S, Bueno E, Hansen AJ, Hansen TW, Goldman S, Nedergaard M. 1998. Gap-junction-mediated propagation and amplification of cell injury. *Nat Neurosci* 1(6):494-500.
- Lin R, Karpa K, Kabbani N, Goldman-Rakic P, Levenson R. 2001. Dopamine D2 and D3 receptors are linked to the actin cytoskeleton via interaction with filamin A. *Proc Natl Acad Sci U S A* 98(9):5258-63.
- Liu QS, Xu Q, Arcuino G, Kang J, Nedergaard M. 2004. Astrocyte-mediated activation of neuronal kainate receptors. *Proc Natl Acad Sci U S A* 101(9):3172-7.
- Lo CM, Wang HB, Dembo M, Wang YL. 2000. Cell movement is guided by the rigidity of the substrate. *Biophys J* 79(1):144-52.
- Loewenstein WR. 1981. Junctional intercellular communication: the cell-to-cell membrane channel. *Physiol Rev* 61(4):829-913.
- Loftis JM, Janowsky A. 2003. The N-methyl-D-aspartate receptor subunit NR2B: localization, functional properties, regulation, and clinical implications. *Pharmacol Ther* 97(1):55-85.
- Lowenstein DH, Thomas MJ, Smith DH, McIntosh TK. 1992. Selective vulnerability of dentate hilar neurons following traumatic brain injury: a potential mechanistic link between head trauma and disorders of the hippocampus. *J Neurosci* 12(12):4846-53.
- Lu YB, Franze K, Seifert G, Steinhauser C, Kirchhoff F, Wolburg H, Guck J, Janmey P, Wei EQ, Kas J and others. 2006. Viscoelastic properties of individual glial cells and neurons in the CNS. *Proc Natl Acad Sci U S A* 103(47):17759-64.

Bibliography

- Lusardi TA, Rangan J, Sun D, Smith DH, Meaney DF. 2004. A device to study the initiation and propagation of calcium transients in cultured neurons after mechanical stretch. *Ann Biomed Eng* 32(11):1546-58.
- MacKintosh FC, Kas J, Janmey PA. 1995. Elasticity of semiflexible biopolymer networks. *Physical Review Letters* 75(24):4425-4428.
- Mandell JW, Gocan NC, Vandenberg SR. 2001. Mechanical trauma induces rapid astroglial activation of ERK/MAP kinase: Evidence for a paracrine signal. *Glia* 34(4):283-95.
- Mathur AB, Collinworth AM, Reichert WM, Kraus WE, Truskey GA. 2001. Endothelial, cardiac muscle and skeletal muscle exhibit different viscous and elastic properties as determined by atomic force microscopy. *J Biomech* 34(12):1545-53.
- McIntosh TK, Smith DH, Meaney DF, Kotapka MJ, Gennarelli TA, Graham DI. 1996. Neuropathological sequelae of traumatic brain injury: relationship to neurochemical and biomechanical mechanisms. *Lab Invest* 74(2):315-42.
- McKeon RJ, Jurynek MJ, Buck CR. 1999. The chondroitin sulfate proteoglycans neurocan and phosphacan are expressed by reactive astrocytes in the chronic CNS glial scar. *J Neurosci* 19(24):10778-88.
- Meme W, Ezan P, Venance L, Glowinski J, Giaume C. 2004. ATP-induced inhibition of gap junctional communication is enhanced by interleukin-1 beta treatment in cultured astrocytes. *Neuroscience* 126(1):95-104.
- Miller RT, Margulies SS, Leoni M, Nonaka M, Chen X, Smith DH, Meaney DF. Finite Element Modeling Approaches for Predicting Injury in an Experimental Model of Severe Diffuse Axonal Injury; 1998; Tempe, Arizona. p 156-167.
- Montana V, Ni Y, Sunjara V, Hua X, Parpura V. 2004. Vesicular glutamate transporter-dependent glutamate release from astrocytes. *J Neurosci* 24(11):2633-42.
- Morrison B, 3rd, Meaney DF, McIntosh TK. 1998. Mechanical characterization of an in vitro device designed to quantitatively injure living brain tissue. *Ann Biomed Eng* 26(3):381-90.
- Movsesyan VA, O'Leary DM, Fan L, Bao W, Mullins PG, Knobloch SM, Faden AI. 2001. mGluR5 antagonists 2-methyl-6-(phenylethynyl)-pyridine and (E)-2-methyl-6-(2-phenylethenyl)-pyridine reduce traumatic neuronal injury in vitro and in vivo by antagonizing N-methyl-D-aspartate receptors. *J Pharmacol Exp Ther* 296(1):41-7.
- Munsch N, Gavaret JM, Pierre M. 1998. Ca²⁺ dependent purinergic regulation of p42 and p44 MAP kinases in astroglial cultured cells. *Biomed Pharmacother* 52(4):180-6.
- Muyderman H, Nilsson M, Blomstrand F, Khatibi S, Olsson T, Hansson E, Ronnback L. 1998. Modulation of mechanically induced calcium waves in hippocampal astroglial cells. Inhibitory effects of alpha 1-adrenergic stimulation. *Brain Res* 793(1-2):127-35.
- Myer DJ, Gurkoff GG, Lee SM, Hovda DA, Sofroniew MV. 2006. Essential protective roles of reactive astrocytes in traumatic brain injury. *Brain* 129(Pt 10):2761-72.

Bibliography

- Nadkarni S, Jung P. 2003. Spontaneous oscillations of dressed neurons: a new mechanism for epilepsy? *Phys Rev Lett* 91(26 Pt 1):268101.
- Nagy JI, Rash JE. 2000. Connexins and gap junctions of astrocytes and oligodendrocytes in the CNS. *Brain Res Brain Res Rev* 32(1):29-44.
- Nakahara K, Okada M, Nakanishi S. 1997. The metabotropic glutamate receptor mGluR5 induces calcium oscillations in cultured astrocytes via protein kinase C phosphorylation. *J Neurochem* 69(4):1467-75.
- Neary JT, Kang Y. 2005. Signaling from P2 nucleotide receptors to protein kinase cascades induced by CNS injury: implications for reactive gliosis and neurodegeneration. *Mol Neurobiol* 31(1-3):95-103.
- Neary JT, Kang Y, Bu Y, Yu E, Akong K, Peters CM. 1999. Mitogenic signaling by ATP/P2Y purinergic receptors in astrocytes: involvement of a calcium-independent protein kinase C, extracellular signal-regulated protein kinase pathway distinct from the phosphatidylinositol-specific phospholipase C/calcium pathway. *J Neurosci* 19(11):4211-20.
- Neary JT, Kang Y, Willoughby KA, Ellis EF. 2003. Activation of extracellular signal-regulated kinase by stretch-induced injury in astrocytes involves extracellular ATP and P2 purinergic receptors. *J Neurosci* 23(6):2348-56.
- Neary JT, McCarthy M, Kang Y, Zuniga S. 1998. Mitogenic signaling from P1 and P2 purinergic receptors to mitogen-activated protein kinase in human fetal astrocyte cultures. *Neurosci Lett* 242(3):159-62.
- Neary JT, Norenberg MD. 1992. Signaling by extracellular ATP: physiological and pathological considerations in neuronal-astrocytic interactions. *Prog Brain Res* 94:145-51.
- Neary JT, Rathbone MP, Cattabeni F, Abbracchio MP, Burnstock G. 1996. Trophic actions of extracellular nucleotides and nucleosides on glial and neuronal cells. *Trends Neurosci* 19(1):13-8.
- Newman EA. 2001. Propagation of intercellular calcium waves in retinal astrocytes and Muller cells. *J Neurosci* 21(7):2215-23.
- Newman EA. 2003. Glial cell inhibition of neurons by release of ATP. *J Neurosci* 23(5):1659-66.
- Nieto-Sampedro M. 1999. Neurite outgrowth inhibitors in gliotic tissue. *Adv Exp Med Biol* 468:207-24.
- North RA, Verkhratsky A. 2006. Purinergic transmission in the central nervous system. *Pflugers Arch* 452(5):479-85.
- Norton WT. 1999. Cell reactions following acute brain injury: a review. *Neurochem Res* 24(2):213-8.
- Ohta Y, Okamoto H, Kanno M, Okuda T. 2002. Atomic force microscopic observation of mechanically traumatized erythrocytes. *Artif Organs* 26(1):10-7.
- Onopriashvili I, Andria ML, Kramer HK, Ancevska-Taneva N, Hiller JM, Simon EJ. 2003. Interaction between the mu opioid receptor and filamin A is involved in receptor regulation and trafficking. *Mol Pharmacol* 64(5):1092-100.
- Panickar KS, Norenberg MD. 2005. Astrocytes in cerebral ischemic injury: morphological and general considerations. *Glia* 50(4):287-98.

Bibliography

- Parpura V, Haydon PG. 2000. Physiological astrocytic calcium levels stimulate glutamate release to modulate adjacent neurons. *Proc Natl Acad Sci U S A* 97(15):8629-34.
- Parpura V, Haydon PG, Henderson E. 1993. Three-dimensional imaging of living neurons and glia with the atomic force microscope. *J Cell Sci* 104 (Pt 2):427-32.
- Pascual O, Casper KB, Kubera C, Zhang J, Revilla-Sanchez R, Sul JY, Takano H, Moss SJ, McCarthy K, Haydon PG. 2005. Astrocytic purinergic signaling coordinates synaptic networks. *Science* 310(5745):113-6.
- Pekny M, Nilsson M. 2005. Astrocyte activation and reactive gliosis. *Glia* 50(4):427-434.
- Pelham RJ, Jr., Wang Y. 1997. Cell locomotion and focal adhesions are regulated by substrate flexibility. *Proc Natl Acad Sci U S A* 94(25):13661-5.
- Perez Velazquez JL, Kokarovtseva L, Sarbaziha R, Jeyapalan Z, Leshchenko Y. 2006. Role of gap junctional coupling in astrocytic networks in the determination of global ischaemia-induced oxidative stress and hippocampal damage. *Eur J Neurosci* 23(1):1-10.
- Porter JT, McCarthy KD. 1996. Hippocampal astrocytes in situ respond to glutamate released from synaptic terminals. *J Neurosci* 16(16):5073-81.
- Powell EM, Meiners S, DiProspero NA, Geller HM. 1997. Mechanisms of astrocyte-directed neurite guidance. *Cell Tissue Res* 290(2):385-93.
- Radmacher M, Fritz M, Kacher CM, Cleveland JP, Hansma PK. 1996. Measuring the viscoelastic properties of human platelets with the atomic force microscope. *Biophys J* 70(1):556-67.
- Raghupathi R, Graham DI, McIntosh TK. 2000. Apoptosis after traumatic brain injury. *J Neurotrauma* 17(10):927-38.
- Rao VL, Baskaya MK, Dogan A, Rothstein JD, Dempsey RJ. 1998. Traumatic brain injury down-regulates glial glutamate transporter (GLT-1 and GLAST) proteins in rat brain. *J Neurochem* 70(5):2020-7.
- Rao VL, Dogan A, Todd KG, Bowen KK, Dempsey RJ. 2001. Neuroprotection by memantine, a non-competitive NMDA receptor antagonist after traumatic brain injury in rats. *Brain Res* 911(1):96-100.
- Regan RF, Choi DW. 1994. The effect of NMDA, AMPA/kainate, and calcium channel antagonists on traumatic cortical neuronal injury in culture. *Brain Res* 633(1-2):236-42.
- Ricci D, Tedesco M, Grattarola M. 1997. Mechanical and morphological properties of living 3T6 cells probed via scanning force microscopy. *Microsc Res Tech* 36(3):165-71.
- Rodrigues RJ, Almeida T, Richardson PJ, Oliveira CR, Cunha RA. 2005. Dual presynaptic control by ATP of glutamate release via facilitatory P2X1, P2X2/3, and P2X3 and inhibitory P2Y1, P2Y2, and/or P2Y4 receptors in the rat hippocampus. *J Neurosci* 25(27):6286-95.
- Rossi DJ, Oshima T, Attwell D. 2000. Glutamate release in severe brain ischaemia is mainly by reversed uptake. *Nature* 403(6767):316-21.
- Rothman SM, Olney JW. 1986. Glutamate and the pathophysiology of hypoxic-ischemic brain damage. *Ann Neurol* 19(2):105-11.

Bibliography

- Rotsch C, Braet F, Wisse E, Radmacher M. 1997. AFM imaging and elasticity measurements on living rat liver macrophages. *Cell Biol Int* 21(11):685-96.
- Royo NC, Shimizu S, Schouten JW, Stover JF, McIntosh TK. 2003. Pharmacology of traumatic brain injury. *Curr Opin Pharmacol* 3(1):27-32.
- Runden-Pran E, Tanso R, Haug FM, Ottersen OP, Ring A. 2005. Neuroprotective effects of inhibiting N-methyl-d-aspartate receptors, P2X receptors and the mitogen-activated protein kinase cascade: A quantitative analysis in organotypical hippocampal slice cultures subjected to oxygen and glucose deprivation. *Neuroscience* 136(3):795-810.
- Rzagalinski BA, Liang S, McKinney JS, Willoughby KA, Ellis EF. 1997. Effect of Ca²⁺ on in vitro astrocyte injury. *J Neurochem* 68(1):289-96.
- Rzagalinski BA, Weber JT, Willoughby KA, Ellis EF. 1998. Intracellular free calcium dynamics in stretch-injured astrocytes. *J Neurochem* 70(6):2377-85.
- Sanderson MJ, Charles AC, Boitano S, Dirksen ER. 1994. Mechanisms and function of intercellular calcium signaling. *Mol Cell Endocrinol* 98(2):173-87.
- Sandvig A, Berry M, Barrett LB, Butt A, Logan A. 2004. Myelin-, reactive glia-, and scar-derived CNS axon growth inhibitors: expression, receptor signaling, and correlation with axon regeneration. *Glia* 46(3):225-51.
- Sato M, Chang E, Igarashi T, Noble LJ. 2001. Neuronal injury and loss after traumatic brain injury: time course and regional variability. *Brain Res* 917(1):45-54.
- Sato M, Nagayama K, Kataoka N, Sasaki M, Hane K. 2000. Local mechanical properties measured by atomic force microscopy for cultured bovine endothelial cells exposed to shear stress. *J Biomech* 33(1):127-35.
- Sato M, Theret DP, Wheeler LT, Ohshima N, Nerem RM. 1990. Application of the micropipette technique to the measurement of cultured porcine aortic endothelial cell viscoelastic properties. *J Biomech Eng* 112(3):263-8.
- Sattler R, Charlton MP, Hafner M, Tymianski M. 1998. Distinct influx pathways, not calcium load, determine neuronal vulnerability to calcium neurotoxicity. *J Neurochem* 71(6):2349-64.
- Sattler R, Xiong Z, Lu WY, MacDonald JF, Tymianski M. 2000. Distinct roles of synaptic and extrasynaptic NMDA receptors in excitotoxicity. *J Neurosci* 20(1):22-33.
- Scatton B. 1993. The NMDA receptor complex. *Fundam Clin Pharmacol* 7(8):389-400.
- Scemes E. 2000. Components of astrocytic intercellular calcium signaling. *Mol Neurobiol* 22(1-3):167-79.
- Scemes E, Giaume C. 2006. Astrocyte calcium waves: what they are and what they do. *Glia* 54(7):716-25.
- Scemes E, Suadicani SO, Spray DC. 2000. Intercellular communication in spinal cord astrocytes: fine tuning between gap junctions and P2 nucleotide receptors in calcium wave propagation. *J Neurosci* 20(4):1435-45.
- Schools GP, Kimelberg HK. 1999. mGluR3 and mGluR5 are the predominant metabotropic glutamate receptor mRNAs expressed in hippocampal astrocytes acutely isolated from young rats. *J Neurosci Res* 58(4):533-43.

Bibliography

- Selkirk JV, Stiefel TH, Stone IM, Naeve GS, Foster AC, Poulsen DJ. 2005. Over-expression of the human EAAT2 glutamate transporter within neurons of mouse organotypic hippocampal slice cultures leads to increased vulnerability of CA1 pyramidal cells. *Eur J Neurosci* 21(8):2291-6.
- Sergeeva M, Ubl JJ, Reiser G. 2000. Disruption of actin cytoskeleton in cultured rat astrocytes suppresses ATP- and bradykinin-induced $[Ca^{2+}]_i$ oscillations by reducing the coupling efficiency between Ca^{2+} release, capacitative Ca^{2+} entry, and store refilling. *Neuroscience* 97(4):765-9.
- Shapira Y, Yadid G, Cotev S, Niska A, Shohami E. 1990. Protective effect of MK801 in experimental brain injury. *J Neurotrauma* 7(3):131-9.
- Shreiber DI, C. BA, Meaney DF. In *Vivo* Thresholds for Mechanical Injury to the Blood-Brain Barrier; 1997; 41st Stapp Car Crash Conference Proceedings. p 277-291.
- Smith DH, Soares HD, Pierce JS, Perlman KG, Saatman KE, Meaney DF, Dixon CE, McIntosh TK. 1995. A model of parasagittal controlled cortical impact in the mouse: cognitive and histopathologic effects. *J Neurotrauma* 12(2):169-78.
- Sneddon IN. 1965. The relation between load and penetration in the axisymmetric Boussinesq problem for a punch of arbitrary profile. *Int J Eng Sci* 3:47-57.
- Sofroniew MV. 2005. Reactive astrocytes in neural repair and protection. *Neuroscientist* 11(5):400-7.
- Stout CE, Costantin JL, Naus CC, Charles AC. 2002. Intercellular calcium signaling in astrocytes via ATP release through connexin hemichannels. *J Biol Chem* 277(12):10482-8.
- Strasser U, Lobner D, Behrens MM, Canzoniero LM, Choi DW. 1998. Antagonists for group I mGluRs attenuate excitotoxic neuronal death in cortical cultures. *Eur J Neurosci* 10(9):2848-55.
- Suadicani SO, Brosnan CF, Scemes E. 2006. P2X7 receptors mediate ATP release and amplification of astrocytic intercellular Ca^{2+} signaling. *J Neurosci* 26(5):1378-85.
- Suadicani SO, Flores CE, Urban-Maldonado M, Beelitz M, Scemes E. 2004. Gap junction channels coordinate the propagation of intercellular Ca^{2+} signals generated by P2Y receptor activation. *Glia* 48(3):217-29.
- Sutton RL, Lescaudron L, Stein DG. 1993. Unilateral cortical contusion injury in the rat: vascular disruption and temporal development of cortical necrosis. *J Neurotrauma* 10(2):135-49.
- Tashiro A, Goldberg J, Yuste R. 2002. Calcium oscillations in neocortical astrocytes under epileptiform conditions. *J Neurobiol* 50(1):45-55.
- Tashlykov V, Katz Y, Gazit V, Zohar O, Schreiber S, Pick CG. 2007. Apoptotic changes in the cortex and hippocampus following minimal brain trauma in mice. *Brain Res* 1130(1):197-205.
- Tian GF, Azmi H, Takano T, Xu Q, Peng W, Lin J, Oberheim N, Lou N, Wang X, Zielke HR and others. 2005. An astrocytic basis of epilepsy. *Nat Med* 11(9):973-81.
- Tordjmann T, Berthon B, Claret M, Combettes L. 1997. Coordinated intercellular calcium waves induced by noradrenaline in rat hepatocytes: dual control by gap junction permeability and agonist. *Embo J* 16(17):5398-407.

Bibliography

- Toulmond S, Serrano A, Benavides J, Scatton B. 1993. Prevention by eliprodil (SL 82.0715) of traumatic brain damage in the rat. Existence of a large (18 h) therapeutic window. *Brain Res* 620(1):32-41.
- Trendelenburg G, Dirnagl U. 2005. Neuroprotective role of astrocytes in cerebral ischemia: focus on ischemic preconditioning. *Glia* 50(4):307-20.
- Trickey WR, Vail TP, Guilak F. 2004. The role of the cytoskeleton in the viscoelastic properties of human articular chondrocytes. *J Orthop Res* 22(1):131-9.
- Turvey MR, Fogarty KE, Thorn P. 2005. Inositol (1,4,5)-trisphosphate receptor links to filamentous actin are important for generating local Ca^{2+} signals in pancreatic acinar cells. *J Cell Sci* 118(Pt 5):971-80.
- Venance L, Stella N, Glowinski J, Giaume C. 1997. Mechanism involved in initiation and propagation of receptor-induced intercellular calcium signaling in cultured rat astrocytes. *J Neurosci* 17(6):1981-92.
- Verkhatsky A, Steinhäuser C. 2000. Ion channels in glial cells. *Brain Res Brain Res Rev* 32(2-3):380-412.
- Volonte C, Merlo D. 1996. Selected P2 purinoceptor modulators prevent glutamate-evoked cytotoxicity in cultured cerebellar granule neurons. *J Neurosci Res* 45(2):183-93.
- Wang CX, Shuaib A. 2005. NMDA/NR2B selective antagonists in the treatment of ischemic brain injury. *Curr Drug Targets CNS Neurol Disord* 4(2):143-51.
- Wang HB, Dembo M, Hanks SK, Wang Y. 2001. Focal adhesion kinase is involved in mechanosensing during fibroblast migration. *Proc Natl Acad Sci U S A* 98(20):11295-300.
- Wang Z, Haydon PG, Yeung ES. 2000. Direct observation of calcium-independent intercellular ATP signaling in astrocytes. *Anal Chem* 72(9):2001-7.
- Weber JT, Rzigalinski BA, Ellis EF. 2001. Traumatic injury of cortical neurons causes changes in intracellular calcium stores and capacitative calcium influx. *J Biol Chem* 276(3):1800-7.
- Williams K. 1993. Ifenprodil discriminates subtypes of the N-methyl-D-aspartate receptor: selectivity and mechanisms at recombinant heteromeric receptors. *Mol Pharmacol* 44(4):851-9.
- Wirkner K, Gunther A, Weber M, Guzman SJ, Krause T, Fuchs J, Koles L, Norenberg W, Illes P. 2006. Modulation of NMDA Receptor Current in Layer V Pyramidal Neurons of the Rat Prefrontal Cortex by P2Y Receptor Activation. *Cereb Cortex*.
- Wirkner K, Koles L, Thummler S, Luthardt J, Poelchen W, Franke H, Furst S, Illes P. 2002. Interaction between P2Y and NMDA receptors in layer V pyramidal neurons of the rat prefrontal cortex. *Neuropharmacology* 42(4):476-88.
- Wolf JA, Stys PK, Lusardi T, Meaney D, Smith DH. 2001. Traumatic axonal injury induces calcium influx modulated by tetrodotoxin-sensitive sodium channels. *J Neurosci* 21(6):1923-30.
- Wu VW, Schwartz JP. 1998. Cell culture models for reactive gliosis: new perspectives. *J Neurosci Res* 51(6):675-81.

Bibliography

- Yamane Y, Shiga H, Asou H, Ito E. 2002. GAP junctional channel inhibition alters actin organization and calcium propagation in rat cultured astrocytes. *Neuroscience* 112(3):593-603.
- Yamane Y, Shiga H, Haga H, Kawabata K, Abe K, Ito E. 2000. Quantitative analyses of topography and elasticity of living and fixed astrocytes. *J Electron Microsc* (Tokyo) 49(3):463-71.
- Yiu G, He Z. 2006. Glial inhibition of CNS axon regeneration. *Nat Rev Neurosci* 7(8):617-27.
- Yong VW. 1998. Response of Astrocytes and Oligodendrocytes to Injury. *Mental Retardation and Developmental Disabilities Research Reviews* 4:193-199.
- Yoshida Y, Tsuchiya R, Matsumoto N, Morita M, Miyakawa H, Kudo Y. 2005. Ca²⁺-dependent induction of intracellular Ca²⁺ oscillation in hippocampal astrocytes during metabotropic glutamate receptor activation. *J Pharmacol Sci* 97(2):212-8.
- Zhang L, Rzigalinski BA, Ellis EF, Satin LS. 1996. Reduction of voltage-dependent Mg²⁺ blockade of NMDA current in mechanically injured neurons. *Science* 274(5294):1921-3.
- Zhang Q, Fukuda M, Van Bockstaele E, Pascual O, Haydon PG. 2004a. Synaptotagmin IV regulates glial glutamate release. *Proc Natl Acad Sci U S A* 101(25):9441-6.
- Zhang Q, Pangrsic T, Kreft M, Krzan M, Li N, Sul JY, Halassa M, Van Bockstaele E, Zorec R, Haydon PG. 2004b. Fusion-related release of glutamate from astrocytes. *J Biol Chem* 279(13):12724-33.
- Zhao X, Ahram A, Berman RF, Muizelaar JP, Lyeth BG. 2003. Early loss of astrocytes after experimental traumatic brain injury. *Glia* 44(2):140-52.